

Abstract

The study concern with using local Kaolin of Duekhla to prepare Anorthite material. The sequence of study started with washing, chemical treatment and sedimentation to produce a fine powder by passing the product through a special sieve (less than 20 μm).then after this step dividing the fine powder product into two groups, the first group with out heat treatment and the second with heat treatment (calcinations) at 400°C. Then the second required material is calcium carbonate, so it is sieved through mesh size (less than 20 μm).the next step was mixed these groups of Kaolin separately with calcium carbonate (CaCO_3) in percentage of (kaolin : CaCO_3) as; (70% :30%, 75% :25%, 80% :20%, 85% :15%) respectively. The process of mixing is done by wet grinding with Ethanol technique; follow that drying and firing at 1200°C for 1hr, 2hrs and 3hrs and 1300 °C for 1hr. The results are XRD and IR for fired sample shows that the groups prepared from (80%:20% and 85%:15%) and treated at 1200°C for 3hrs gives the excellent results as Anorthite material ($\text{CaAl}_2\text{Si}_2\text{O}_8$). The chemical analyses study for acceptable Anorthite product was in coincidence with that defined by Ternary phase diagram. Additional study was done is dielectric properties give the same results. The conclusion behind this study is the Anorthite can be prepared from Kaolin Duekhla under specified treatment with calcium carbonate at certain mixing and firing condition.

List of contents

Contents		
	Abstract	i
	Contents	ii
	List of symbols	v
	List of figures	vi
	List of tables	x
Chapter One “Introduction”		
1.1	Introduction	1
1.2	The Calcium Ortho- Silicate Group	2
1.3	Feldspar	3
1.3.1	Mineralogy of Feldspar	4
1.4	Anorthite	5
1.5	Literature Review:	8
1.6	Process Parameters	11
1.6.1	Mixing	11
1.6.2	Drying	11
1.6.3	Shrinkage	13
1.6.4	Sintering &Firing	14
1.7	Analytical Technique	16
1.7.1	X-Ray Powder Crystal Diffraction	16
1.7.2	Infrared Analysis:	17
1.7.3	Dielectric Properties	19
1.7.4	Factors affecting on dielectric properties	22
1.8	Raw Materials	24
1.8.1	Kaolin	24
1.8.2	Calcium Carbonate	25
1.9	Aim of thesis	26
Chapter Two “Theoretical Part”		
2.1	Two Components Miscible System	27
2.2	Polymorphous Changes in Solid Solution.	35
2.3	Binary Systems in Ceramic Materials	36
2.4	Ternary System in Ceramic Materials	47

2.5	The Mechanism of Fusion in Ceramic Materials	48
2.5.1	Rate of Fusion	49
2.5.2	The Vaporization Point	50
2.5.3	Boiling Point	50
2.5.4	Thermal Effects Accompanying Reaction	51
2.6	Changes in Composition on Firing Silica Materials	51
Chapter Three “Practical and Results Part ”		
3.1	Sample preparation procedure	56
3.1.1	Kaolin treatment	56
3.1.2	Calcium carbonate treatment	61
3.1.3	Sample preparation	62
3.2	Measurements	63
3.2.1	X- Ray Diffraction Measurement	63
3.2.2	Chemical composition	63
3.2.3	IR measurement	63
3.2.4	Dielectric Properties Measurements	94
Chapter four Discussion of Results, Conclusion & Future Work		
4.1	Raw and product Material Characterization	99
4.2	XRD characterization	100
4.3	IR characterization	102
4.4	dielectric properties	104
4.5	Chemical analyses	104
4.6	Conclusion	106
4.7	Future Work	106
	Reference	107

Figure No.	Captions	Page No.
(1.1)	Reduced growth rate versus under cooling relation for Anorthite	7
(1.2)	Rate of drying curve	12
(1.3)	The change in the volume of ceramic body as the moisture is removed during drying	13
(1.4)	During sintering, diffusion produces bridges between the particles and event causes the pores to be filling in	16
(2.1)	The phase diagram of a binary mixture where the components are completely miscible in both the liquid and solid form	29
(2.2)	The phase diagram of miscible components with a maximum point	32
(2.3)	The phase diagram of miscible components with a minimum point	33
(2.4)	The phase diagram of miscible components with partial solid solution	34
(2.5)	The effect of polymorphic changes on the phase relationships in a binary solid solution	36
(2.6)	The alumina / silica phase diagram	37
(2.7)	The equilibrium phase diagram of CaO – SiO ₂	39
(2.8)	The magnesia / silica phase diagram	40
(2.9)	The iron oxide / silica phase diagram	41
(2.10)	The sodium oxide / silica phase diagram	42
(2.11)	The amount of liquid formed with mixtures of silica with (1%) of various oxides at different temperatures	43

List of Figure

Figure No.	Captions	Page No.
(2.12)	The partial phase diagram of the lime / alumina system	44
(2.13)	The partial phase diagram of the magnesia alumina system	45
(2.14)	Temperature / concentration diagram of the lime magnesia system	45
(2.15).	The phase diagram of iron oxide and lime	46
(2.16)	Phase diagram of lima – alumina - silica	47
(3.1)	In this figure length between 1 and2 is40 cm, 2 and3 is 30cm, 3 and4 is 30cm	57
(3.2)	IR analysis for kaolin raw material	58
(3.3)	IR analysis for kaolin washed by HCL	58
(3.4)	XRD pattern for Kaolin Duekhla raw material	59
(3.5)	XRD pattern for Kaolin Duekhla washed by HCL	59
(3.6)	XRD pattern for calcinated kaolin duekhla	60
(3.7)	XRD pattern for calcinated kaolin duekhla washing with HCL	60
(3.8)	IR analysis for CaCO ₃	61
(3.9)	IR analysis for sample No. M ₃	64
(3.10)	IR analysis for sample No. M ₄	64
(3.11)	IR analysis for sample No. M ₇	65
(3.12)	IR analysis for sample No. M ₈	65
(3.13)	XRD pattern for sample 70% K+30% CaCO ₃ fired 1200 °C for one hours	66
(3.14)	XRD pattern for sample 70% K+30% CaCO ₃ fired 1200 °C for two hours	67
(3.15)	XRD pattern for sample 70% K+30% CaCO ₃ fired 1200 °C for three hours	68

Figure No.	Captions	Page No.
(3.16)	XRD pattern for sample 75% K+25% CaCO ₃ fired 1200 °C for one hours	69
(3.17)	XRD pattern for sample 75% K+25% CaCO ₃ fired 1200 °C for two hours	70
(3.18)	XRD pattern for sample 75% K+25% CaCO ₃ fired 1200 °C for three hours	71
(3.19)	XRD pattern for sample 80% K+20% CaCO ₃ fired 1200 °C for one hours	72
(3.20)	XRD pattern for sample 80% K+20% CaCO ₃ fired 1200 °C for two hours	73
(3.21)	XRD pattern for sample 80% K+20% CaCO ₃ fired 1200 °C for three hours	74
(3.22)	XRD pattern for sample 80% K+20% CaCO ₃ fired 1300 °C for one hours	75
(3.23)	XRD pattern for sample 85% K+15% CaCO ₃ fired 1200 °C for one hours	76
(3.24)	XRD pattern for sample 85% K+15% CaCO ₃ fired 1200 °C for two hours	77
(3.25)	XRD pattern for sample 85% K+15% CaCO ₃ fired 1200 °C for three hours	78
(3.26)	XRD pattern for sample 85% K+15% CaCO ₃ fired 1300 °C for one hours	79
(3.27)	XRD pattern for sample 70%K+30% CaCO ₃ fired 1200 °C for one hours	80
(3.28)	XRD pattern for sample 70%K+30% CaCO ₃ fired 1200 °C for two hours	81
(3.29)	XRD pattern for sample 70%K+30% CaCO ₃ fired 1200 °C for three hours.	82
(3.30)	XRD pattern for sample 75%K+25%CaCO ₃ fired 1200 °C for one hour.	83
(3.31)	XRD pattern for sample 75%K+25% CaCO ₃ fired 1200 °C for two hours.	84
(3.32)	XRD pattern for sample 75%K+25% CaCO ₃ fired 1200 °C for three hours	85

Figure No.	Captions	Page No.
(3.33)	XRD pattern for sample 80%C K+20% CaCO ₃ fired 1200 °C for one hour.	86
(3.34)	XRD pattern for sample 80%C K+20% CaCO ₃ fired 1200 °C for two hours.	87
(3.35)	XRD pattern for sample 80%C K+20% CaCO ₃ fired 1200 °C for three hours	88
(3.36)	XRD pattern for sample 80%C K+20% CaCO ₃ fired 1300°C for one hour	89
(3.37)	XRD pattern for sample 85%C K+15% CaCO ₃ fired 1200 °C for one hours	90
(3.38)	XRD pattern for sample 85%C K+15% CaCO ₃ fired 1200 °C for two hours	91
(3.39)	XRD pattern for sample 85%C K+15% CaCO ₃ fired 1300 °C for three hours	92
(3.40)	XRD pattern for sample 85%C K+15% CaCO ₃ fired 1300 °C for one hours	93
(3.41)	(a) Dielectric Constant (b) Dielectric Loss Index; for sample M ₁	95
(3.42)	(a) Dielectric Constant (b) Dielectric Loss Index; for sample M ₂	95
(3.43)	(a) Dielectric Constant (b) Dielectric Loss Index; for sample M ₃	96
(3.44)	(a) Dielectric Constant (b) Dielectric Loss Index; for sample M ₄	96
(3.45)	(a) Dielectric Constant (b) Dielectric Loss Index; for sample M ₅	97
(3.46)	(a) Dielectric Constant (b) Dielectric Loss Index; for sample M ₆	97
(3.47)	(a) Dielectric Constant (b) Dielectric Loss index; for sample M ₇	98
(3.48)	(a) Dielectric Constant (b) Dielectric Loss; for sample M ₈	98
(4.1)	Ternary phase diagram	105

List of Tables

Table NO.	Captions	Page NO.
(1.1)	The feldspar group	5
(1.2)	chemical composition of Kaolin Duekhla	24
(2.1)	Some important features of divalent oxide /silica system	40
(2.2)	spinal ($MgOAl_2O_3$), with melting point of $2135^{\circ}C$ and the three eutectics	44
(2.3)	Compounds formed in the $CaO / Al_2O_3 / SiO_2$ system	48
(2.5)	the proportions of liquid formed in mixtures of silica with alumina and Lima or magnesia	63
(3. 1)	sample preparation from Kaolin and calcent Kaolin with $CaCO_3$	62
(3. 2)	Chemical composition of the samples preparation	63
(3.3)	dielectric constant and those Dielectric loss indexes at frequency of 1MHZ.	94
(4.1)	ASTM for Anorthite peak	101
(4.2)	Standard peaks of anorthite	103
(4.2)	represents the chemical analyses for pure Anorthite and the samples prepared	105

List of Symbols

A	Cross section area.
C	Capacitance of capacitor in medium.
CaCO ₃	Calcium carbonate.
d	Parallel plate capacitor distance.
D _d	Dielectric displacement.
d _s	Sample thickness.
E	Electric field in the medium.
E _o	External electric field.
K	Thickness of electric double layer is known Debye length.
R _p	Resistance of the material.

The Greek Symbols

ϵ	Dielectric constant of the medium (permittivity).
ϵ_0	Dielectric constant of vacuum (vacuum permittivity).
ϵ'	Relative dielectric constant.
K''	Dielectric loss index ($K'' = \epsilon'' / \epsilon_0$)
K*	Complex dielectric ($K^* = K' - iK''$)
Tan δ	Loss angle
Φ_s	Phase angle.
ρ_c	Charge density.
σ	Conductivity.



جمهورية العراق
وزارة التعليم العالي والبحث العلمي
جامعة النهرين / كلية العلوم
قسم الفيزياء

تحضير مادة الانورثايت من مواد محلية عراقية

رسالة

مقدمة الى كلية العلوم - جامعة النهرين
وهي جزء من متطلبات نيل درجة الماجستير في الفيزياء

من قبل

معمار عبدالعزيز كامل

بكلوريوس 2000 (جامعة النهرين)

بأشراف

د. فاضل عبد رسن

1427 هـ
2006 م

ربيع الاول
نيسان

بِسْمِ اللَّهِ الرَّحْمَنِ الرَّحِيمِ

﴿ رَبِّ أَوْزِعْنِي أَنْ أَشْكُرَ نِعْمَتَكَ الَّتِي أَنْعَمْتَ عَلَيَّ

وَعَلَى وَالِدِي وَأَنْ أَعْمَلَ صَالِحًا تَرْضَاهُ وَأُدْخِلْنِي

بِرَحْمَتِكَ فِي عِبَادِكَ الصَّالِحِينَ ﴾

صدق الله العظيم

﴿ النمل: 19 ﴾

الخلاصة

ان الدراسة تركزت حول استخدام كاؤولين دويخله العراقي وكاربونات الكالسيوم لتحضير مادة الانورثايت. ان خطوات الدراسة تبدأ من الغسل والمعاملة الكيميائية والتركيد للحصول على مسحوق ذو حجم حبيبي صغير جداً وذلك من خلال امرار المسحوق الناتج من التركيد خلال مرشح خاص ذو حجم حبيبي (اقل من 20 مايكروميتر) بعد هذه العملية تم تقسيم المسحوق الناتج الى قسمين (الكاؤولين) القسم الاول تم استخدامه بدون معاملة حرارية والثاني تم اجراء عملية الكلسنة عليه لدرجة حرارة 400 درجة مئوية. اما المادة المطلوبة الثانية في التحضير هي كاربونات الكالسيوم وهذه ايضا تقوم بامرارها من مرشح خاص الحجم الحبيبي له (اقل من 20 مايكروميتر).

الخطوة اللاحقة هي خلط مجاميع الكاؤولين وكاربونات الكالسيوم وبنسب وزنيه, كاؤولين: كاربونات الكالسيوم (70% : 30%, 75% : 25%, 80% : 20%, 85% : 15%) على التوالي. ان عملية الخلط تمت بطريقة الطحن الرطب بوجود كحول الايثانول, تبع ذلك عملية التجفيف والحرق لدرجات حرارية 1200 درجة مئوية لمدة 1 و2 و3 ساعة على التوالي و1300 درجة مئوية لمدة 1 ساعة ان الناتج من عملية الحرق اجريت له فحوص IR, XRD حيث اعطت النتائج ان افضل خلطه لانتاج الانورثايت كانت (80% / 20%, 85% / 15%) ولدرجة حرارة 1200 درجة مئوية لمدة 3 ساعات . تمت معاينة مادة الانورثايت المحضره باجراء التحليل الكيميائي ومطابقة المادة الناتجة مع النسب المطلوبه لمنحني التحول الطوري الثلاثي. لقد اعطى استخدام المواد المحليه العراقيه بعد المعالجه مطابقة لمكونات الاوكسيد في الانورثايت.

ان الاستنتاج هو تحقق تحضير الانورثايت من استخدام الكاؤولين العراقي بعد المعامله مع كاربونات الكالسيوم وبتركيز ومعالجه حرارية معينين.

Chapter One

Introduction

1.1 Introduction:

A ceramic material for modern high-temperature uses in which the natural cement occurs in large proportions is generally application unless it is very highly siliceous or argillaceous and is itself refractory.

The cement or bond produced by the burning process is usually of a very complex nature and is generally in the form of a glass composed of various silicates such as alumina-silicates, etc.; in stoneware and porcelain such a bond is essential [1].

Alumina-silicates is found in porcelain, stoneware, fired silica and in some clay bricks; these consist of crystals of mullite, quartz and other forms of silica, cemented together by a glassy mass composed of various complex silicates and alumina-silicates which sometimes include minerals such as wollastonite and anorthite. The whole mass is usually coloured by the iron compounds present. The granular matter may be either crystalline or amorphous and either coarse or fine [2].

Feldspars which are commonly used in the manufacture of glazes and in the preparation of vitrified bodies. Pegmatites, Aplites and Cornish Stone are natural rock formations which are rich in feldspars and are frequently used in place of the pure minerals. Feldspar is a constituent of pegmatite's, such as granite and other igneous rocks which are predominantly alkali-bearing; it may be present in amounts up to 60 per cent. Feldspar is also found in a reasonably pure state in Norway, Sweden, Russia and the United States, and it is readily purified from many rocks which contain it [3].

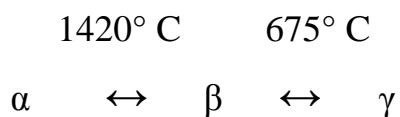
Feldspars are the most valuable fluxes used in the ceramic industries, both in bodies and glazes, particularly in the manufacture of fine earthenware, china ware, porcelain and stoneware. Orthoclase and albite are preferred, but anorthite is

sometimes used; for many purposes, feldspars can be replaced by the cheaper china stone. None of the commercial feldspars is quite pure and their selection requires great care. One essential is that the feldspar should melt at a temperature not exceeding 1260° C. to form a smooth, glossy, vitreous mass, free from any discolorations, such as iron [4].

1.2 The Calcium Ortho-Silicate Group:

Calcium-silicates are commonly-occurring minerals in refractory materials and slags, yet the relationships between them are not simple. A study of their crystal structures has explained many of the perplexing changes which take place when they are heated.

There are two chemical phases of orthosilicate of calcium, tricalcium silicate, $3\text{CaO} \cdot \text{SiO}_2$, and dicalcium silicate, $2\text{CaO} \cdot \text{SiO}_2$. Dicalcium is capable of existing in at least three modifications named α , β and γ phases. If lime and silica are mixed in the molecular proportions of 2:1 and heated to a sufficiently high temperature both α - and β -*dicalcium silicate*, which have similar properties, are formed. On cooling, however, these forms convert slowly to the γ -variety with a large increase in volume. The temperature stability ranges of the different forms are given as [5]



Tricalcium silicate which is formed by heating lime and silica in the correct, molecular proportions is stable under normal conditions, mixture can be converted to β -dicalcium silicate and lime by slowly cooling between 1250° C. and 1600° C. And at lower temperatures, in turn, changes into γ -dicalcium silicate. The relationship between γ - and β -dicalcium silicate depends upon the coordination of calcium with oxygen at low and high temperatures [6]. Under normal conditions,

calcium forms a silicate which has a similar structure to olivine, so calcium is in octahedral linkage with oxygen and the formula may be written as Ca_2SiO_4 ; its lattice constants are [7]

At high temperatures, however, calcium has a different co-ordination. The mineral *merwinite*, $\text{Ca}_3\text{Mg}(\text{SiO}_4)_2$, is considered by Bredig to have a similar structure to β -dicalcium silicate may not be a definite compound but a high-temperature isomorphous mixture of forsterite in the high-temperature form of Ca_2SiO_4 ; the forsterite component may act as a stabilizer.

Goldschmidt and Rait have suggested that merwinite is based on the perovskite structure where each calcium is surrounded by twelve oxygen atoms. Tricalcium silicate also exists in the, α , β and γ modifications but all three are similar in property and structure. The crystal structures of this mineral have not been established with certainty [5].

1.3 Feldspar:

Feldspars may be technically defined as alumina silicates of sodium, potassium, and calcium. Also, feldspars may be formed with other alkaline or alkaline-earth cations, but these rare minerals are of little interest to the ceramist.

A pure end-member of a feldspar series is seldom found, so that our commercial materials are mixtures containing potassium, sodium, and calcium feldspars in various proportions as solid solutions or as mixed crystals [6].

Feldspars are used in the fine ceramic industry as a flux to form a glassy phase in bodies, thus promoting vitrification and translucency. They are also used as a source of alkalis and alumina in glazes and glasses. Their value lies in their low cost and in the fact that they are one of the few sources of water-insoluble alkali compounds.

The first regular mining of feldspar [8] in the United States is believed to have taken place in Connecticut in the year 1825, for shipment to England.

However, small amounts may have been exported as early as 1744. The first feldspar mill was set up near Middletown, Connecticut, about 1850. This was a granite chaser mill pulled by oxen. The early American white ware potters imported Cornish stone until it was completely displaced by domestic feldspar at about the beginning of the nineteenth century [5].

1.3.1 Other Feldspars:

Few other rare feldspars and feldspar like minerals have been reported such as: Spodumene: $\text{Li} [\text{Al}, \text{Si}_2] \text{O}_6$, Petalite: $\text{Li}_2\text{O} \cdot \text{Al}_2\text{O}_3 \cdot 4\text{SiO}_2$, Celsian (isomorphism with orthoclase): $\text{Ba} [\text{Al}_2, \text{Si}_2] \text{O}_8$, Rubidium microcline: $\text{Rb} [\text{Al}, \text{Si}_3] \text{O}_8$, Pollucite: $4\text{CsAlSi}_2\text{O}_6 \cdot \text{H}_2\text{SiO}_3$, Strontium feldspar: $\text{Sr} [\text{Al}_2, \text{Si}_2] \text{O}_8$ (laboratory mineral), Beryl: $\text{Be} [\text{Al}, \text{Si}_2] \text{O}_6$ (approximate) [5].

The most common constituents of igneous rock formations are the feldspars. These important minerals are used extensively in the manufacture of porcelains. Feldspars are used in the fine ceramic industry as a flux to form a glassy phase in bodies [6].

There are two clearly – defined groups:-

(1) Based on orthoclase KAlSi_3O_8 , orthoclase was used in general as K – feldspar with monoclinic optical properties.

(2) Termed the plagioclase group, which are solid solution of albite, $\text{NaAlSi}_3\text{O}_8$, and anorthite, $\text{CaAl}_2\text{Si}_2\text{O}_8$; celsian $\text{BaAl}_2\text{Si}_2\text{O}_8$, which is not of common occurrence, is similar to orthoclase [9, 10].

The structure of all feldspars is based on framework of oxygen–silicon tetrahedrons sharing four corners, there is replacement of silicon by aluminum ions, however which results in charge–deficiencies, balanced by cat ions of K^+ , Na^+ , or Ca^{2+} entering the lattice. The relative ionic radii of these cat ions are 1.33 \AA , 0.98 \AA , and 1.06 \AA respectively, the structure varies with the cat ion.

The feldspar minerals with small Na^+ and Ca^{2+} are considered as a “collapsed “ structure and thus lose some symmetry to make them triclinic, on the other hand, the K^+ minerals are generally monoclinic [11, 5].

The important feldspars are classified in **Table (1.1)** which also gives their crystallographic details.

Crystal habit	Mineral	Composition	Space group	Crystallographic dimensions					
				a	b	c	α	β	γ
Monoclinic	Orthoclase	KAlSi_3O_8	C2/m	8.56 Å	12.99 Å	7.19 Å	90°	116°	90°
	Hyalophane	KAlSi_3O_8	”						
	Celsian	$\text{BaAl}_2\text{Si}_2\text{O}_8$	”	8.63	13.10	14.41	90°	116°	90°
	Microcline	KAlSi_3O_8	”	8.44	13.00	7.21	90° 65'	115° 50'	87° 70'
Triclinic	Albite (Ab)	$\text{NaAlSi}_3\text{O}_8$	CI	8.14	12.86	7.17	94°	116° 30'	89°
	Oligoclase	Ab_6An to Ab_3An	”						
	Andesine	Ab_3An to Ab An	”	8.14	12.86	7.17	93° 23'	116° 28'	89° 59'
	Labradorite	AbAn to AbAn_3	”						
	Bytownite	AbAn_3 to AbAn_6	”						
Anorthite (An)	$\text{CaAl}_2\text{Si}_2\text{O}_8$	”	8.21	12.95	14.16	93° 13'	115° 56'	91° 12'	

TABLE (1.1) the feldspar group [11]

1.4 Anorthite ($\text{CaAl}_2\text{Si}_2\text{O}_8$) :

Anorthite is the lime – rich end member of the plagioclase feldspar solid solution series. The natural mineral has triclinic symmetry and is composed of a frame work of (Si,Al) — O Tetrahedral with Ca^{+2} ions residing in the interstices [12]. Are an end member and one of the rarer members of the plagioclase series . The plagioclase series comprises minerals that range in chemical composition from pure $\text{NaAlSi}_3\text{O}_8$ (Albite) to pure $\text{CaAl}_2\text{Si}_2\text{O}_8$ (anorthite). Anorthite by definition must contain no more than 10% sodium and no less than 90% calcium in the sodium/calcium position in the crystal structure. The various plagioclases feldspars are identified from each other by gradations

in index of refraction and density in the absence of chemical analysis and optical measurements [13].

All plagioclase feldspars show a type of twinning that is named after albite. Albite Law twinning produces stacks of twin layers that are typically only fractions of millimeters to several millimeters thick. These twinned layers can be seen as striation like grooves on the surface of the crystal and unlike true striations these also appear on the cleavage surfaces. The Carlsbad Law twin produces what appears to be two intergrown crystals growing in opposite directions. Two different twin laws, the Mane Bach and Baveno laws, produce crystals with one prominent mirror plane and penetrate angles or notches into the crystal. Although twinned crystals are common, single crystals showing a perfect twin are rare and are often collected by twin fanciers. [14]

The crystallization behavior of anorthite from a melt of the same composition has been determined over the ranges of temperature between 1173° and 1273°K and between 1523° and 1773°K. The triclinic form is invariably observed as the crystallization product. The interface morphology is faceted under all conditions of growth, indicative of significant growth rate anisotropy, and growth takes place preferentially in the *c* direction. By combining the present crystallization data with viscosity data previously determined in this laboratory the approximate reduced growth rate versus under cooling relation has been constructed. The positive slope and positive curvature of this relation indicate that the fraction of preferred growth sites on the interface increases continuously with increasing under cooling over the full range investigated (between 52° and 652°C of under cooling) [15].

Although this observation suggests that growth takes place by a surface nucleation mechanism, the logarithm of growth rate times viscosity versus $1/T\Delta T$ does not exhibit the simple straight line of negative slope predicted by the standard models for surface nucleation growth but is characterized by negative slope and positive curvature.

This form is consistent with recent computer simulations of crystal growth in materials with large entropies of fusion. By combining the present kinetic data with results of the computer studies the heat of fusion of a northite is estimated as $2.8-4.5 \times 10^4$ cal mol [16].

The Color of Anorthite is usually white, gray or colorless but can be pale shades of other colors. Transparency crystals are translucent to opaque and only sometimes transparent.

Crystal Habits include blocky or tabular crystals. Rarely are free crystals seen but they have a nearly rectangular or square cross-section with slanted dome and pinacoid terminations. Twinning is almost universal in all plagioclases.

Crystals can be twinned according to the Albite, Carlsbad, Manebach and Baveno laws. Anorthite is usually found in contact metamorphic limestones and as a constituent in mafic igneous rocks as shown in figure (1.1) [17].

The cleavage is perfect in one and good in another direction forming nearly right angled prisms. And the fracture is conchoidal. Hardness is 6 - 6.5. And we saw that the specific Gravity is approximately 2.76 (average) [18].

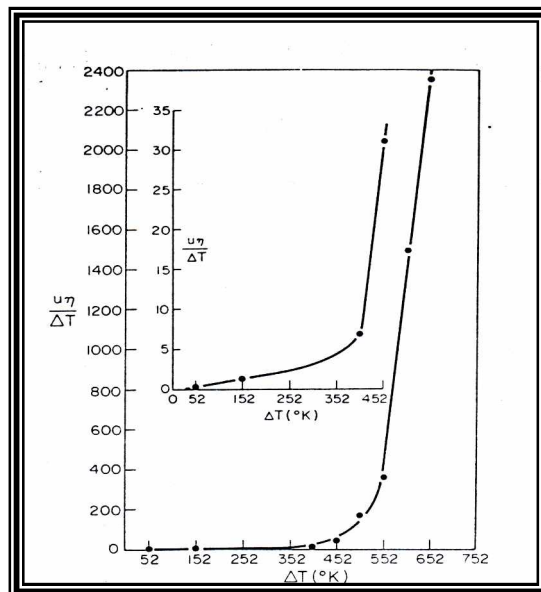


Figure (1.1) Reduced growth rate versus under cooling relation for Anorthite

1.5 Literature Review:

R. JAMHS KIRKPATRICK IN (1976) the kinetics of crystal growth from silicate melts was studied by using a microscope heating stage The rates of linear crystal growth have been measured law diopside and anorthite growing from their own melts by using a microscope heating stage [19].

M.CUKIE RAMAN IN (1993) studied the viscosity of liquid anorthite has been determined over the temperature ranges between 1450°-1620°C and 820°-950°C. The high-temperature data agree well with previous experimental data and with predictions of the Bottinga and Weill model. The overall log (viscosity) versus 1/T relation exhibits pronounced and rather continuous curvature. The viscosity of anorthite is higher at any given temperature and more strongly temperature dependent than that of the anorthite-rich lunar compositions. The room temperature density of glassy anorthite (2.64 gm cm^{-3}) and the thermal expansion coefficients of glassy and liquid anorthite have also been determined. The volume expansion coefficient, for the glass $\sim 1.8 \times 10^{-5} \text{ }^{\circ}\text{C}^{-1}$, and that for the liquid is $\sim 4.8 \times 10^{-5} \text{ }^{\circ}\text{C}^{-1}$. These values are used to relate the high-temperature flow data to the predictions of free volume theories [20].

YUICHI IN (1994) prepare anorthite by using NZ kaolin with calcite by this experiment. Preliminary ball-milled calcite was used for mixing with NZ kaolin since the particle-size distribution of calcite would affect the sintering process at low temperature. To prevent aggregation after drying, calcite was ball-milled with ethanol in high-alumina mills. The mean particle sizes of the calcite were 1.5, 2.5, 4.5, and 12 μm . Ball-milled calcite, and NZ kaolin were mixed in a composition such that the *dehydrated* kaolin: CaO ratio was 80:20 (wt %). This composition was 1.09CaO. Al₂O₃.2.36 SiO₂ in molar ratio, rich in CaO and SiO₂ in comparison with anorthite (CaO.Al₂O₃.2SiO₂). The crystalline phases were identified using XRD [21].

TAKASHI MURAKAMI in (1998) studied the formation of secondary minerals and its effect on anorthite dissolution. To examine the relationship between product secondary minerals and dissolution of anorthite, anorthite batch dissolution experiments were carried out. The dissolution experiments were done at 90, 150, and 210 °C for 3 to 355 days at pH 4.56 measured at 25 °C, which corresponds to 4.69, 4.97, and 5.40 at the respective experimental temperatures. A sequence of secondary minerals including bonhomie, "modified bonhomie," and kaolinite formed with increasing time. Modified bonhomie, probably a detestable phase, is basically similar to bonhomie in structure, but their stacking orders of the Al octahedral layers as well as morphologies and chemistries are different, and contains 3 to 30 mol% Si. Silicon may be present between the Al octahedral layers of modified bonhomie. The anorthite dissolution is incongruent under the above conditions and approximated by a two-stage process. The first is characterized by the formation of bonhomie, and the second by formation of modified bonhomie. The dissolution rate in the second stage is slower than the first by approximately one order of magnitude because of the saturation state with respect to anorthite. To estimate the effect of the formation of secondary minerals on the anorthite dissolution, Gibbs free energies of anorthite dissolution (AG) were calculated, assuming conditions without the formation of secondary minerals. The calculations reveal that the formation of secondary minerals decreases the AG values significantly, and thus we can predict that the dissolution rates of anorthite increase due to the influence of the secondary minerals on AG Modified bonhomie functions as a sink for Si, and thus accelerates the dissolution rate of anorthite.

The results indicate that the overall dissolution rate near equilibrium is affected by both the saturation with respect to a primary mineral and the formation of secondary minerals, but in the opposite sense [22].

R.A.GDULA IN (2004) studied the Production of anorthite ceramics suitable for dielectric applications are described. The ceramic processing used was simple and conventional, and the raw materials inexpensive. Air sintering at 1200°C gave fine grained bodies that are 98% of theoretical density. Their dielectric properties are Mil-1-10 grade L-6 with a dielectric constant of 6.2 at 1 Mc and room temperature. The linear thermal expansion coefficient was $48.2 \times 10^{-7}/^{\circ}\text{C}$ up to 700°C, a reasonable match to silicon semiconductor chips. These ceramics are also stable in hydrogen atmospheres [12].

Yunbin Guan and Laure A.Leshin (2005) studied the oxygen isotope distribution in anorthite – spinel – rish inclusion from the ningqiang carbonaceous chondrite. Intriguing oxygen isotopic data were observed for perovskite in the two Ningqiang ASIs. . Anorthite in Ningqiang ASIs was formed by reaction of melilite with gaseous components [23].

1.6 Process Parameters:

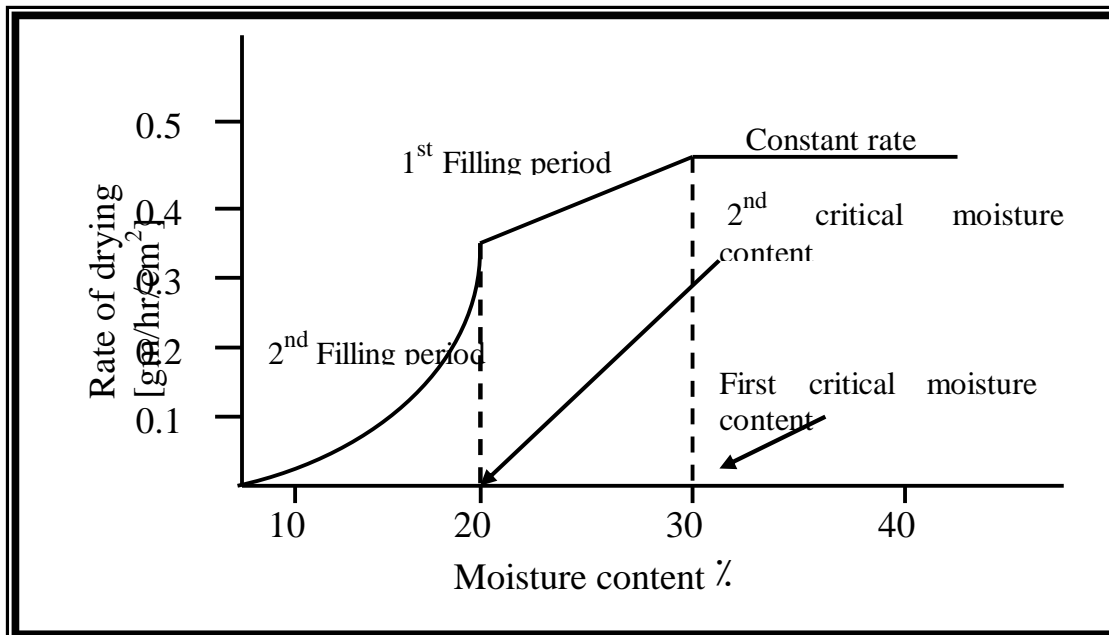
1.6.1 Mixing:

The mechanism of mixing is influenced by many factors such as the shape and size of the mixing vessel, the physical properties of the solid particle and the operating condition [24]. Mixing, an important operation in chemical process industries can be divided into five areas: – liquid–solid dispersion, gas–liquid dispersion, liquid–liquid dispersion, the blending of miscible liquids, and the production of fluid motion. Mixing performance is

evaluated by two criteria, the first is physical uniformity, i.e., a physical relationship required in terms of samples of uniformity in various parts of mixing vessel, the other criterion is based on mass transfer or chemical reaction. The elements of mixer design are the process design fluid mechanics of impellers, impeller power characteristics–relate impeller power, mechanical design shafts and drive assembly [25].

1.6.2 Drying:

Drying can be defined as the removal of water from a granular material by evaporation [26]. This process involves both the transfer of heat from the surrounding environment to the solid–water system and the simultaneous transfer of water vapor in the reverse direction [27]. Drying is accomplices by shrinkage, which tends to bring the particles so close together that attractive forces become so strong that water can no longer penetrate between them, the wetting and moderate drying, frequently tend to increase the plastic properties of clay mineral [28]. **Fig. (1–2)** represents the drying behavior expressed in terms of the drying rate versus the moisture content percentage [29].



On such curve three intervals can be distinguished, the first: – The constant rate intervals, during which the rate of evaporation is independent of moisture content. The second is the first filling–rate intervals, during which the rate of drying is very often a linear function of the moisture content, and the third is the second filling–rate intervals, with a curvilinear relation between rate of drying and moisture content. The constant–rate intervals and the first Falling–rate period ends are termed the first and second moisture content respectively [29].

1.6.3 Shrinkage:

Shrinkage on drying is profound concern to the structure clay products industry. Since clay minerals are responsible for shrinkage, the amounts percentage and their particles sizes determine the shrinkage potential; then, the amount of water present in the plastic clay is proportional to, but not equal to shrinkage.

Differential shrinkages set up stresses during drying that can cause warping and cracking of the sample. Variations in moisture content in the piece are largely responsible for shrinkage differences from one part of the body to another. Another unique feature of clays is increased in the strength on drying, the shear strength of clay bodies increases from the plastic strength to a maximum when all the absorbed water is removed.

During drying, large dimensional changes occur as **Fig. (1.3)** Most of the shrinkage occurs during the initial stages of drying as the inter particle water evaporates; the temperature and humidity are carefully controlled during drying to minimize stress, distortion, or cracking [30].

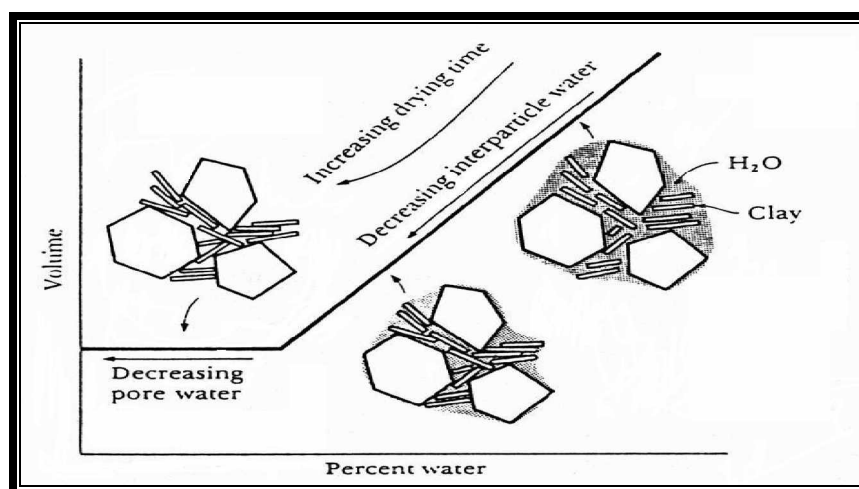


Figure (1.3) the change in the volume of ceramic body as the moisture is removed during drying [30].

Other factors also influence shrinkage, one of these is body thickness; non uniform shrinkage and defect formation are more pronounced in thick pieces than in thin ones. Water content of the formed body is also critical; the greater the water content, the more extensive the shrinkage. Consequently, the water content is ordinarily kept as low as possible.

Clay particle size also has an influence; shrinkage is enhanced as the particle size decrease, to minimize shrinkage, the size of the particle may be increased, or nonplastic material having relatively large particles may be added to the clay [31]. The value of linear firing shrinkage is, in the percent of shrinkage, due to variations in the size and shape of sample particles, linear shrinkage is approximately proportional to the inverse of the particle radius but is not greatly affected by sintering time [32]. Size distribution is important in practical system where shrinkage is to be minimized. Mostly large particles and sufficiently small particles to fill in the interstices will give a particle compact of highest green density. The linear firing shrinkage also varies with composition and tends to increase as fluxing components increase with the production of relatively more glassy material and less-high-temperature crystalline phases during the firing [31].

1.6.4 Sintering & Firing:

Sintering is common term for the process by which a slight (non-densification) or large (densification) reduction in pore volume occurs when heating a powder compact to temperatures close to melting [33]. The process has been recognized as a very complicated evolution of microstructure through the action of several different transport mechanisms.

The most general concept of sintering is the interface elimination process, i.e. the particles sinter together by atomic motions that act to eliminate the high surface

energy associated with an unsintered powder, therefore, during the process the total free energy of the system would decrease.

As important step in production of most ceramic products in firing, where the purpose is to agglomerate particles into mass by sintering, the sintering operation brings about several significant changes in ceramic product: The total surface area is reduced, the bulk volume is reduced, and the strength is increased. The dimensional changes which occur during firing are just as important as those which occur during drying; in fact, probably more so, because shrinkage take place in almost all aggregated materials during firing [34]. During firing, the rigidity and strength of ceramic increase firing or Sintering, cause additional shrinkage of the ceramic body as the pore size between the particles is reduced. We must control four features of the final sintered microstructure—grain size, pore size, pore shape, and amount of a glass.

During sintering, ion first diffuses along grain boundaries and surfaces to the points of contact between particles, providing bridging and concenection of the individual grains. Further grain boundary diffusion closes the pores and increases the density, while the pores become more rounded. Firing initial particle size and higher temperatures accelerated the rate of pore shrinkage, when the pores become so small that they no longer pin the grain boundary, grain growth occurs as **Fig. (1. 4)** [30].

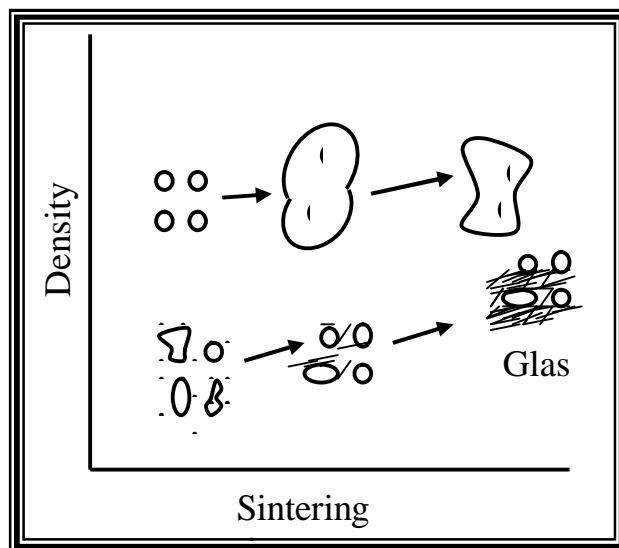


Figure (1. 4).During sintering, diffusion produces bridges between the particles and event causes the pores to be filling in [30] .

1.7 Analytical Technique:

1.7.1 X-Ray Powder Crystal Diffraction:

X-rays are electromagnetic waves whose wave lengths are in the neighborhood of 1°A , which is the same order of magnitude as the lattice constants of crystal and it are which makes X-rays useful in the analysis of crystal structures [35].

The energy of the X-ray photon is given by the Einstein relation ($E=h\nu$), where (h) is Planck's constant and (ν) is the frequency ($\nu=c/\lambda$); c is the velocity of light, λ is X-ray wave length.

When a monochromatic X-ray beam incident on the surface of a crystal, it is reflected. This reflection is well-defined by Bragg's law for constructive interference [36], which is

$$2d \sin \theta = n \lambda \text{ (Bragg's law)}$$

The angles determined by Bragg's law, for a given inter planner distance (d) and X-ray wave length (λ), are the only angles at which reflection takes place the

maximum frequency of the continuous spectrum ν_0 is related to the acceleration potential by [$eV = h\nu_0$], since the maximum energy of a photon can not exceed the kinetic energy of incident electron, the corresponding wave length λ_0 is then given by

$$\lambda_0 (\text{\AA}) = 12.3/V, \text{ where } V \text{ in kilovolts [37]}$$

1.7.2 Infrared Analysis:

Infrared spectroscopy can be described as the use of instrumentation in measuring a physical property of matter, and then relating the data to chemical composition. The instruments used are called infrared spectrophotometers and physical property measured is the ability of matter to absorb, transmitted, or reflect infrared radiation. The basic principle of infrared instruments is to measure the vibrational spectrum of a sample by passing infrared radiation through it, that wavelengths have been absorbed and what extent. Since the amount of energy absorbed is a function of the number of molecules present. The source of infrared may be a glowing filament or hot silicon carbide rod, both of which emit radiation over a wide range of frequency.

The infrared beam passes through a collimator to the specimen which should be in the form of a thin film. The transmitted rays then pass through a system of mirrors on the rock salt prism, which can be rotated, so vary the frequency of radiation received on the detector [38]. The details are as following:

1. Wave number between 3500 and 3700 cm^{-1} :-

Buswell and Dudenbostel [39] first showed that absorption in this range is due to hydroxyl group (O–H). In the structure of decahedral minerals, each pair of aluminum ions shares two hydroxyl groups, which are related by a center of

symmetry between the aluminum ions. Sarasota [40] through that the absorption frequency of (O–H) bonds depends on the degree of association of these groups. Miller [41] concluded that the bands at 3718 and 3677 cm^{-1} for kaolin are due to stretching vibrations of relatively unassociated (O–H) groups, i.e. due to hydroxyl groups nearly free of hydrogen bounding to the other atoms.

In general, the layer–silicate structural OH groups that are comparatively slightly show absorption of high frequencies of 3600 to 3700 cm^{-1} , where as the absorbed Water shows absorption at low frequencies 3400 cm^{-1} , and another band 1640 cm^{-1} corresponding to the deformation vibration of water [42].

2. Wave number between 1500 and 600 cm^{-1} .

The position and sharpness of the perpendicular vibration varied with physical state; thus in the spectra of kaolin of large crystal size, the node appears as a broad shoulder near (1080) cm^{-1} [42,43].

The band intensities and shift to higher frequencies in the spectra of smaller crystals until in very finely ground material the band is at 1109 cm^{-1} smaller but distinct shifts in frequency, together with sharpening and intensification of bands as particle size decreases [44].

1- The major these bands of kaolin Duekhla raw material (particle size <20 μm) are 3699.2, 3662.1 and 3652.9 cm^{-1} .

2- Washed kaolin Duekhla by hydrochloric acid affect the intensity of major bands was lowered and the band 3652.9 cm^{-1} was disappeared.

1.7.3 Dielectric Properties:

Dielectric Constant

The capacitance of the parallel plate capacitor, with distance (d) and cross – section area A, in vacuum [45, 46] is given by:

$$C_o = \epsilon_o(A / d) \quad \text{----- (1-1)}$$

Where ϵ_o is the vacuum permittivity, when a dielectric material replaces the vacuum between the parallel capacitors, then the capacitance is

$$C = \epsilon(A / d) \quad \text{----- (1-2)}$$

Where ϵ is the permittivity of the material, normally the ability of material to polarize and store electrical charge is described by relative permittivity (dielectric constant), ϵ' which may defined as the permittivity of the material to the vacuum permittivity

i.e.:

$$\epsilon' = \epsilon / \epsilon_o \quad \text{----- (1-3)}$$

By substitution of equation (1-2) in equation (1-3), the dielectric constant is given in the relation

$$\epsilon' = (1 / \epsilon_o)[(d / A)C] \quad \text{----- (1-4)}$$

Where C is the measured value for the charge capacitance of the material. The dielectric constant of ceramic samples is affected by changes in its composition, manufacturing technique and porosity as well as by testing factors including the effect of temperature and voltage frequency [47].

Dielectric loss Index

Firstly the above term is agreed upon internationally, while in the U.S.A., it is formally called the loss factor [48]. The dielectric loss index is defined as the magnitude of imaginary part of relative complex permittivity. The representations of the alternating electric field and dielectric displacement in complex notation [46, 2] are given by:

$$E = E_0 \exp. (i\omega t) \quad \text{----- (1-5)}$$

$$D_d = D_0 \exp.i (\omega t - \delta) \quad \text{----- (1-6)}$$

As the electric field (E) is caused to vary with time, E and D_d are no longer necessarily in phase, and for sinusoidal fields a complex dielectric constant K^* can be employed in this equation:-

$$D_d = \epsilon E \quad \text{----- (1-7)}$$

Then equation (1-7) become

$$D_d = K^* E \quad \text{----- (1-8)}$$

Where $K^* = k' - ik'' = \frac{\epsilon}{\epsilon_0} = 1 / \epsilon_0 (\epsilon' - i\epsilon'')$

Dividing equation (1-6) by (1-5) and then by simplification, one gets

$$\tan \delta = \frac{k''}{k'} = \frac{\epsilon''}{\epsilon'} \quad \text{----- (1-9)}$$

Where $\tan\delta$ is a loss tangent. This phase shift corresponds to time lag between an applied voltage and induced current, which cause loss current and energy dissipation in circuits which do not require charge carrier migration.

The loss index, in terms of electrical conductivity can be written as [49]

$$\sigma = \omega \epsilon'' = \omega \epsilon' \tan \delta \quad \text{----- (1-10)}$$

$$\text{Since } K'' = \frac{\epsilon''}{\epsilon_0}; K' = \frac{\epsilon'}{\epsilon_0} \quad \text{----- (1-11)}$$

$$\text{Its follows that } K'' = \frac{\epsilon''}{\epsilon_0} = \sigma / \omega \epsilon_0 \quad \text{----- (1-12)}$$

By substitution ($\sigma = 1/\rho$; $R_p = \rho \cdot (d_s / A)$).and by substitution, then

$$K'' = [(1/R_p \omega \epsilon_0) d_s / A] \quad \text{----- (1-13)}$$

Where R_p is the measured value for the material resistance [48]. A theoretically perfect insulator would throw current and voltage wave entirely out of phase, in which case the phase angle ϕ_s would be 90° , for actual insulator the phase angle is some what less than 90° . Energy losses in dielectrics result an Electronic polarization occurs easily even at frequencies as high as 10^{16} Hz. Since no rearrangement of atoms is necessary. The ion vibration and deformation losses become important in the infrared but are not a major concern for frequencies below about 10^{10} Hz. The far aspect the major factor affecting on the using of ceramic materials is the ion migration losses which tend to increase at low frequencies and as the temperature raised. However, materials that rely no molecular polarization are very sensitive to frequency, since entire atoms or groups of atoms must be rearranged [50].

1.7.4 Factors affecting on dielectric properties:

Frequency

1. The insulating material used for all rang of frequency from 50 HZ to $3E+10$ HZ and there are few materials will not effecting by loss index, dielectric constant for this rang like Polystyrene, Polyethylene and fused Silica. For this reason we must measure these characters at dielectric frequency for this dielectric or measure at different frequencies.
2. The change in these two characters with frequency comes from dielectric polarization in the material.
3. The d – c conductance in dielectric com from because the free electrons or ions will not effect directly on the dielectric constant and this made dissipation factor will change inversely with frequency and become infinite at zero frequency.

Temperature

1. The major electrical effect of temperature on an insulating material is to increase the relaxation frequencies of its polarization.
2. The temperature coefficient of dielectric constant at the lower frequencies would always be positive except for the fact that the temperature coefficients of the dielectric constant resulting from much atomic and electric polarization are negative.
3. The temperature coefficient of dielectric constant will then be negative at high frequency and positive as the relaxation frequency of the dipole or interfacial polarization is approached.

4. the temperature coefficient of loss index and dissipation factor may be either positive or negative depending on the relation of the measuring to the relaxation frequency

+ve for $f > \text{RF}$ and -ve for $f < \text{RF}$

5. Since the relaxation frequency of interfacial polarization is usually below 1HZ.

So the corresponding temperature coefficient of loss index and dissipation factor will be positive at all usual measuring frequencies.

6. Since the d – c conductance of a dielectric usually increases exponentially with decrease of the reciprocal of absolute temperature, the values of loss index and dissipation factor arising there from will increase in a similar manner and will produce a larger positive temperature coefficient [51].

Voltage

1. All dielectric polarization except interfacial are nearly independent of the existing potential gradient until such a value is reached that ionization occurs in the voids in the material or on its surfaces, or that breakdown occurs.
2. In the interfacial polarization the number of free ions may increase with voltage and change both the magnitude of the polarization and its relaxation frequency.
3. The d-c conductance is similarly affected.

Humidity

1. The major electrical effect of humidity on an insulating material is to increase greatly the magnitude of its interfacial polarization, thus increasing both its dielectric constant and loss index and also its d-c conductance.
2. These effects of humidity are caused by absorption of water into the volume of the material and by the formation of an ionized water film on its surface.

1.8 Raw Materials:

1.8.1 Kaolin:

The term kaolin is coming from the Chinese word kaoliang (meaning “high ridge “), from which the clay originally came [52]. The kaolin’s groups are koalinite, nacrite, dickite and halloysite. Their basic structure consists of oxygen atoms arranged to give alternate layers of tetrahedral holes and octahedral holes. Where these layers are filled with silicon in tetrahedral holes and aluminum in two-third of the octahedral ones we get the common mineral kaolinite, and more perfect and rarer minerals dickite and nacrite. The structure applies equally to all the members of kaolin group; the distribution feature in the way in which the units are stacked one upon into her [13]. In this study Kaolin Duekhla is used where chemical composition as shown in **table (1.2)**

SiO₂	52.35%	TiO₂	0.13%	SO₃	0.45%	Lo.I	12.54%
Al₂O₃	34.02%	CaO	1.2%	Na₂O	—		
Fe₂O₃	1.31%	MgO	1.11%	K₂O	—		

Table (1.2) chemical composition of Kaolin Duekhla [52]

1.8.2 Calcium Carbonate:

Properties: Crystals, white or grayish-white lumps, or granular powder; commercial material sometimes has a yellowish or brownish tint.

The *chief* calcium compounds in clays are (a) *calcite* (CaCO_3), which occurs as white or grey hexagonal crystals, with a hardness of 3 and a specific gravity of 2.71, or as amorphous grains; (b) *aragonite* (CaCO_3), which occurs as white, grey or greenish orthorhombic crystals, with a hardness of 3.5 - 4 and a specific gravity of 2.94, or as amorphous grains; calcium carbonate may be present in the form of chalk or other form of limestone and occasionally fragments of shells may be observed, and (c) various *calcium silicates and alumina-silicates* which include some feldspars, micas and other primary minerals or their alteration products. Residual clays derived from an igneous rock are more likely to contain such mineral impurities, for most of them are readily decomposed by weathering and water transportation. [53].

1.9 Aim of thesis:

This work aims to utilize the Kaolin clay of Duekhla in preparing calcium feldspar (**Anorthite**). The study of the effect of washing chemical treatment and sintering processes on the properties of the product is also included in the work. The work aims also to study the effects of mixing proportions in weight and thermal treatment on the dielectric properties of the resulting of calcium feldspar (**Anorthite**) product.

Chapter Two

Theoretical Part

2.1 Two components miscible system:

In such systems both the solid and liquid phases are homogeneous and the two components form solid or crystalline solutions [54]. A *solid solution* is where two crystalline substances merge their chemical entities, three groups are known:

(a) Where two crystalline materials of similar habit and lattice dimensions form a single crystal and such an example is the mineral dolomite which is a double carbonate of calcium and magnesium. The crystal habit and lattice of dolomite are not unlike those of the single carbonates, the only difference being that calcium and magnesium cations are both present in the lattice at the same time and are mutually interchangeable. The compound must not be confused with a mixture of the two components. Each part of the crystal is identical with all other parts [55]. The formula of dolomite should be written $(\text{Ca.Mg})\text{CO}_3$ and not expressed as a mixed carbonate. Ideally, this type of, crystalline solution will most readily occur when the interchangeable components or I ions are almost identical in size and charge. One of the best known naturally-occurring solid solutions is the plagioclase feldspars, where the interchange is $(\text{Na}^+ + \text{Si}^{4+})$ for $(\text{Ca}^{2+} + \text{Al}^{3+})$. A whole series of minerals is known between the two extremes [54]. Albite $\text{Na}_2[\text{Al}_2\text{Si}_6]\text{O}_{16}$ and anorthite $(\text{Ca Al}_2\text{Si}_2\text{O}_8)$. (b) Where foreign ions are contained in holes or defects within the crystal lattice of a mineral. Occasionally, two entirely different crystalline components form solid solutions, but usually in only a limited range of composition. Ionic substitution or replacement is impossible yet the foreign ion is held firmly within the lattice [56]. The formation of such complexes is most common when the crystalline structure is open.

This is the case in silicates which are based on the framework structure and it is here that solid solutions of this type are most common [55].

(c) Diffusion-type complexes. Many solid substances, when placed in contact with others, will slowly diffuse into the crystal lattice of the other component. This process is usually greatly accelerated at high temperatures and the extent of penetration may, in some uses, cause a breakdown in the crystal lattice. The complex formed may be random in structure with dissimilar ions occupying equivalent positions in the same lattice. Eventually, such diffusion-type complexes may lead to compound formation, but, in the initial stages, they have all the characteristics of true solid solutions [56]. Although they may be extremely variable in composition, solid solutions are not to be confused with glass. Unlike the latter, they have all the properties of true crystalline solids. On the other hand the term solid solution does not imply compound formation where the combination of components is in a fixed invariable stoichiometric ratio. The term infers that one solid phase is incorporated into another in such a way that a continuum or single phase is formed in which the properties of the parent substances are modified, but not completely changed. The main distinction between a solid solution and a compound is that the melting point in the former extends over a range of temperature whilst in the latter it is usually sharp. There are, however, exceptions to this rule, for some well-defined compounds are known which decompose in the solid state and so have an extended melting range [5]. The simplest equilibrium diagram for components with a complete range of solid and liquid solution is illustrated in **Fig.(2.1)** There is two phase boundary lines; the upper of which is known as the liquids and represents the maximum temperature at which solid phase can exist at all compositions; the lower curve or solids indicates the minimum temperature at which liquid can form in any particular mixture.

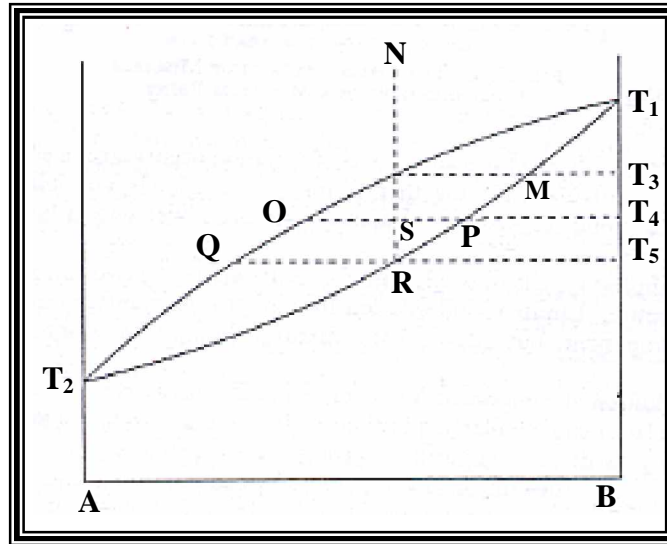


Fig. (2.1). the phase diagram of a binary mixture where the components are completely miscible in both the liquid and solid form [54]

The addition of component A (of lower melting point) to component B depresses its melting point, although amounts of B increase the melting temperature of A [54]. The region between the two phase boundary lines is known as the field of heterogeneous melting where liquid and solid phase can exist together. The extreme ends of the horizontal lines, known as *tie lines*, drawn across this region represent the composition of the liquid and solid phases which exist in equilibrium with each other at particular temperatures [5]. The phases which form on cooling are clearly indicated by a mixture of composition N which, when cooled from a temperature above the liquids line, has a single uniform phase until the temperature T_a is reached. Crystallization commences, but the solid phase first formed has a composition represented by the point M, i.e. richer in the component of higher melting point than is the initial mixture. At this point only two phases are present hence the system is invariant and the temperature can be progressively lowered. As the cooling continues, the composition of the liquid phase changes (due to crystallization of an excess of component B), and follows the path of the liquids

curve. At temperature T_4 for example the liquid has the composition of the point O. The solid which is in equilibrium with this liquid has the composition given by the point P, the point of intersection of a horizontal line through O and the solids phase boundary curve. Hence, not only does the liquid phase change in composition as the temperature is lowered, but so does the solid being crystallized. Ideally, if the rate of cooling were sufficiently slow, the solid phase formed would constantly be re-dissolved and re-crystallized with an ever-changing composition. This cooling process would continue with more solid being formed of a progressively increasing concentration of component A until the temperature T_5 was reached. Here liquid of composition Q is in equilibrium with solid R and as R is along the *tsopleth* (line of constant composition) of N, all liquid must disappear and only a solid solution of uniform composition will be present. The relative amounts of liquid and solid phase at any stage of the crystallization are given by applying the 'lever principle' about the point of initial composition.

At T_4 for example, liquid O is in equilibrium with solid P, and the relative amounts of each are expressed as [2].

$$\frac{\text{Amount of liquid O}}{\text{Amount of solid P}} = \frac{\text{PS}}{\text{SO}}$$

Thus at the temperature T_5 the amount of liquid of composition Q will be infinitesimal. Systems of two completely miscible components in both the liquid and solid states are common in both rock-forming minerals and in slag compositions. In general, such mixtures do not cool sufficiently slowly to allow equilibrium to be attained at all temperatures. In some igneous rocks there is evidence that, although cooling may have extended over a geological age, there has been insufficient time for the resolution and solid diffusion reactions to proceed to completion and form homogeneous crystals. Many minerals which occur in eruptive rocks exhibit characteristic *zoning or fractional crystallization*

and this phenomenon is even more common in the typical silicate minerals found in slag [57].

The formation of zoned structures is clearly demonstrated by considering the cooling of a mixture of composition N **Fig. (2.1)**, but under more rapid non-equilibrium conditions. Once again crystallization begins at a temperature T_3 and the composition of the first solid phase to appear is represented by the point M. The liquid phase becomes deficient in component B and its composition follows the path of the liquid's curve. If conditions were ideally those of equilibrium cooling, the solid phase would be constantly changing in composition due to resolution and re-crystallization or to solid diffusion, but, under practical conditions, these processes do not proceed rapidly enough and crystallization of material of ever-changing composition continues with the original deposits acting as seeds for later crystallization. This process continues until all the liquid disappears with the result that the final solid consists of zones of material, the centre core of which is comparatively rich in component B but with the composition changing and being more enriched in A towards the outer edges. The overall composition is equivalent to the original composition of the liquid mixture N. Zoning of this type is a typical feature of the plagioclase feldspars where Albite ($\text{Na}_2\text{O}.\text{Al}_2\text{O}_3.6\text{SiO}_2$) and anorthite ($\text{CaO}.\text{Al}_2\text{O}_3.2\text{SiO}_2$) are the extreme end members of a solid solution series. It is also found in the olivine, pyroxene and mellitus series. In every case the 'core' of zoned crystals is richer in the component of higher melting point [5]. The system illustrated in **Fig. (2.1)** is the simple case of two components which are completely miscible in the solid and liquid states. Other cases are known where a maximum or minimum point occurs in the diagram as shown in **Fig. (2.2)** and **(2.3)**. These maxima or minima are of interest because they are examples of invariant points where apparently the Phase Rule does not so predict. At the points M in both diagrams, only two phases can

co-exist, namely a homogeneous liquid phase and a solid phase of identical composition with complete miscibility of the components. Hence, with $P = 2$ and $F = 1$, the points are theoretically invariant [56].

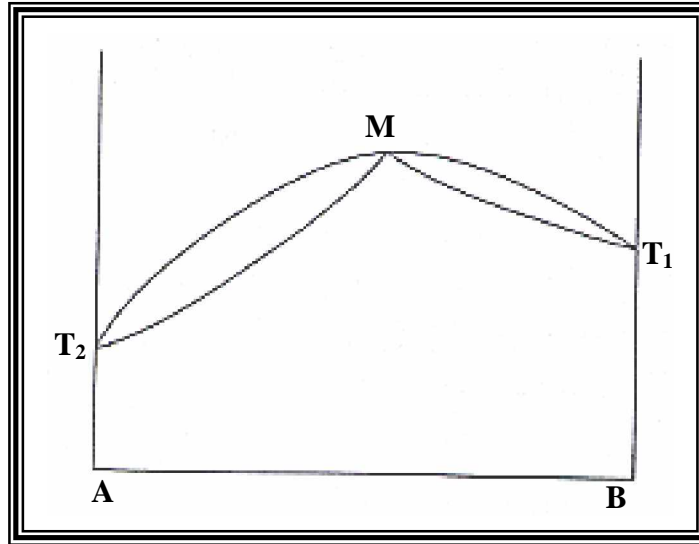


Fig. (2.2) the phase diagram of miscible components with a maximum point [57]

A concise explanation of this apparent anomaly is outside the scope of this volume - it arises as a result of an over-simplification of the Phase equation. Terms which appear in the original form cancel out in the vast majority of systems, but in this one case they have to be considered and contribute to the equation to make the maximum and minimum points invariant. Examples of a maximum-point diagram **Fig.(2.2)** are not common in ceramic systems, but they are the usual form of constant melting or boiling point systems, such as' alcohol and water. There are, however, some important mineral systems with a minimum point and the iron-calcium Monticellite $2(\text{CaO}, \text{FeO}) \text{SiO}_2$ is an example [57].

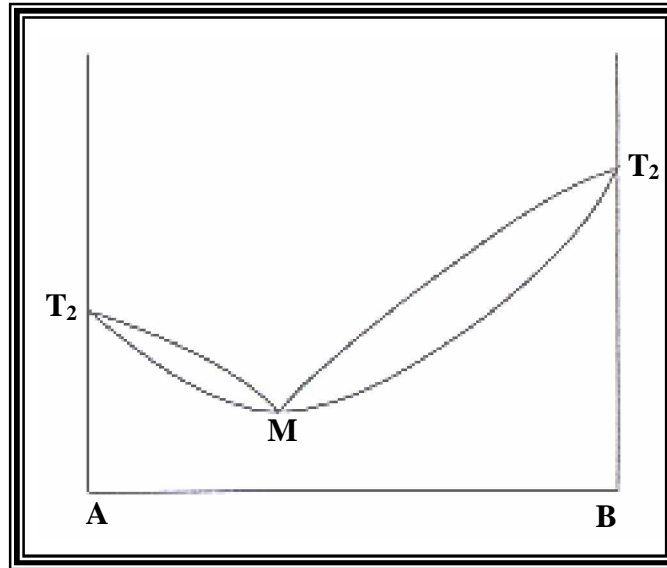


Fig. (2.3). the phase diagram of miscible components with a minimum point [57]

Partial miscibility in the solid state is of common occurrence in silicate systems. Many components will mix together to form a completely miscible liquid but a homogeneous, solid, crystalline solution is produced over only a limited range of compositions.

The simplest type is illustrated in **Fig. (2.4)** where the two components form a eutectic mixture. Limited solid solution formation is encountered in mixtures rich in either component, but intermediate mixtures do not form a homogeneous solid phase.

The addition of component A to component B causes a reduction in the melting point of the latter and, similarly, additions of B to A also produce a lowering. When a melt of any particular composition is cooled, crystallization will begin at the temperature of the liquids line in that region. The composition of the first solid phase to form is given by drawing a horizontal tie-line to cut the solids line.

The composition of the liquid phase follows the phase boundary line and, ideally, the solid solution changes in composition progressively. This process will

continue until all liquid disappears when one solid homogeneous phase will be the result or until the liquid reaches the composition of the eutectic mixture E [33].

At this point liquid can be in equilibrium with two solid solutions of composition M and N. True invariant conditions exist and the two solid phases are distinctly separate. Any mixture with a composition between the points M and N will solidify to give two separate crystalline solutions. Mixtures richer in component A than the point M or richer in B than is mixture N will finally crystallize as one homogeneous solid solution phase, provided equilibrium cooling has taken place. The composition of this single phase will be that of the original mixture.

Solid solutions may also be associated with both stable and incongruent compound formation. The establishment of the amount of solid solution in silicate systems is difficult and it is only in recent years that exhaustive studies using specialized techniques have established their existence. [57, 5]

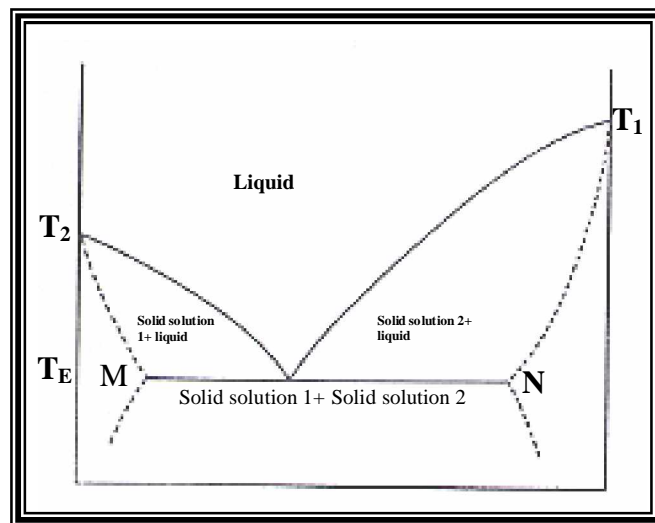


Fig. (2.4). the phase diagram of miscible components with partial solid solution [33]

2.2 Polymorphous changes in solid solution:

The transformation of a pure mineral into a polymorphic variety invariably takes place at a definite temperature although such changes are sometimes very sluggish. When solid solution occurs, however, an inversion-interval may replace the invariant point and the change or changes take place at temperatures removed from those in the pure material. Miscibility in the solid state is most likely when the components are similar in crystalline form. When polymorphic changes in crystal structure take place in one component of such a mixture, the ratio of the two components which can take part in the high temperature solid solution will probably be different from that in the original mixture. Furthermore, the formation of solid solutions usually results in an alteration of the temperature of inversion in a comparable way to the change in the melting or boiling point produced by mixing components. Solid phase relationships in the region of polymorphic changes are complex but can be represented by characteristic equilibrium diagrams. Polymorphic inversions in systems with solid solution are commonly found in silicate mixtures, but the importance of these changes and the way in which they are influenced by other components has only been recognized. The invariable result of introducing a component capable of forming solid solutions with a polymorphic material is to alter the temperature at which inversions take place. As in the case of the melting of a binary solid solution, a heterogeneous field is present, bounded by two phase-boundary lines. **Fig. (2.7)** represents the transformation of a high to a low form in the presence of varying amounts of the second miscible component, whilst the lower phase-boundary curve indicates the variation in the low to high transformation with the degree of solid solution [5].

At any one particular temperature, therefore, a solid solution of the high temperature modification of an inverting mineral can be in equilibrium with a solid solution of the low temperature form. The inversion effect thus takes place over a temperature interval and not at one specific point.

There are two well-established cases covered by Konowalow Rules which state if the low temperature or α -phase of the inverting material contains *less* of the additional miscible component than the high or β -form, the inversion temperature of the resulting solid solution will be *lower* than that of the pure mineral. Conversely, if the high or β -variety is *less rich* in the other component than the low form, the inversion temperature in the solid solution will be *raised* with respect to that of the pure mineral [44]. These two cases are shown in **Fig. (2.8)**

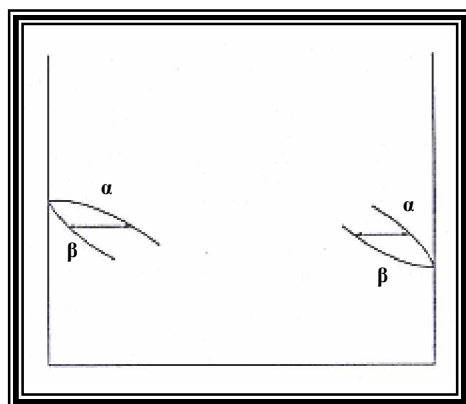


Fig. (2.5) the effect of polymorphic changes on the phase relationships in a binary solid solution [44]

2.3 Binary Systems in Ceramic Materials:

There are many binary systems of importance to ceramists, and almost all the phase equilibrium conditions described previously are to be found.

The American Ceramic Soc. Inc., publish at frequent intervals up-to-date information on phase equilibrium diagrams of importance in ceramic studies [49].

The *alumina /silica* diagram shown in **Fig. (2.9)** is perhaps the most commonly encountered binary system. Seger, in 1893, was the first to attempt its construction

by noting the temperature at which a liquid phase appeared in mixtures of different composition. The system in more detail and deduced a phase diagram in which the salient features included a eutectic point at a temperature of 1545° C [58]. At a composition of 5.5 % alumina, 94.5 % silica. A paratactic point at 1810° C. suggested that a compound was formed which was not stable to its melting point. This is the well-known mineral, mullite ($3\text{Al}_2\text{O}_3 \cdot 2\text{SiO}_2$) which is produced by heating almost all alumina-silicate mixtures and which at 1810° C was thought to dissociate into corundum ($\alpha\text{-Al}_2\text{O}_3$) and a liquid phase.

Since the earlier work was published, several authors have studied sections of the diagram in great detail. It has been suggested that limited solid solution exists and that compounds other than mullite are stable in the solids region [59]. And mullite is in fact a congruently melting compound - but only just, the new phase diagram is shown in Fig. (2.9).

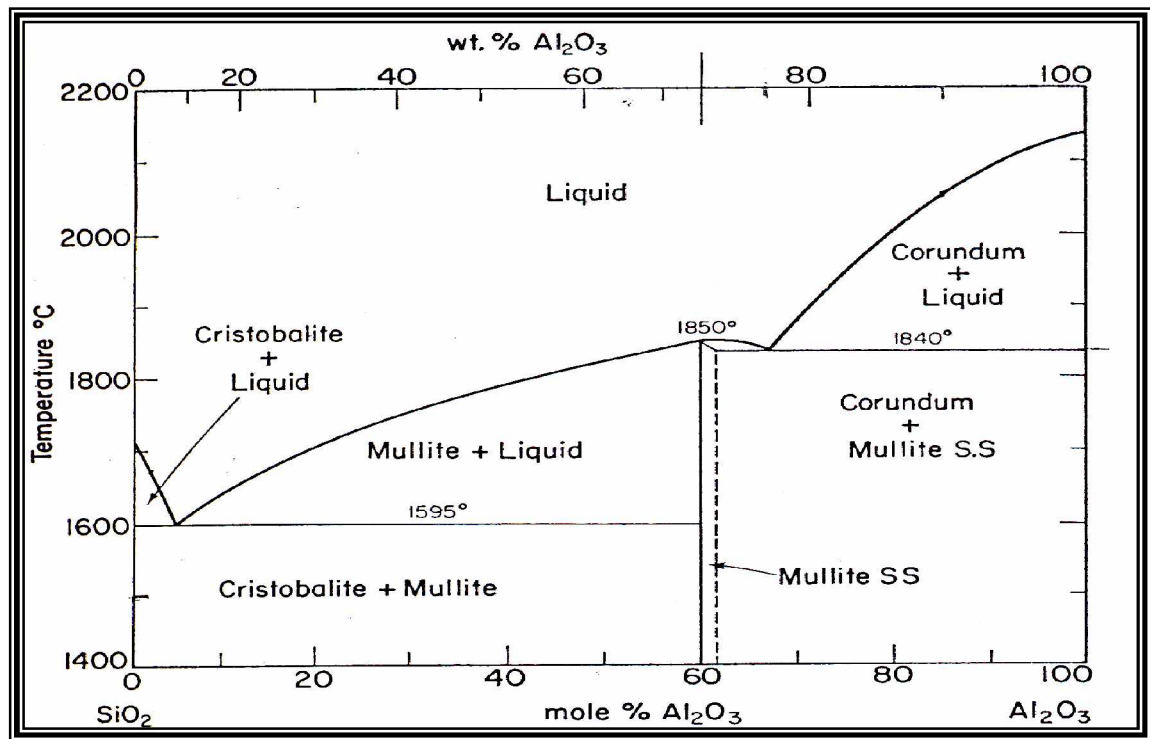


Fig. (2.6). The alumina / silica phase diagram [58]

The inter-relationship of the alumina-silicate minerals, kyanite, andalusite, sillimanite and mullite has been established as the result of the work of Newton and Haskell and DeVries. They have studied the pressure/temperature relationship up to 50kbars pressure and shown that whereas sillimanite is the favoured phase at high temperatures, kyanite is stable at higher pressures; andalusite has a limited stability range but mullite will form at equilibrium at normal pressures, from all other types [60].

The *lime-silica* system has been examined in detail by Rankin and Wright and modified by Rex [61]. There are three eutectic points as follows:

1. At a temperature of 1436° C. a eutectic mixture consisting of Tridymite and Pseudo-Wollastonite $2\text{CaO}.\text{SiO}_2$ is formed.
2. At 1460° C. a eutectic containing 53 per cent of lime and 47 per cent of silica consisting of pseudo-wollastonite and $3\text{CaO}.\text{SiO}_2$ is formed.
3. At 2065° C. a eutectic containing 67.5 per cent of lime and 32.5 per cent of silica and consisting of calcium Orthosilicate and lime is formed.

Four definite binary compounds are shown in the equilibrium diagram **Fig.(2.10)**, namely, calcium Orthosilicate ($2\text{CaO}.\text{SiO}_2$) which melts at 2130°C, calcium metasilicate ($\text{CaO}.\text{SiO}_2$) which melts at 1544° C; a compound with the formula $3\text{CaO}.\text{SiO}_2$, which melts incongruently at 1464°C; and Tricalcium silicate, $3\text{CaO}.\text{SiO}_2$, which dissociates into CaO and $2\text{CaO}.\text{SiO}_2$ at 1900 °C. Which is below the eutectic temperature (2065° C).

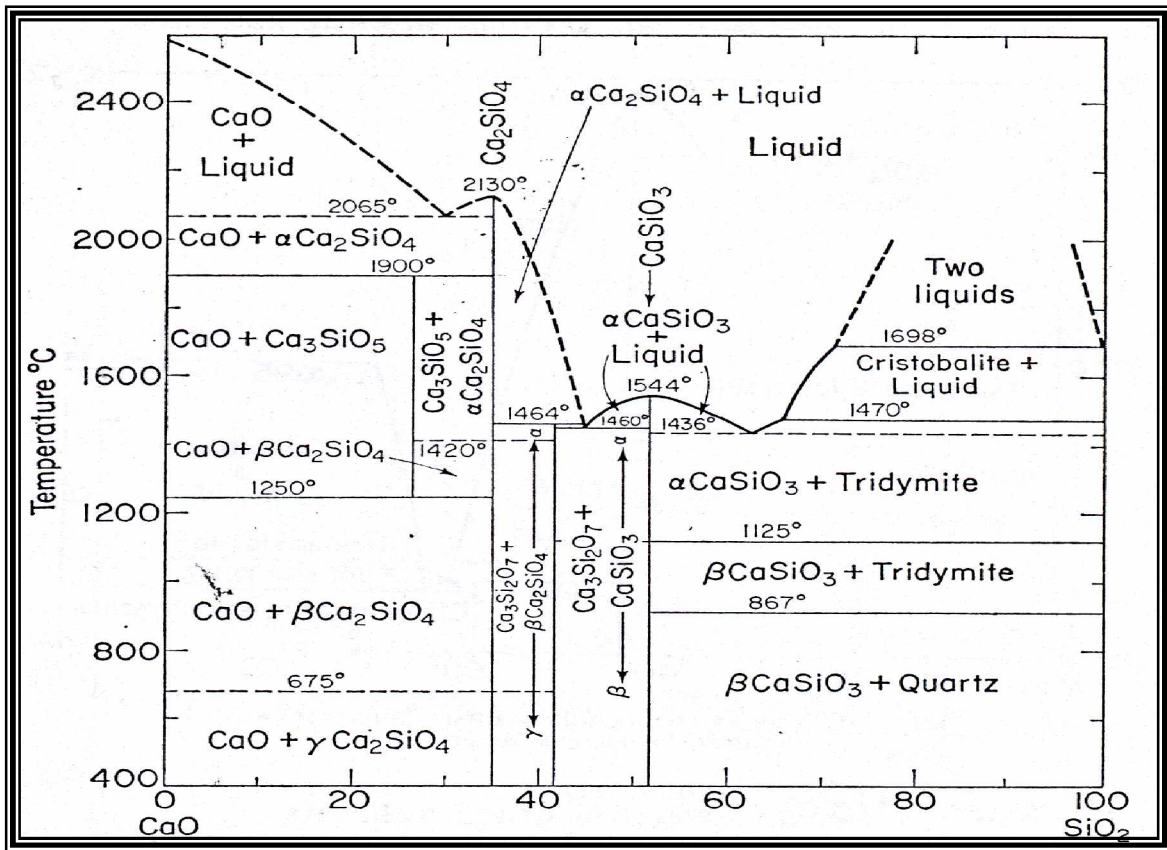


Fig. (2.10). the equilibrium phase diagram of CaO – SiO₂ [62]

Calcium Orthosilicate (Ca₂SiO₄) exists in three forms:

α Stable above 1410° C — monoclinic; specific gravity 3.27; hardness, 5 - 6. β Stable 1410° C - 675° C — orthorhombic; specific gravity 3.28. γ Stable below 675° C — monoclinic; specific gravity 2.97.

Calcium metasilicate (wollastonite) (CaSiO₃) exists in two forms:

α Stable between 1125° C. and the melting-point (1540° C). β Stable up to 1125° C.

In the *magnesia-silica* system examined by Rex [62] Fig.(2.11), there are two compounds (a) Clinoenstatite MgSiO₃ (incongruent, melting point 1557° C.) and (b) Forsterite Mg₂SiO₄ (melting point 1890° C). This is a particularly difficult system to investigate as the products are so viscous, even at high temperatures, that there is always uncertainty as to whether equilibrium has been reached.

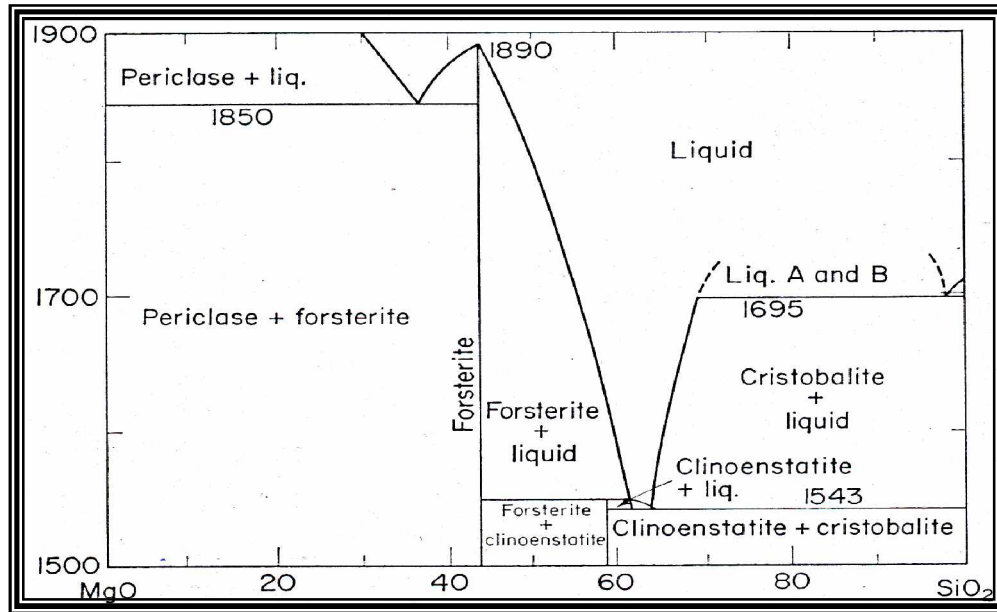


Fig. (2.11). the magnesia / silica phase diagram [62]

The phase diagrams of divalent oxides with silica show interesting and similar features in the important silica-rich region. A close correlation with the size of the cation is observed if the range of immiscible liquids and the composition of the first eutectic are compared. This is illustrated by the data in **(Table 1)**.

Oxide	Cation Size $^{\circ}A$	Immiscible Liquids Rang	SiO ₂ -rich eutectic	
		SiO ₂ molar rang	Molar %SiO ₂	Temp. $^{\circ}C$
BaO	1.35	—	73	1380
SrO	1.13	80-97	67	1360
CaO	0.90	72-97	63	1440
MgO	0.65	59-97	45	1550
PbO	1.20	40-97	29	728
MnO	0.80	52-97	56	1200
FeO	0.76	62-97	38	1180
ZnO	0.74	66-97	52	1432
CoO	0.74	48-97	39	1381
NiO	0.72	57-97	41	1650

Table (2.1). Some important features of divalent oxide /silica system [63]

It is of interest to note that with the exception of barium oxide, all alkaline earth oxide-silica systems have a range in the silica-rich part of the diagram where the two components form immiscible liquids. This is of importance in basic open

hearth practice, where silica bricks are used as roof bricks. The dusts rich in free lime are not exceptionally corrosive if the silica is of high purity because there is little tendency to mix. Should a third component, such as alumina, be present, even in small amounts, this desirable feature is destroyed and complete homogeneity in the liquid phase develops.

All the divalent oxide/silica systems contain a great complexity of compounds and eutectics, but it is also of interest to observe that oxides of elements of large cationic size (e.g. Ba) have the greatest complexity whilst the smaller ones (e.g. Mg) are relatively simple. The beryllium oxide/silica system where the Cation (Be^{2+}) is extremely small (0.31 Å) has only a single eutectic in the liquid us range at 1670°C. And with 94 % molar concentration of SiO_2 . A compound ($2\text{BeO} \cdot \text{SiO}_2$) forms but only in the solid phase; it dissociates into the component oxides at 1560°C well below the eutectic point. The *iron oxide-silica systems* are complicated by the existence of three iron oxides and by the comparative ease with which the red ferric and the black magnetic oxide can be reduced to form the dark ferrous oxide. At temperatures in excess of about 1000°C however, all forms convert more or less readily into *Wustite*, FeO, and Rex [63] have deduced the relationships between this component and silica as shown in Fig.(2.12).

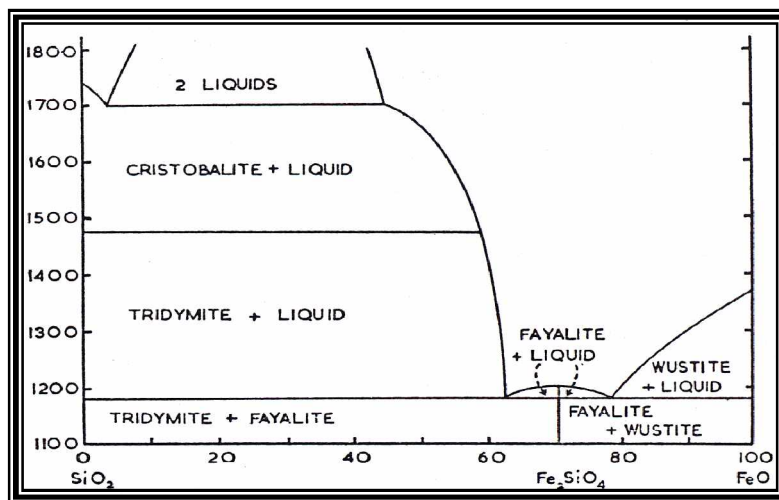


Fig. (2.9). the iron oxide / silica phase diagram [63]

One compound, *fayalite*, Fe_2SiO_4 , has been found and there are eutectic points at 1183°C and 1181°C containing 62 % and 77 % FeO respectively. Two immiscible liquid phases form in the silica-rich region in a similar way to alkaline earth-silica and the phase diagram of soda/silica is in **Fig. (2.13)**.

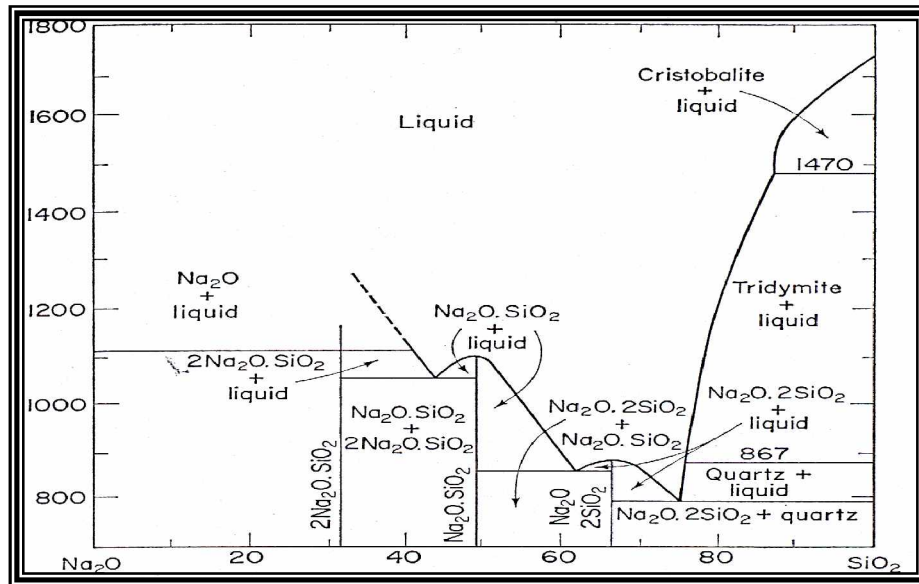


Fig. (2.10). the sodium oxide / silica phase diagram [64]

The full diagram is probably even more complicated [64]. Have proved that an incongruently melting compound $\text{Na}_6\text{Si}_8\text{O}_{19}$ exists in the region of the 799°C eutectic. Much interesting information can be derived from a comparison of the various binary systems with silica as one component. The amount of liquid formed as the temperature is raised when a small amount of impurity is present in silica may be predicted. If (1 %) molar concentration of the various oxides is mixed with pure silica, a liquid will first form at the appropriate eutectic point and its amount is given by applying the lever principle around the composition point. The amount of liquid at all temperatures above the eutectic may be similarly assessed until the liquids line is reached, when no solid matter remains **Fig.(2.14)** shows the amount of liquid forming as the temperature is rays several (1%) oxide-silica mixtures.

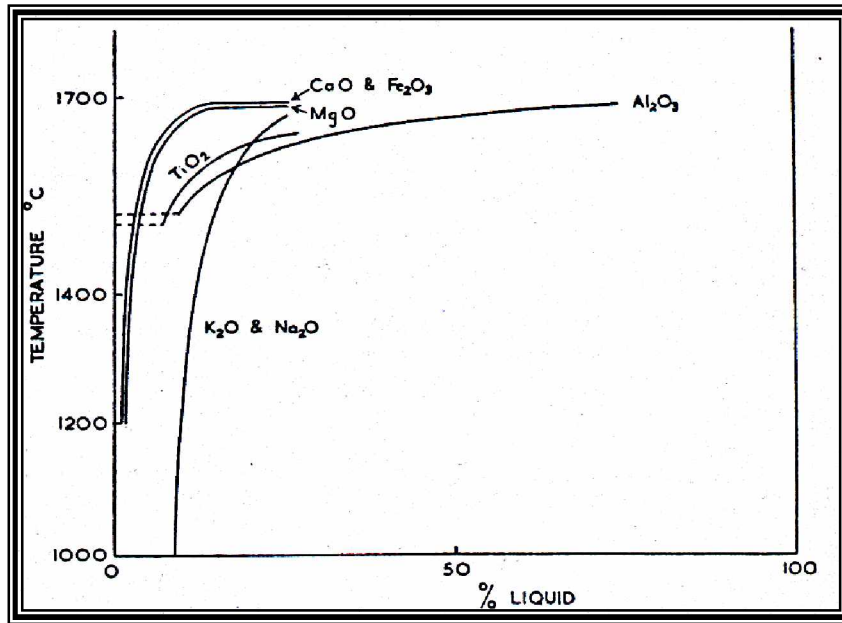


Fig. (2.11). the amount of liquid formed with mixtures of silica with (1%) of various oxides at different temperatures [64]

It is significant that although with alumina, liquid does not form until 1545°C , the amount present at 1650°C is in excess of that in the sodium oxide-silica mixture. For this reason, alumina is an undesirable impurity in the raw materials for the manufacture of silica bricks. The lime-alumina system includes various calcium aluminates which are much more fusible than either lime or alumina. Free lime and alumina begin to react at about 800°C and equilibrium, completely in the solid state, is reached rapidly at 1300°C . No liquid forms in the system below 1400°C . There are many compounds known between the two components -some are congruently so that there are several eutectics. There are others which melt incongruently. The phase diagram shown in Fig. (2.15) [65].

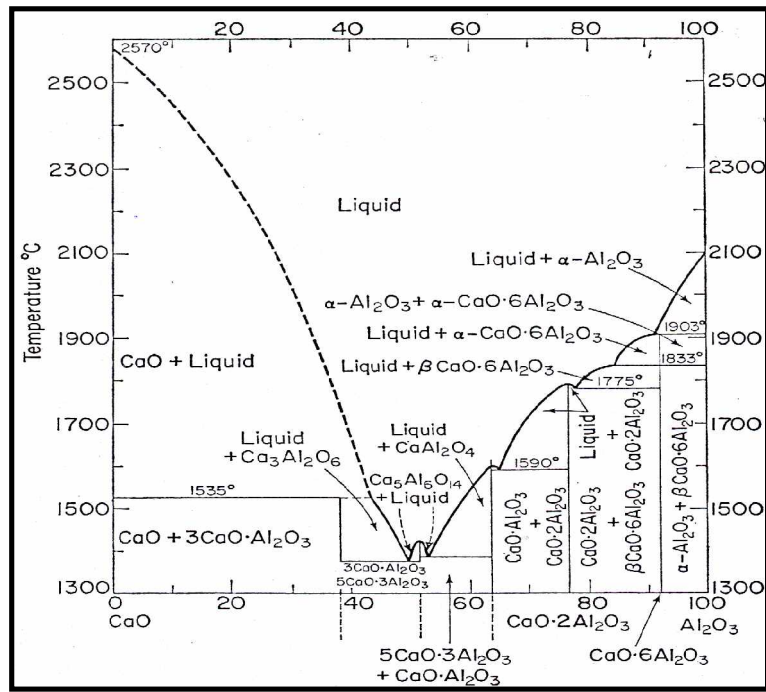


Fig (2.12). The partial phase diagram of the lime / alumina system [65]

The *magnesia-alumina system* [66] yields one compound - spinal (MgOAl_2O_3), with melting point of 2135°C and the three eutectics shown in (Table.2).

Constituents	Magnesia %	Alumina %	Melting point
Spinal / magnesia	45	55	2030°C
Spinal / α - alumina	98	2	$1925 \pm 40^\circ\text{C}$
Spinal / β - alumina	92	8	$1925 \pm 40^\circ\text{C}$

Table (2.2) spinal (MgOAl_2O_3), with melting point of 2135°C and the three eutectics

Spinal forms a series of solid solutions with α -alumina. The phase diagram is shown in Fig. (2.16). the *lime-magnesia system* [67] contains one eutectic composed of 67% of lime and 33 % of magnesia; it melts at 2300°C . Trojer and Konopicky [68] have suggested that partial solid solution of magnesia in lime takes place, and this view has been confirmed by Doman [69] whose diagram is shown in Fig.(2.17).

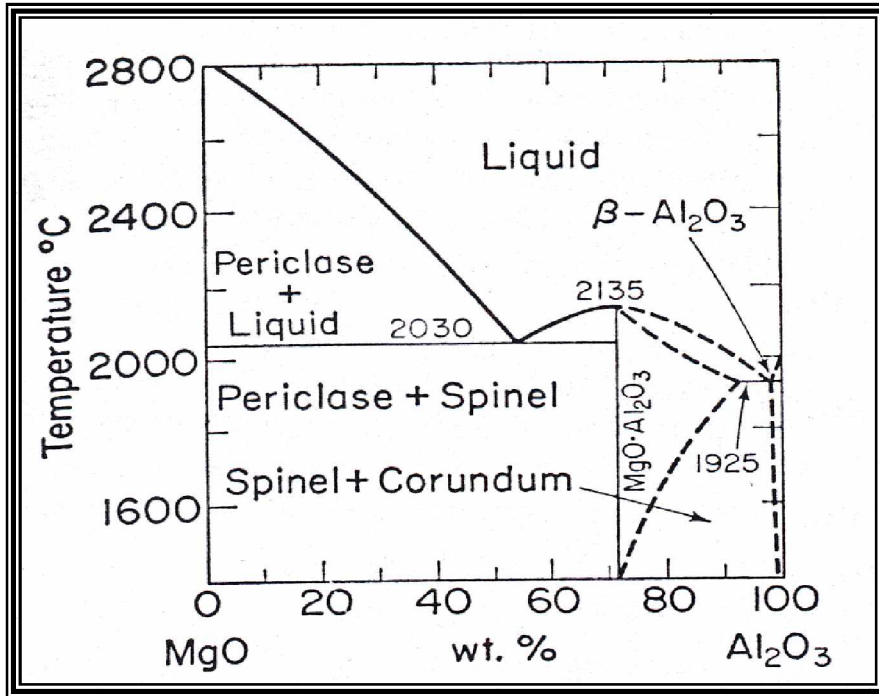


Fig. (2.16). The partial phase diagram of the magnesia alumina system [67]

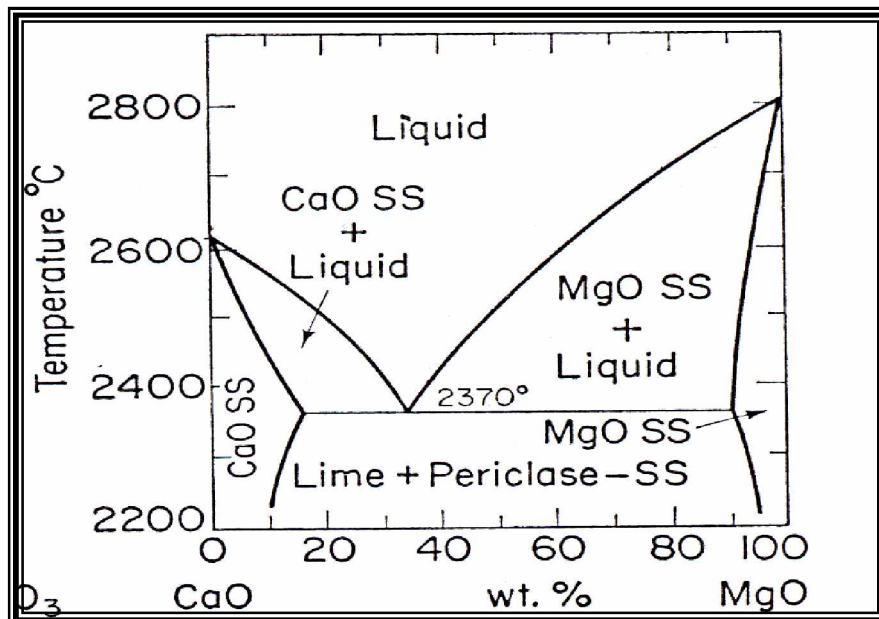


Fig. (2.17). Temperature / concentration diagram of the lime magnesia system [69]

The *iron oxide-alumina* system like the corresponding silica system is complicated by the existence of three iron oxides. So far as the ferrous oxide-alumina system is concerned the chief compound is *Hercynite* (FeOAl_2O_3). The *iron oxide-alumina* system is complicated like the corresponding ones containing alumina and silica respectively. When lime and iron oxide are heated together ferrites may be formed. The two chief compounds are calcium met ferrite (CaOFe_2O_3), which melts at 1215°C , and dissociates at the same temperature, forming long, black, needle-shaped crystals, whilst the second compound calcium Orthoferrite ($2\text{CaOFe}_2\text{O}_3$) melts at 1436°C . And almost immediately dissociates, forming black crystals having a yellowish-brown tinge by reflected light. The eutectic contains 8 % of lime and 92 % of ferric oxide; it melts at 1203°C . The phase diagram, due to Rex [5] is shown in **Fig. (2.18B)**.

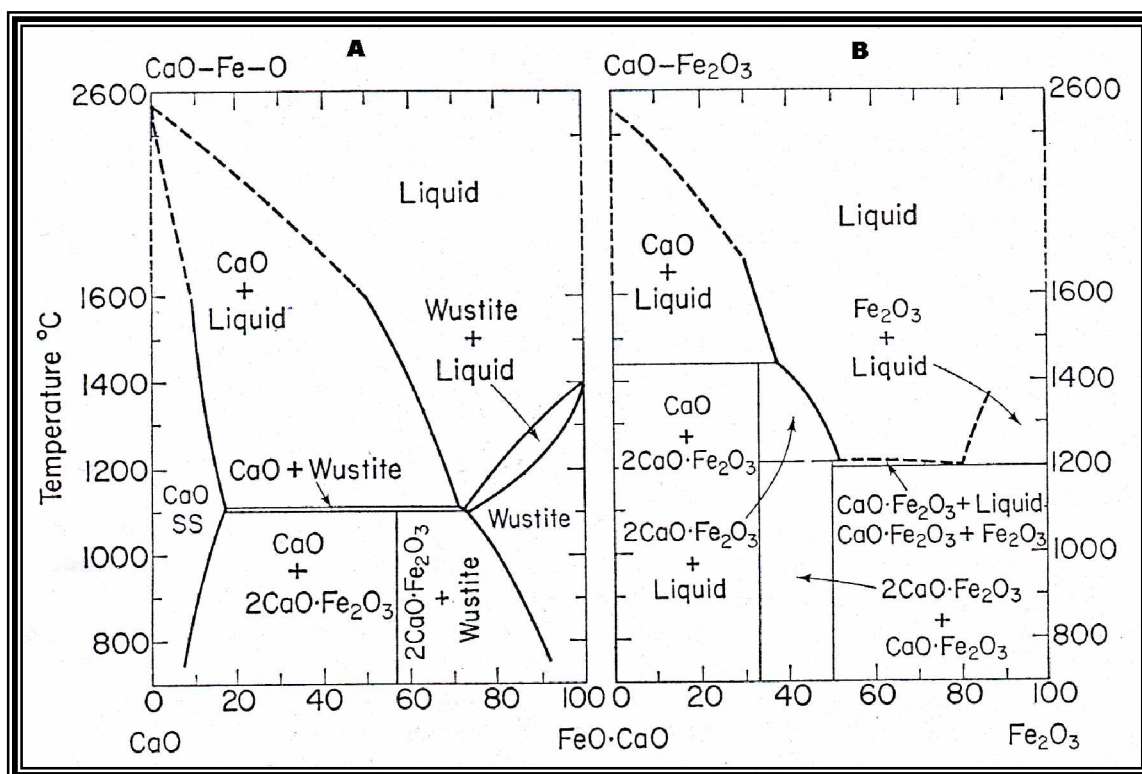


Fig. (2.18). the phase diagram of iron oxide and lime [70, 5]

Very little calcium Meta - ortho -ferrite is formed when clays are burned as the proportion of iron oxide is not usually sufficient.

When the iron oxide is in the partially reduced state, which is so often the case when burning clays and other ceramic materials, Wustite (FeO) is one component of the system and the phase diagram can be entirely different in form [70,5] Fig.(2.18A).

2.4 Ternary Systems in Ceramic Materials:

The lime-alumina-silica equilibrium diagram Fig. (2.19) has been deduced by Rankin and Wright are modified by Stephen [71] and although it appears highly complex, the phases which would crystallize from any mixture of components can be deduced by drawing the conjugation triangle embracing three adjacent phases and applying the principles laid down in the preceding pages.

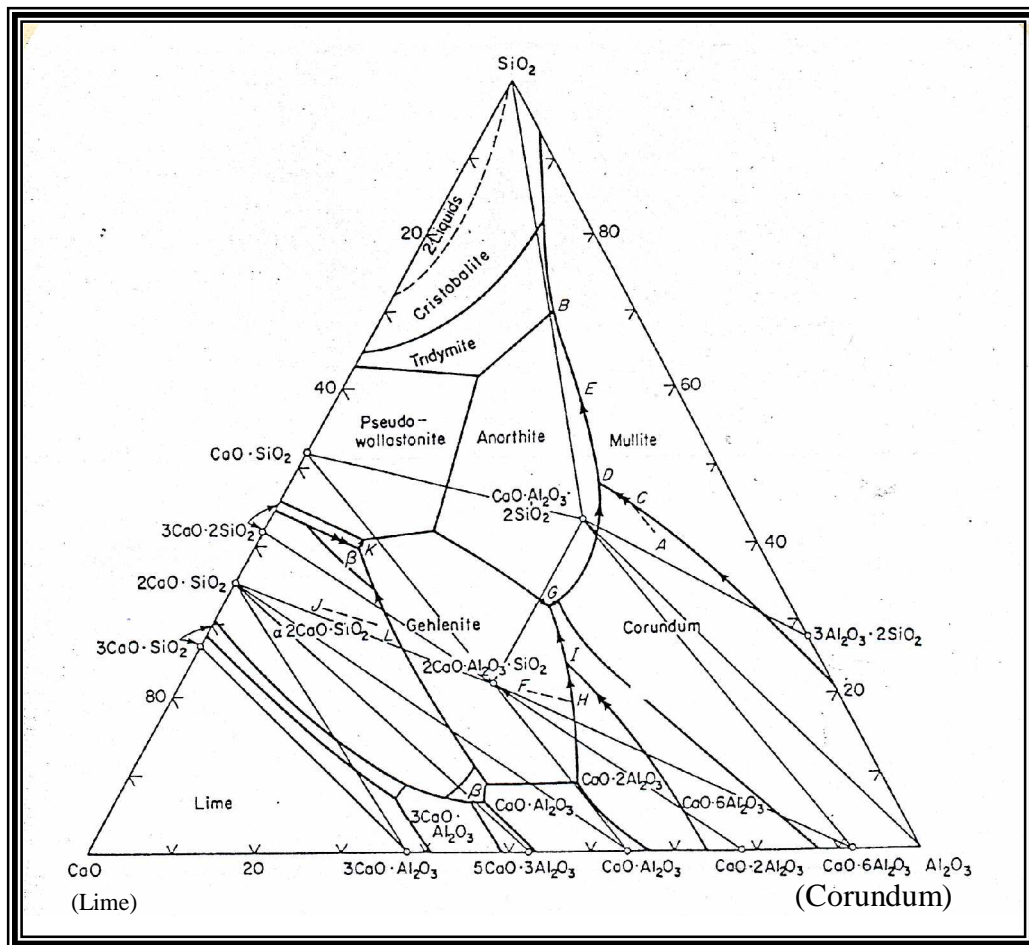


FIG. (2.19) Phase diagram of Lime – alumina - silica [5]

There are ten binary and two ternary compounds formed in the system as shown in **Table (2.3)** The lowest temperature at which liquid can be present is 1170 ° C. corresponding to a mixture of 23 parts CaO, 15 parts Al₂O₃, 62 parts SiO₂,

Binary Compounds	Melting Point	Nature
3CaO.SiO ₂	1900 °C	Congruently melting in a limited ternary field only.
2CaO.2SiO ₂	2130 °C	Congruently melting.
3CaO.2SiO ₂	1475 °C	Incongruent over both binary and ternary fields.
CaO.SiO ₂	1540 °C	Congruently melting.
3CaO.Al ₂ O ₃	1535 °C	Incongruent over both binary and ternary fields.
5CaO.3Al ₂ O ₃	1455 °C	Congruently melting.
CaO.Al ₂ O ₂	1600 °C	Congruently melting in binary fields but only over a limited ternary field.
CaO.2SiO ₂	1720 °C	Congruently melting.
CaO.6SiO ₂	1903 °C	Incongruent over both binary and ternary fields.
3Al ₂ .2SiO ₂	1830 °C	Congruently melting –but only just.
Ternary Compounds		
2CaO.Al ₂ O ₃ .SiO ₂ (Gehlenite)	1590 °C	Congruently melting.
CaO.Al ₂ O ₃ .2SiO ₂ (Anorthite)	1550 °C	Congruently melting.

Table (2.3).Compounds formed in the CaO / Al₂O₃ / SiO₂ system

2.5 The Mechanism of Fusion in Ceramic Materials

There are three principal reasons why ceramic materials fuse over a range of temperature: several different minerals may be present in any one sample, each of which may have a different melting temperature, many bond types may occur in one particular crystal and eutectics may be formed.

Sharp melting points are known in ceramic mixtures but they are rare and can only occur in the following cases; a pure component or congruently melting

compound with only one type of linkage throughout its structure, a mixture of the composition of a eutectic point and specific mixtures corresponding to a maximum or minimum in a solid solution diagram [70]. Even in these cases, melting will take place at one particular temperature only when the rate of heating is extremely slow, and when the quantity of material involved is very small in amount. When large quantities are heated, especially if the substance has a low thermal conductivity, or contains impurities, signs of fusion may appear at a temperature much below that at which liquefaction is complete.

The fusion point of ceramic substances is greatly complicated by the heterogeneous nature of these substances. Localized concentrations of individual complicated points may give rise to partial fusion at temperatures well below those predicted by equilibrium studies. Conversely, a mass that is non-homogeneous may not liquefy until a temperature well above the theoretical fusion point because equilibrium is attained very slowly [5].

2.5.1 Rate of Fusion: It is impossible to devise simple formulae which will indicate the rate of fusion in terms of time and temperature because such fusion also depends very largely on the size of the grains of material in the surface exposed to heat or chemical action, and on the viscosity of the fused products; this viscosity depends on the nature of these products, some substances producing much more viscous fluids than others [63]. Thus, magnesia produces a very viscous slag or glass and, consequently, the range of temperature through which fusion occurs (sometimes termed the *vitrificatit. range*) is much longer where magnesia is the chief flux than when lime is present in considerable proportion. Thus, articles containing magnesia as a flux are less likely to soften and lose their shape than those in which lime is used. The rate of fusion also depends on the solubility of the less fusible materials in the liquid portion. This,

in turn, depends partly on their mutual reactivates—a fusible mobile silicate, rich in bases having a much greater solvent action than one—such as feldspar—of a more neutral character. The action of feldspar is very slow, that it does not cause the ware to lose shape very quickly as is the case with some other fluxing minerals [1].

2.5.2 The vaporization point of a substance: is that temperature at which it is converting into a vapor at normal atmospheric pressure. Many substances vaporize at temperatures well below their boiling point. Thus, iron oxide does so at about 1250° C. and more rapidly as the temperature is increased. Chromium oxide, copper oxide barium oxide, and zinc oxide also vaporize freely at the temperatures reached firing stoneware and porcelain. At the temperature of the electric are most ceramic materials vaporize. The rate at which vaporization occurs depends partly on the temperature and partly on the vapor pressure [29].

2.5.3 Boiling point:

The boiling point of a substance is the temperature at which it is converted into vapor at such a rate that its vapor pressure is that of a column of mercury 760 mm in length i.e. 1 atmosphere. Most ceramic materials have boiling points which are I high as to be outside the range of attainable temperatures. The boiling point of any substance reduced if the pressure of the atmosphere in which it is heated is also reduced, that water can be boiled rapidly *in vacua* at about 60° C and slowly at lower temperatures.

If a liquid is heated above its boiling point in a closed vessel so that the vapor of the liquid cannot escape, the vapor pressure will increase in proportion to the heat absorbed. A typical example of this is the pressure of steam in an ordinary boiler. Water heated under pressure has more solvent action than that at the ordinary boiling point, and this is probably one cause of the decomposition of feldspar and other minerals from which clay is derived. Any substances which dissolve in a liquid will increase the boiling point of the latter in proportion to the concentration of the solution [72].

2.5.4 Thermal effects accompanying reaction:

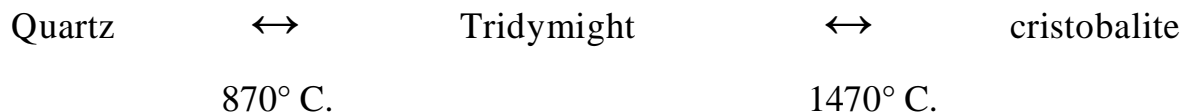
Reactions are accompanied by an energy change which is usually manifested as a heat effect. Thus a heat change may occur when substances form, dissolve, combine, dissociate, melt or crystallize. The amount of energy involved in such changes depends on the initial and final states of the material. If the final state has lower energy content than the original, heat will be evolved and the reaction is termed *exothermic*; conversely, if the final state has higher energy content, energy will be absorbed and the change is *endothermic* [1, 29].

2.6 Changes in Composition on Firing Silica Materials:

Silica may exist in a variety of crystalline forms, each of which is stable over a fixed range of temperature. Two quite distinct types of thermal change are associated with the changes in the silica minerals; these are (a) conversions, and (b) inversions.

a. Conversions: involve a pronounced change in crystal type, they proceed at a sluggish rate and, although reversible, the change takes place so slowly at the critical temperature that it is not observable under ordinary conditions.

The stability ranges of the minerals have been quoted by R. Greene [76] as



The transformation of quartz is not as simple as the above scheme suggests, nor is that of Tridymite to cristobalite.

The changes are so slow that pure quartz can be maintained at temperatures well above 870° C. without pronounced change and, once the high temperature varieties are formed, they can be cooled and maintained at room temperature for an indefinite period of time without reconvertng into quartz.

Pure quartz crystals are highly stable even at temperatures well above 870°C. The critical temperature for the change was deduced by assessing the rate constant at various temperatures and extrapolating back to zero conversion. The initial product of the decomposition of quartz is probably a transitional, unstable entity which then slowly reverts to one of the other crystalline modifications. All the naturally-occurring siliceous materials contain small proportions of a wide variety of minerals present as impurities. Sericite or hydrous mica is common in British silica rocks and this is usually the source of alumina in the material. Silicate, a crypto-crystalline silica rock, mined in Germany, Italy and South Africa frequently contains up to 5 % of titanium-bearing minerals.

On firing, such materials are converted to the high temperature modifications but, usually at a far faster rate than are crystals of pure quartz. This is mainly because of the smaller particle-size and the presence of colloidal or crypto-crystalline material which changes rapidly and then acts as 'seeds' for the

reaction of the more crystalline varieties. The presence of an amount of such rapidly-converting material is probably essential if a quartzite is to be suitable for the manufacture of siliceous refractoriness. Pure quartz reacts too slowly under commercial conditions; but, on the other hand, an excess of amorphous silica is also unsuitable. So rapidly does this substance convert that a shape prepared from it may be shattered by the excessive rate of change in volume on heating under fairly rapid heating conditions, the transformation in amorphous silica may be detected by observing the thermal change at about 1250° C. Quartzite's of good quality may contain up to 98 % silica, but the small percentage of impurity minerals is sufficient to produce an appreciable amount of liquid on firing.

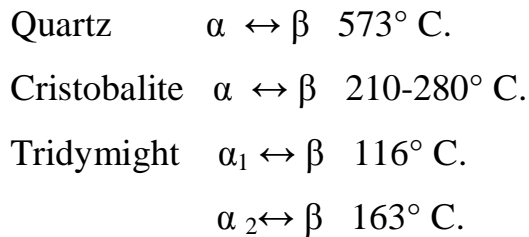
This is augmented by the action of the catalyst or promoter added to the raw material to accelerate the rate of conversion.

Lime or iron oxide (the two principal additives) do not readily form a liquid with silica, but the presence of a small proportion of alumina is sufficient to cause fluidity at a kiln-firing temperature of 1450 °C.

Most of this liquid which is produced on firing becomes a glass on cooling which surrounds the crystals of cristobalite and Tridymite which have formed. The properties of this glass are, however, unusual and it may be that, as it is highly siliceous, a structure can be induced in it by the embedded silica crystals. Alumina when present in siliceous materials not only gives rise to undesirable liquid formation at high temperatures but also inhibits the degree of conversion. This is especially noticeable in siliceous clays where even at high temperatures and on prolonged heating, quartz grains are converted only slowly to one of the high temperature varieties of silica. Quartz can often be detected in fireclay refractoriness which has been in constant service at temperatures over 1250° C. for periods of many years.

b. Inversion. The silica minerals each undergo additional changes when heated which do not involve a pronounced change in crystallographic form these small rearrangements in structure are termed *inversions* and take place at well-defined temperatures. In contrast to the conversions these reactions are rapid and instantaneously reversible.

They may be summarized as:



It is now known that quartz inverts over a short range of temperature although in most cases it occurs within a degree of 573° C. The variations in the inversion temperature are attributed by Jianzhong and Huagao [72] to possible defects in the structure or the incorporation of foreign ions. The variability of the inversion temperature of cristobalite is most probably due to a similar cause. The higher the temperature and the longer the duration of firing, the higher is the inversion temperature of cristobalite, but, the presence of foreign ions also exerts a marked influence; thus, sodium catalyses the formation of cristobalite from quartz and the material so produced after heat treatment at 1350° C. inverts at 268° C. Under the same conditions, calcium- magnesium and other cat ions form cristobalite with an inversion at 232° C.; but cristobalite formed on heating pure kaolin at 1250° C. has an inversion point at about 216° C. The inversion effect may be measured by the small thermal change which accompanies the reaction; the total heat change is about +2.8 calories per g. and the reaction is thus an endothermic effect on heating but, on cooling, is exothermic i.e. will liberate heat [74]. Cristobalite prepared in

different ways is frequently different in thermal behaviors; the presence of magnesium gives a cristobalite in which the inversion is sharp and the heat is liberated over only a small range of temperature; lime and, an even greater extent sodium compounds catalyst the formation of a form which inverts over a range of up to 10 °C.

The range of temperature in the inversion effect of cristobalite samples is due to many individual crystallites which each invert instantaneously but at different temperatures. Berry and Flynn [75] have demonstrated this fact by microphotography on a thin-section of a silica brick which was slowly heated or cooled through the inversion range of cristobalite on a hot-stage microscope; the change from $\alpha \leftrightarrow \beta$ cristobalite in a crystallite was accompanied by an instantaneous increase in transparency [76].

Chapter Three Practical and Results Part

3.1 Sample preparation procedure

3.1.1 Kaolin treatment and characterization:

The first step of treatment is to wash Kaolin Duekhla with distilled water in order to remove some impurities and salts present in the Kaolin. Then the Kaolin is washed by HCL of (10N) concentration for time duration 24 hours, with stirring at room temperature, this is to remove the free iron oxide and other impurities. By this process we can remove all minerals and oxides which can be dissolved in HCL which are not required for the production of the Anorthite martial. Another wash with water is to remove the acid from the Kaolin till it become at 5-6 PH. Then the separated materials dried by using oven (GCA\PRECTIONSIENTIFC, model 16) at temperature rang 50-70 °C for 10 hours. This treatment studied qualitatively by IR measurement .The measurements has been made by using (Shimadzu Fourier Transforms Infrared model FTIR 8300 (Kyoto, Japan)).The IR spectrum for kaolin raw material in (fig 3.2), (fig 3.3) is for kaolin treated with HCL. The dried powders of kaolin was divided in to tow groups, one of these group was heat treated at 400 °C for 1hr. follow this process each of these groups are milled using ball mill of porcelain body with different size of spheres for 24 hours .these group are sediment separately by using locally made glass-tube system having dimensions 5cm in diameter and 1m in length as illustrated in the figure bellow (fig 3.1).

Float powder for each groups get on through aperture 3 and sieved by using special sieved with particle size 20 μm . The powder pass this sieves will be used in the study.

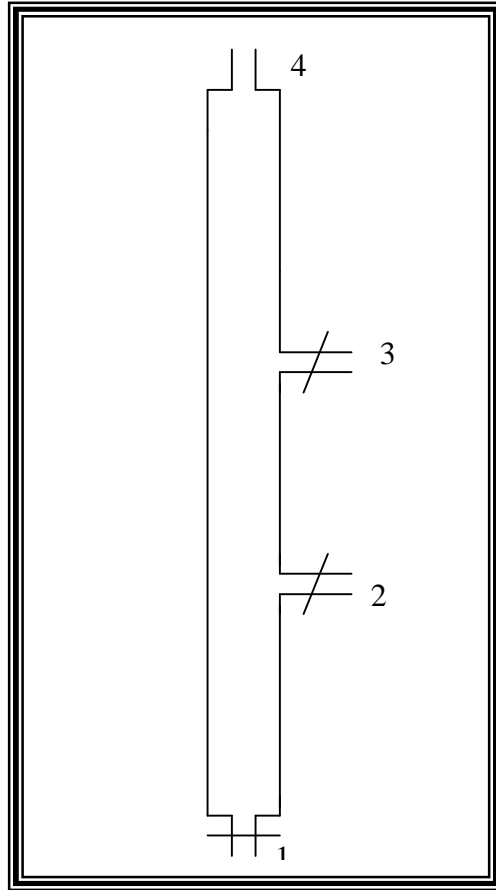


Figure (3.1) in this figure length between 1 and2 is40 cm, 2 and3 is 30cm, 3 and4 is 30cm

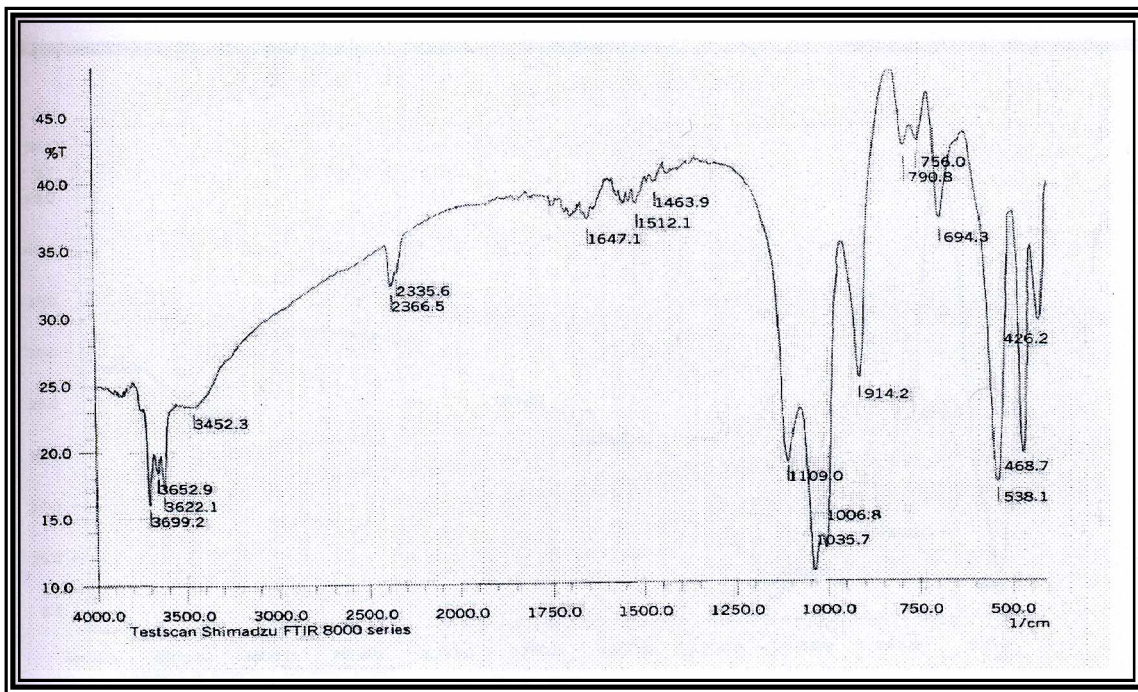


Figure (3.2). IR analysis for kaolin raw material.

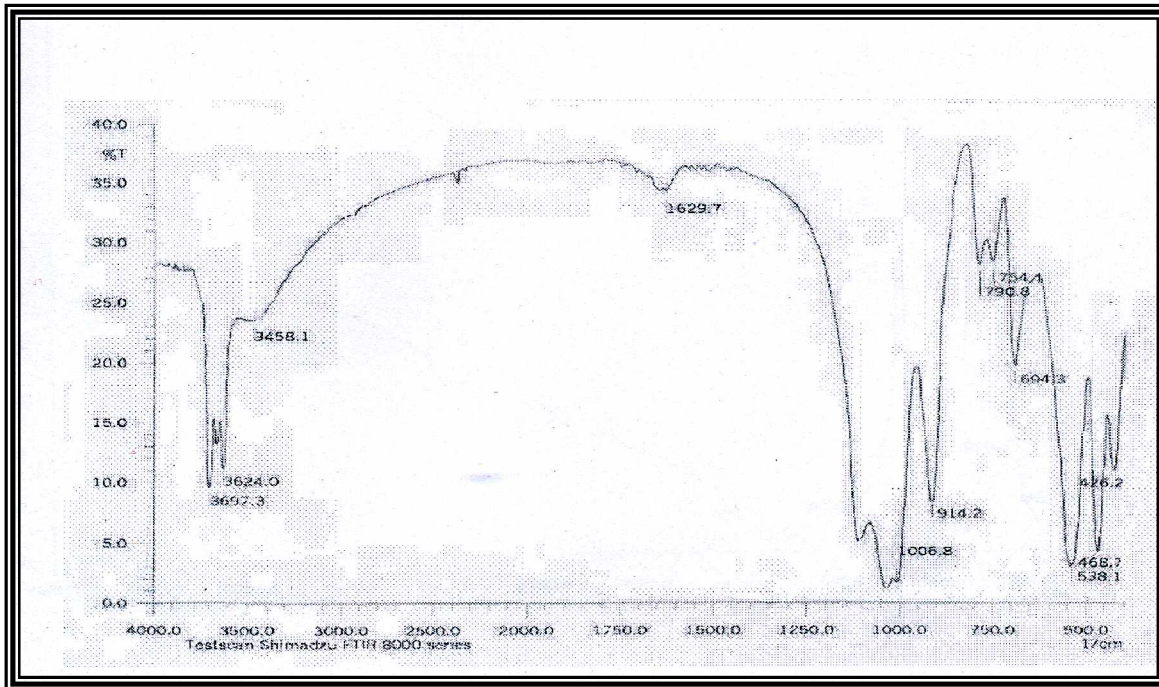


Figure (3.3). IR analysis for kaolin washed by HCL.

And then by using XRD analysis the result for kaolin raw material, washed by HCL and centering kaolin for 400 °C, washed by HCL.as shown in figures, (3.4), (3.5), (3.6) and (3.7).

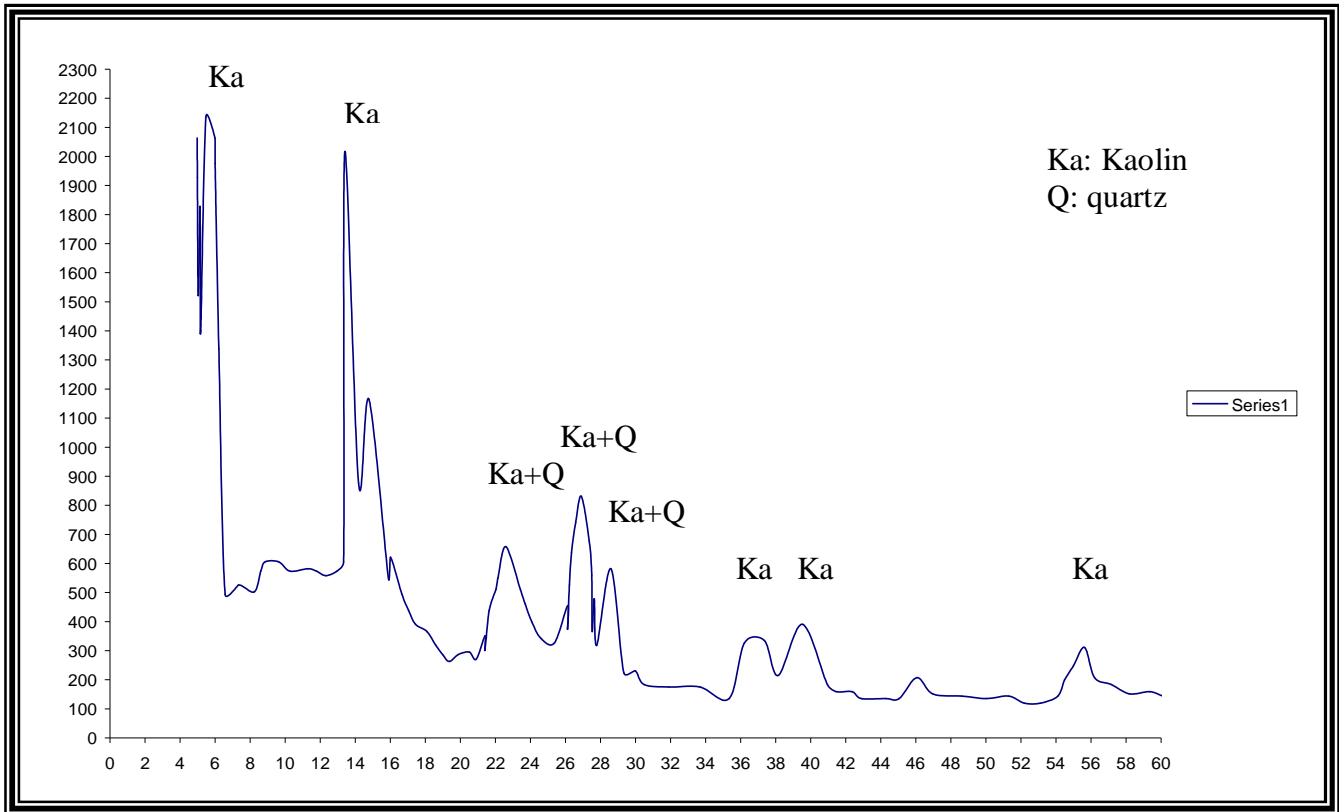


Fig (3.4) XRD pattern for Kaolin Duekhla raw material

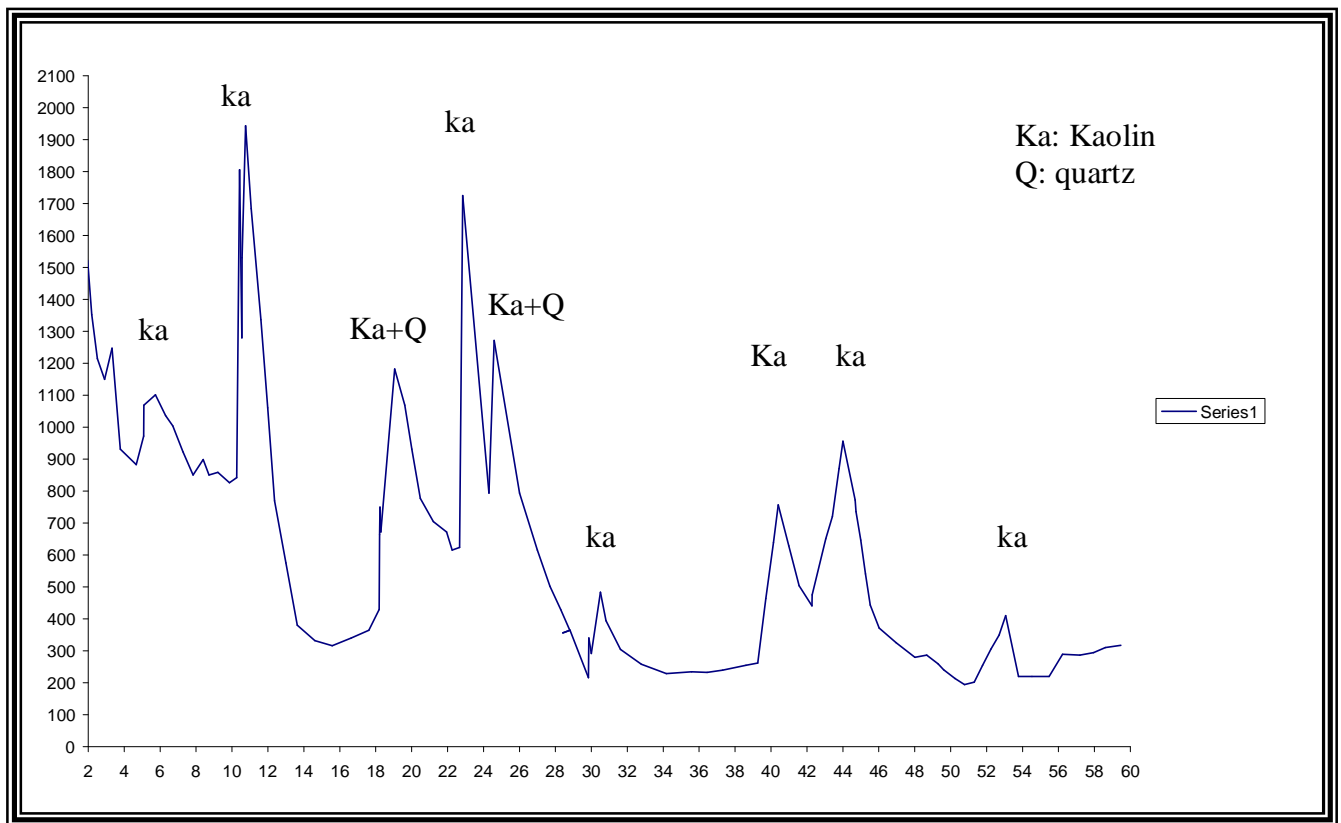


Fig (3.5) XRD pattern for Kaolin Duekhla washed by HCL

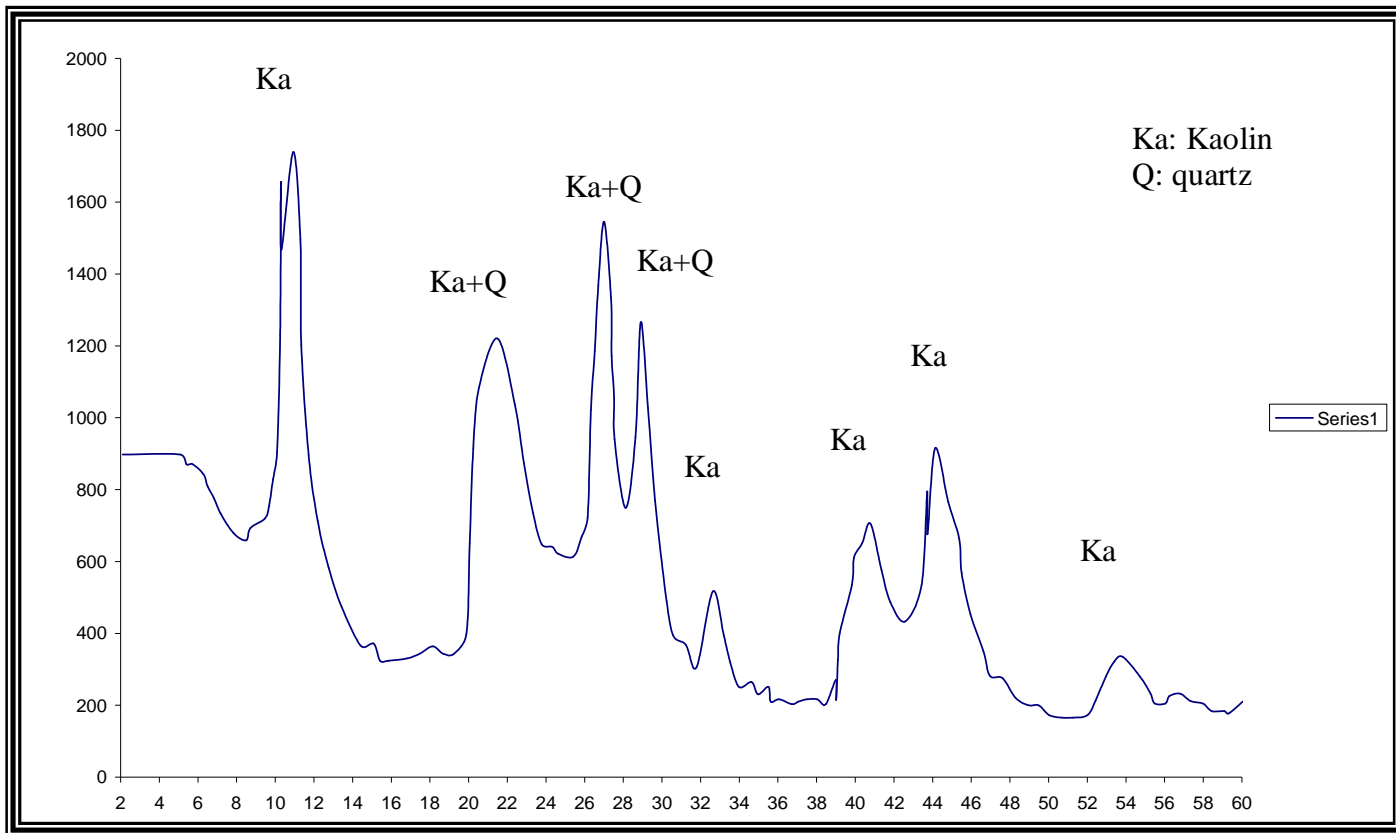


Fig (3.6) XRD pattern for calcinated kaolin duekhla

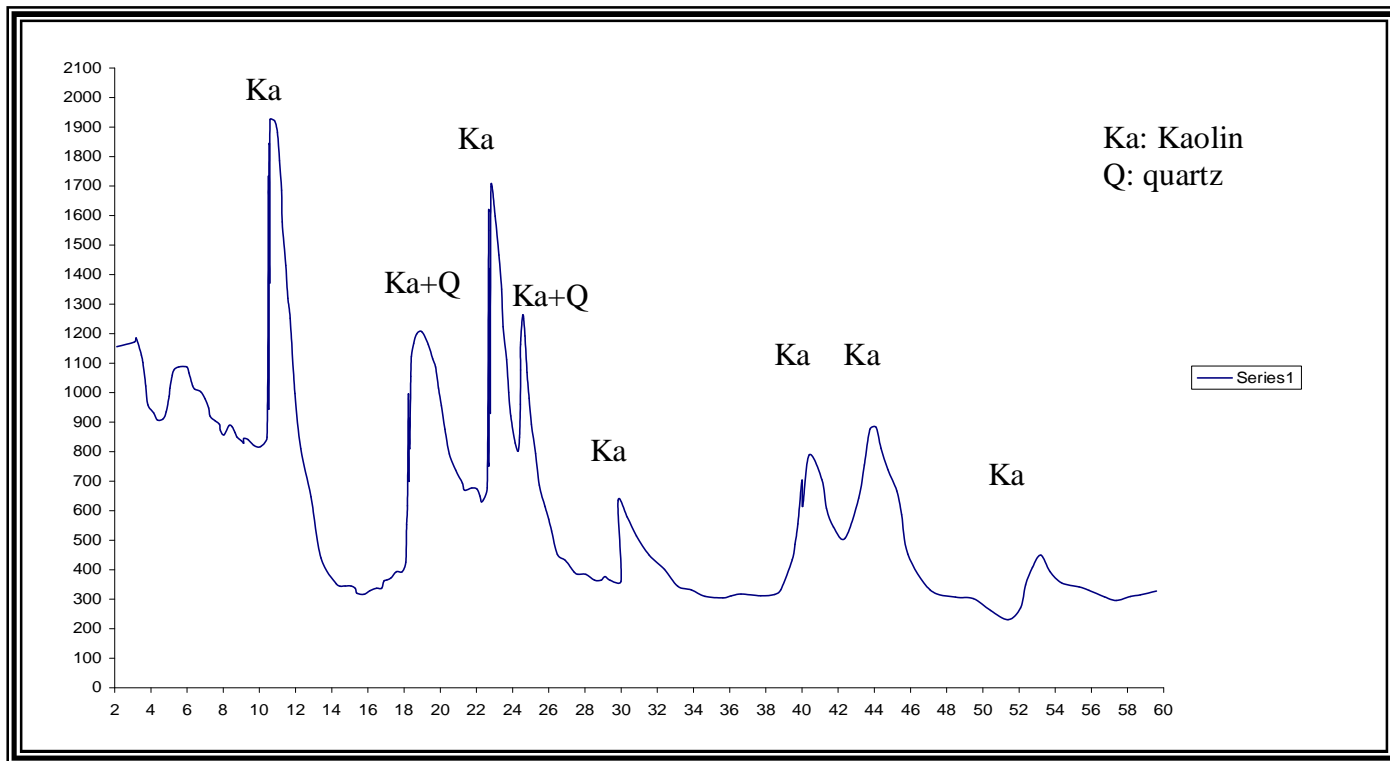


Fig (3.7) XRD pattern for calcinated kaolin duekhla washing with HCL

3.1.2 Calcium carbonate treatment and characterization:

At the first mixed (CaCO_3) with ethanol, then milled using ball mill of porcelain body with different size of spheres for 12 hours ethanol will prevent the aggregation under milling. Then this mixture dried by using furnace at temperature rang 50-70 °C for 5 hours. The dried powders of mixture were sediment by using the same glass tube. Float powder get on from aperture 3 sieved by using special sieved size 20. Then dried the powder by using oven. The IR analyses for CaCO_3 as shown in figure (3.8).

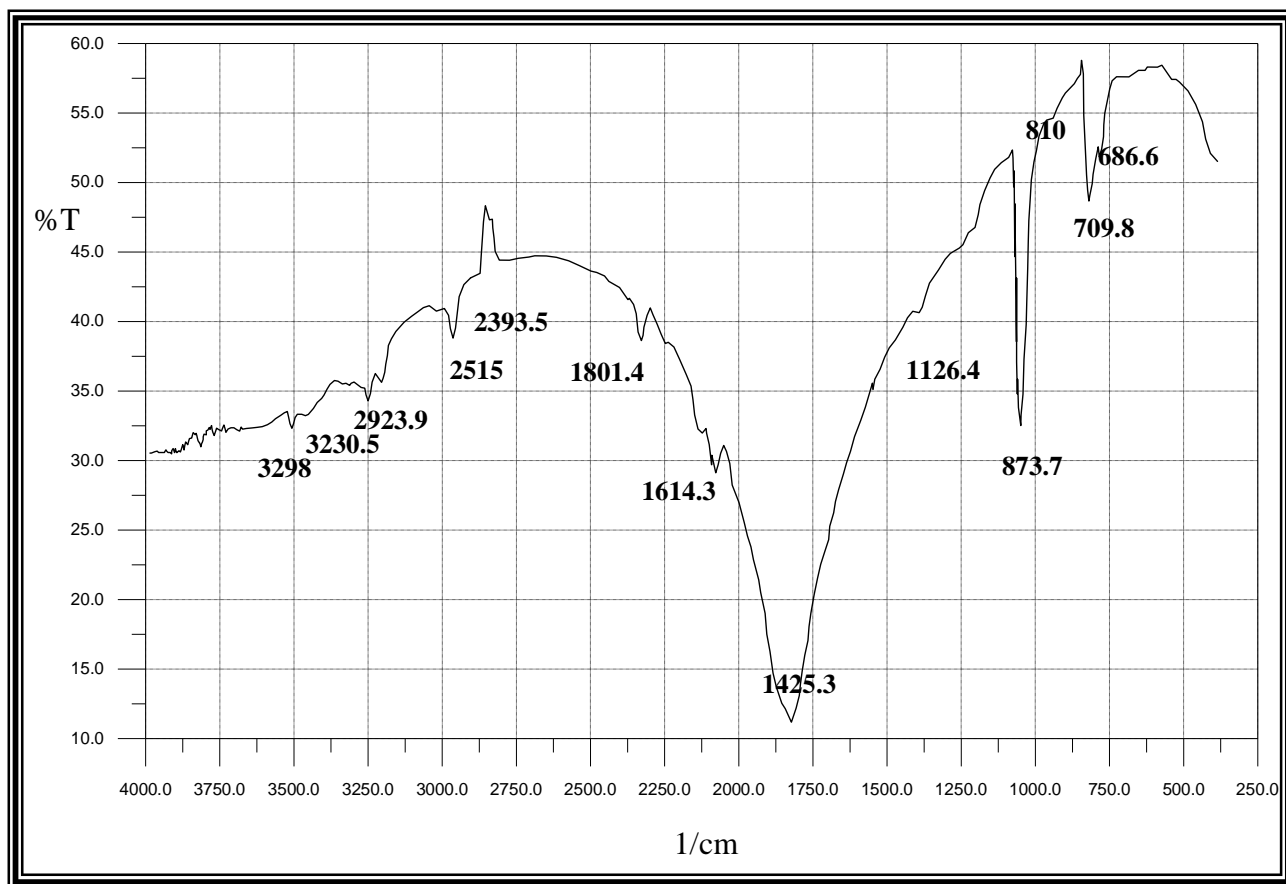


Figure (3.8). IR analysis for CaCO_3

3.1.3 Sample preparation:

Table (3.1) shown the composition weight percent for the groups of samples preparation.

Group No.	Samples No.	Calcinations Kaolin washed by HCL, particle size < 20µm	Kaolin washed by HCL, particle size < 20µm, with out Calcinations	Calcium Carbonate Powder particle size < 20µm
1	M₁	70 %		30 %
	M₂	75 %		25 %
	M₃	80 %		20 %
	M₄	85 %		15 %
2	M5		70 %	30 %
	M6		75 %	25 %
	M7		80 %	20 %
	M8		85 %	15 %

Table (3. 1) .sample preparation from Kaolin and calcent Kaolin with CaCO₃

Proper mixing and homogeneity of these mixtures by using the ultrasonic and magnetic stirrer another succession of drying, grinding and sieving is made. The prepared samples are firing at temperatures (**1200 °C**) for soaking time 1hr,2hr,3hr and then (**1300 °C**) for 1hr .The fine powders prepared by milling this fired sample were tested by XRD and IR analyze. From homogeneity mixture compact samples are prepared using press (model (38888.4D10A00, mad in USA)), with pressure 3MPa as a disc form of diameter 30 mm and 5mm thickness. Then fired at the same rang of temperature and soaking time..

3.2 Measurements:

3.2.1 X- Ray Diffraction Measurement:

The phase structure for these samples are measured by XRD tech. by using (SIEMENS X-RAY DIFFRACTION, UNIT MODEL D-500, KV=40, CUK α =line, $\lambda = 1.542 \text{ \AA}$). These results are shown in figures (3.12) to (3.40).

3.2.2 Chemical composition:

Table (3, 2) shows the chemical composition of the samples that gives the best results of the Anorthite material according to the XRD results.

Samples No.	Samples ,heat treatment 1200°C/3hrs	SiO ₂ %	Fe ₂ O ₃ %	Al ₂ O ₃ %	CaO %	Na ₂ O %	K ₂ O %
M ₃	80% K +20% CaCO ₃	42.48	1.78	33.45	19.1	0.36	0.23
M ₄	85% K +15% CaCO ₃	43.54	1.34	30.08	23.12	0.22	0.34
M ₇	80% CK +20% CaCO ₃	43.78	1.48	32.57	19.5	0.25	0.35
M ₈	85% CK +15% CaCO ₃	45.88	1.22	30.47	21.7	0.20	0.15

Table (3. 2) Chemical composition of the samples preparation

3.2.3 IR measurement:

The chemical components for these samples as shown in table (3.3) are measured by the IR technique by using (Shimadzu Fourier Transform infrared model FTIR 8300 (Kyoto, Japan)). And the results are shown in figures,(3.9),(3.10),(3.11)and(3.12).

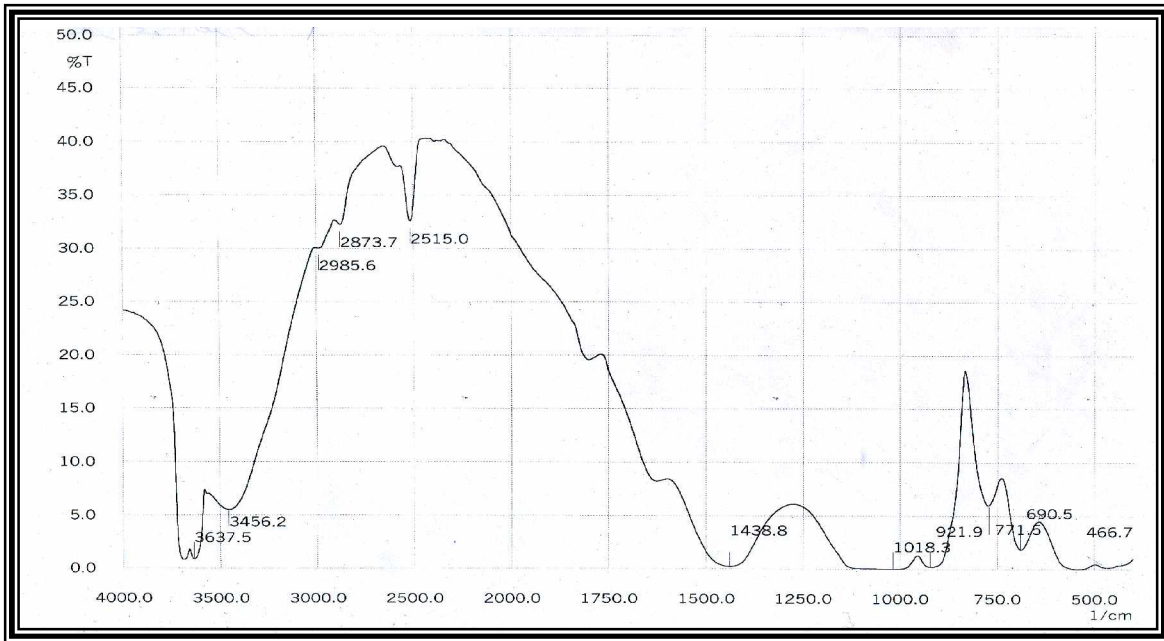


Figure (3.9). IR analysis for sample No. M₃

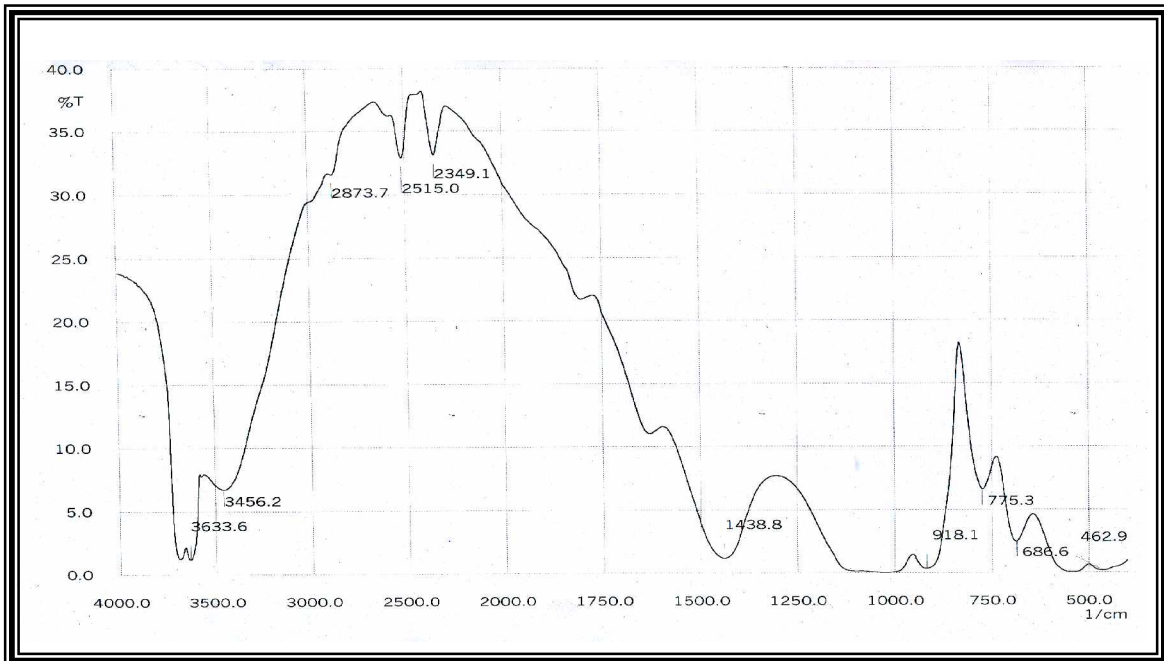


Figure (3.10). IR analysis for sample No. M₄

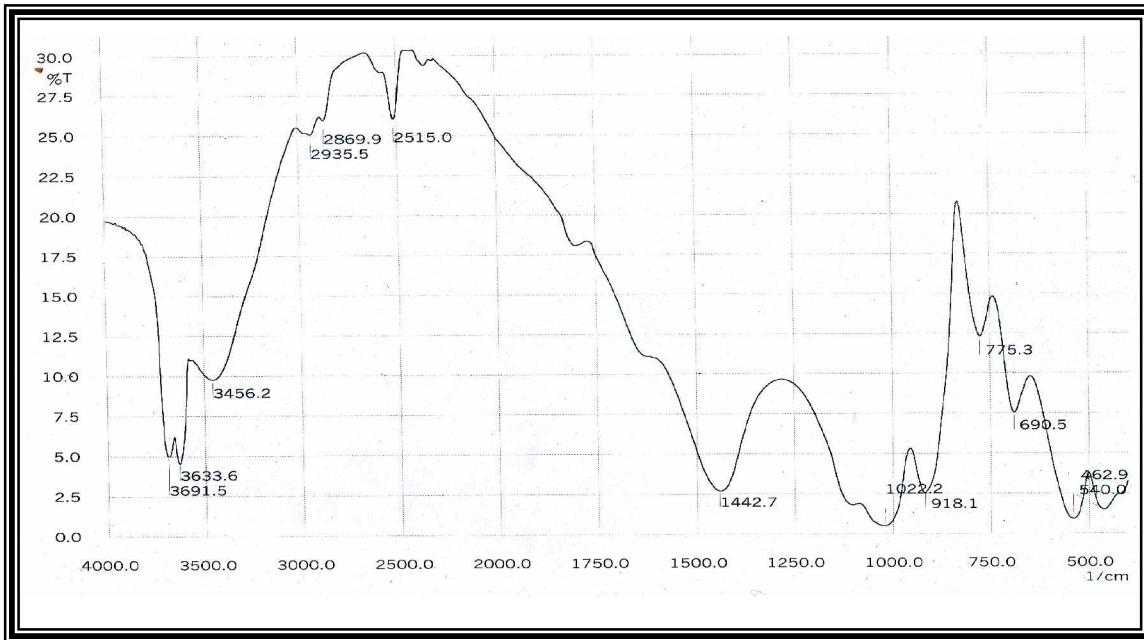


Figure (3.11). IR analysis for sample No. M₇

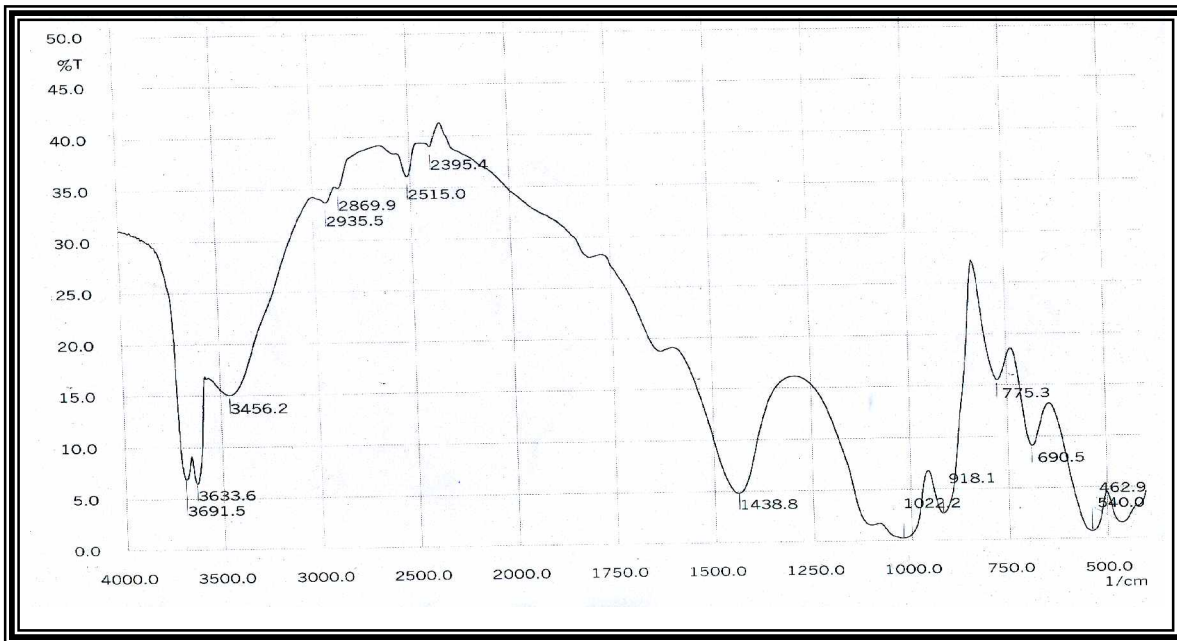


Figure (3.12). IR analysis for sample No. M₈

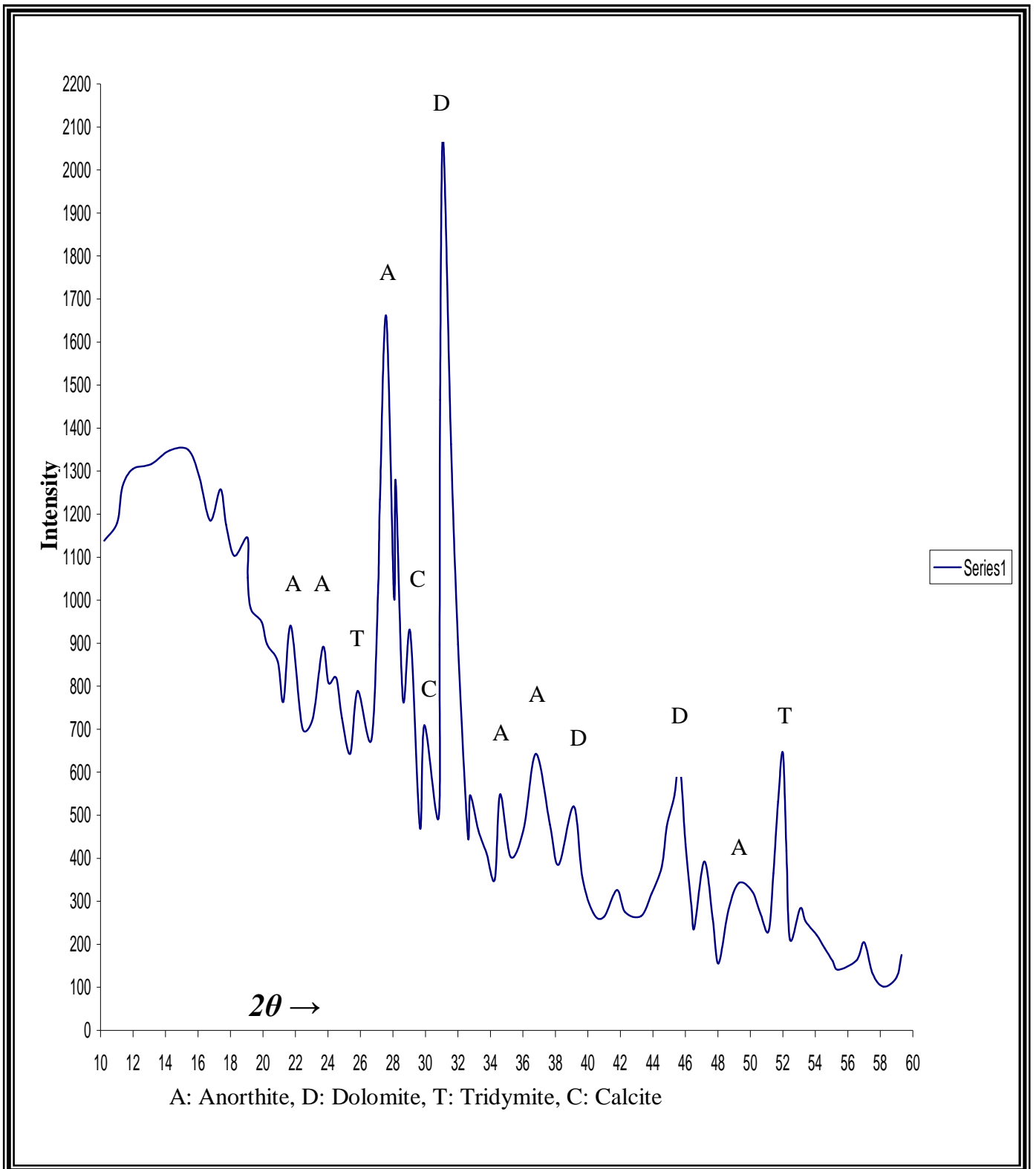


Fig . (3.13) XRD pattern for sample 70% K+30% CaCO₃ fired 1200 °C for one hours [M5]

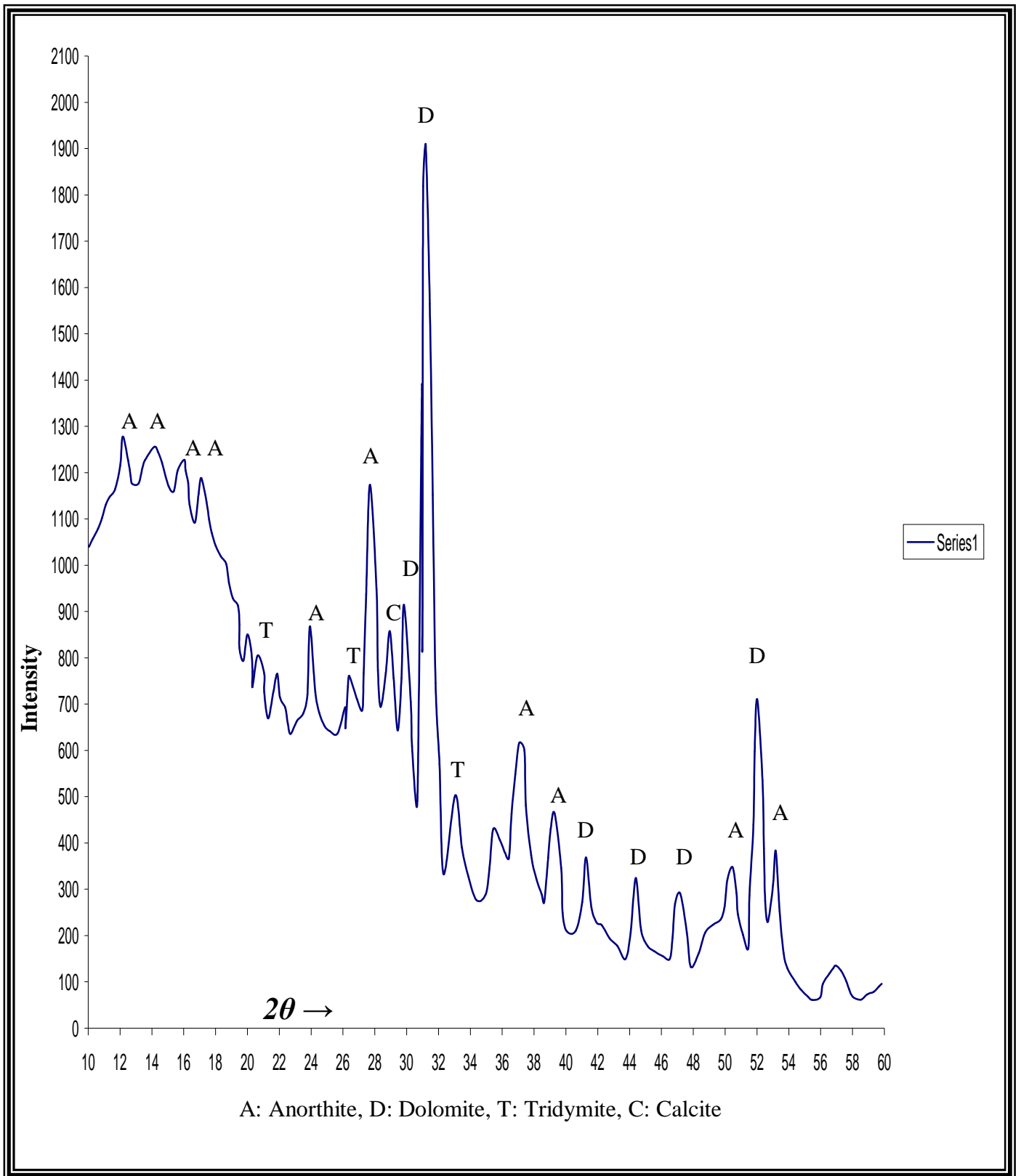


Fig.(3.14) XRD pattern for sample 70% K+30% CaCO₃ fired 1200 °C for two hours [M5]

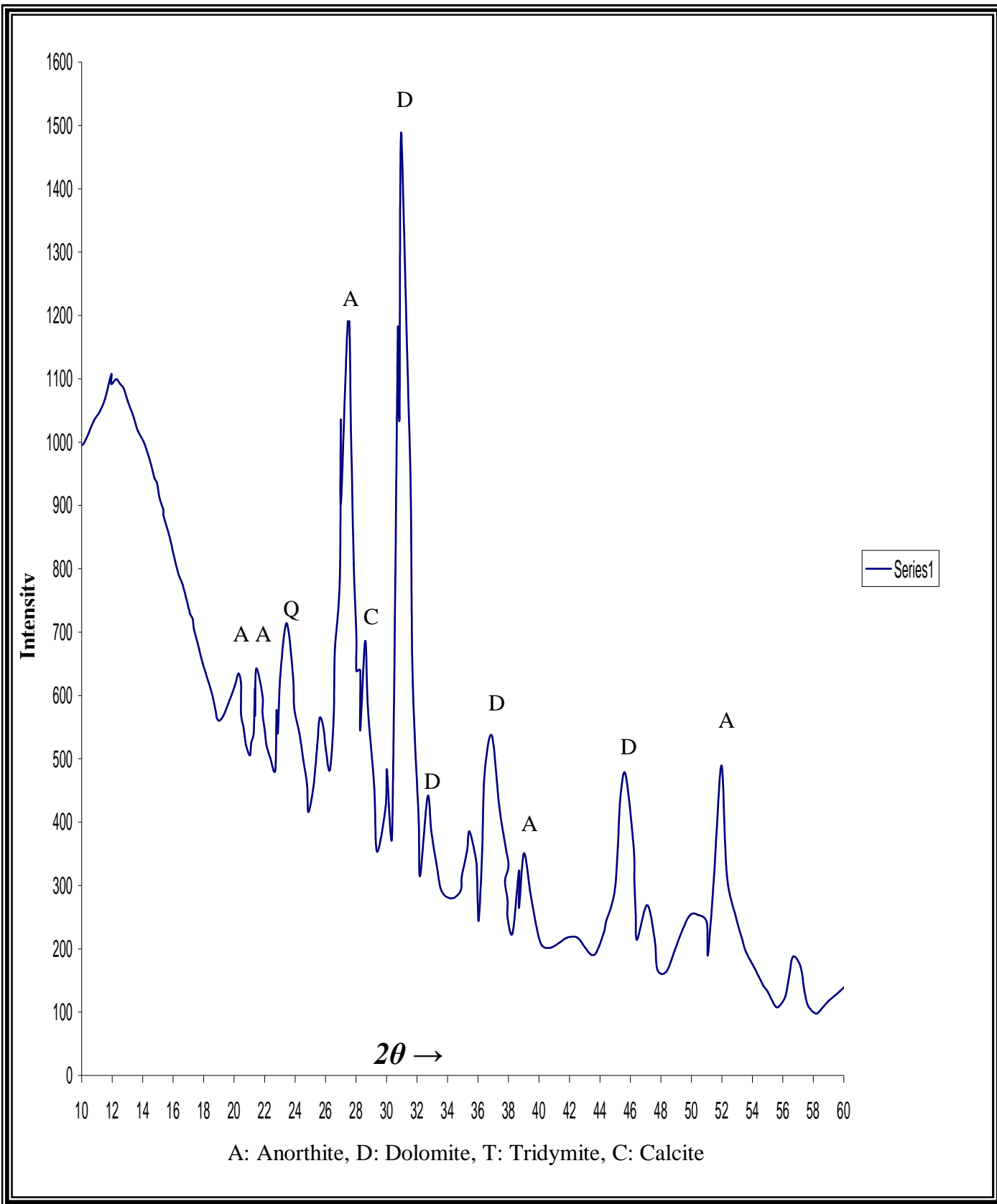


Fig.(3.15)XRD pattern for sample 70% K+30% CaCO₃ fired 1200 °C for three hours IM51

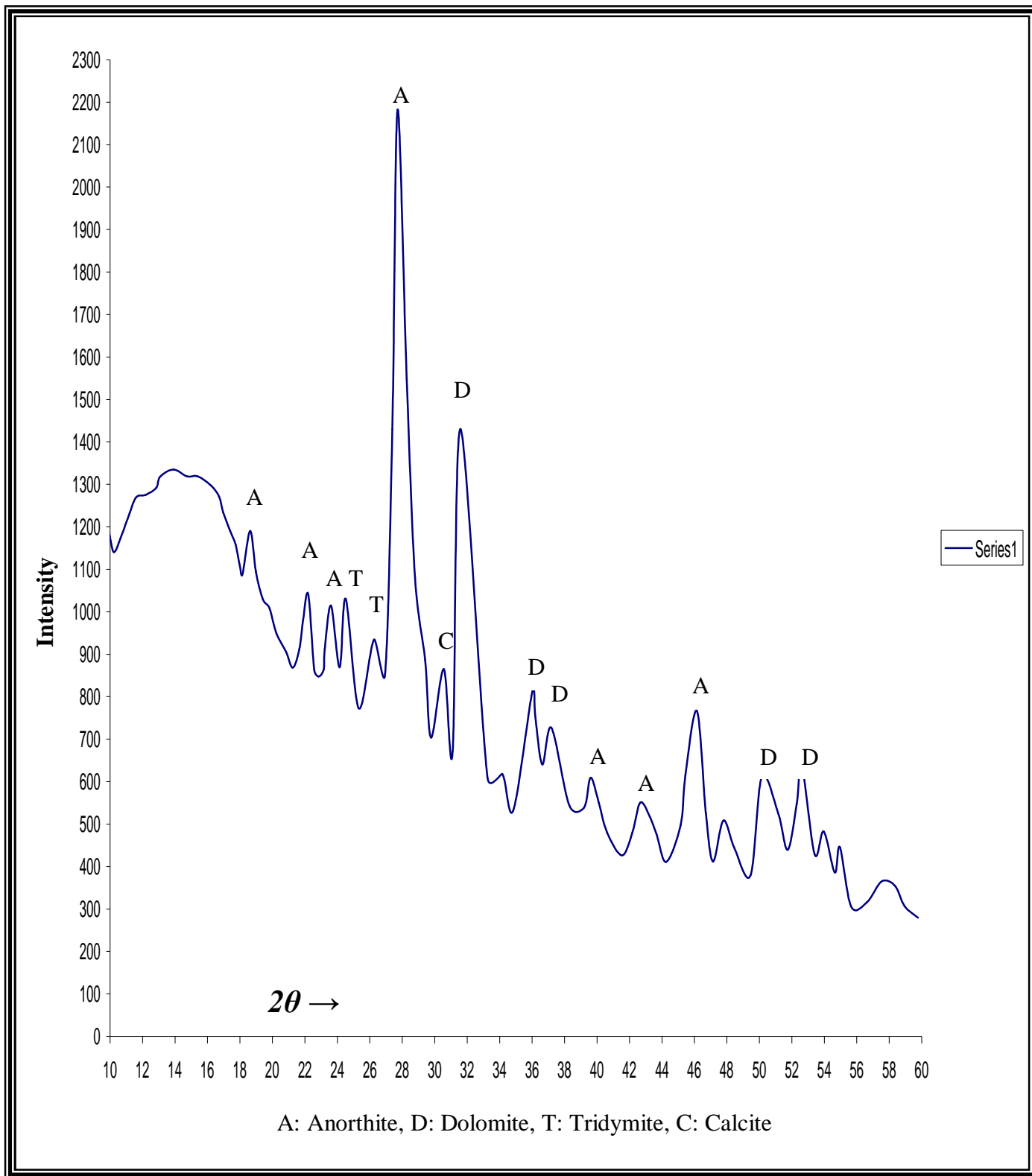


Fig.(3.16)XRD pattern for sample 75% K+25% CaCO₃ fired 1200 °C for one hour [M6]

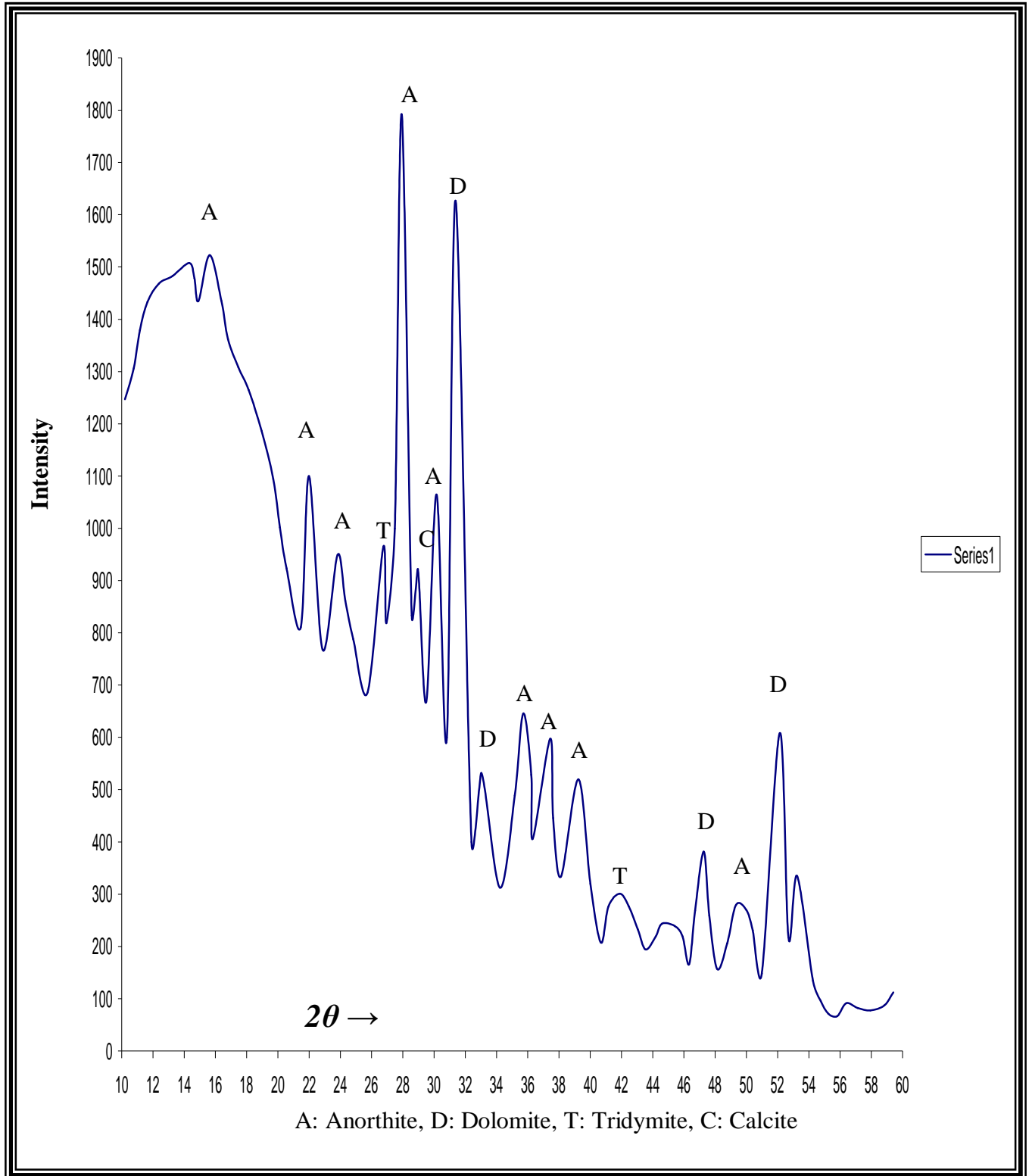


Fig.(3.17)XRD pattern for sample 75% K+25% CaCO₃ fired 1200 °C for two hours [M6]

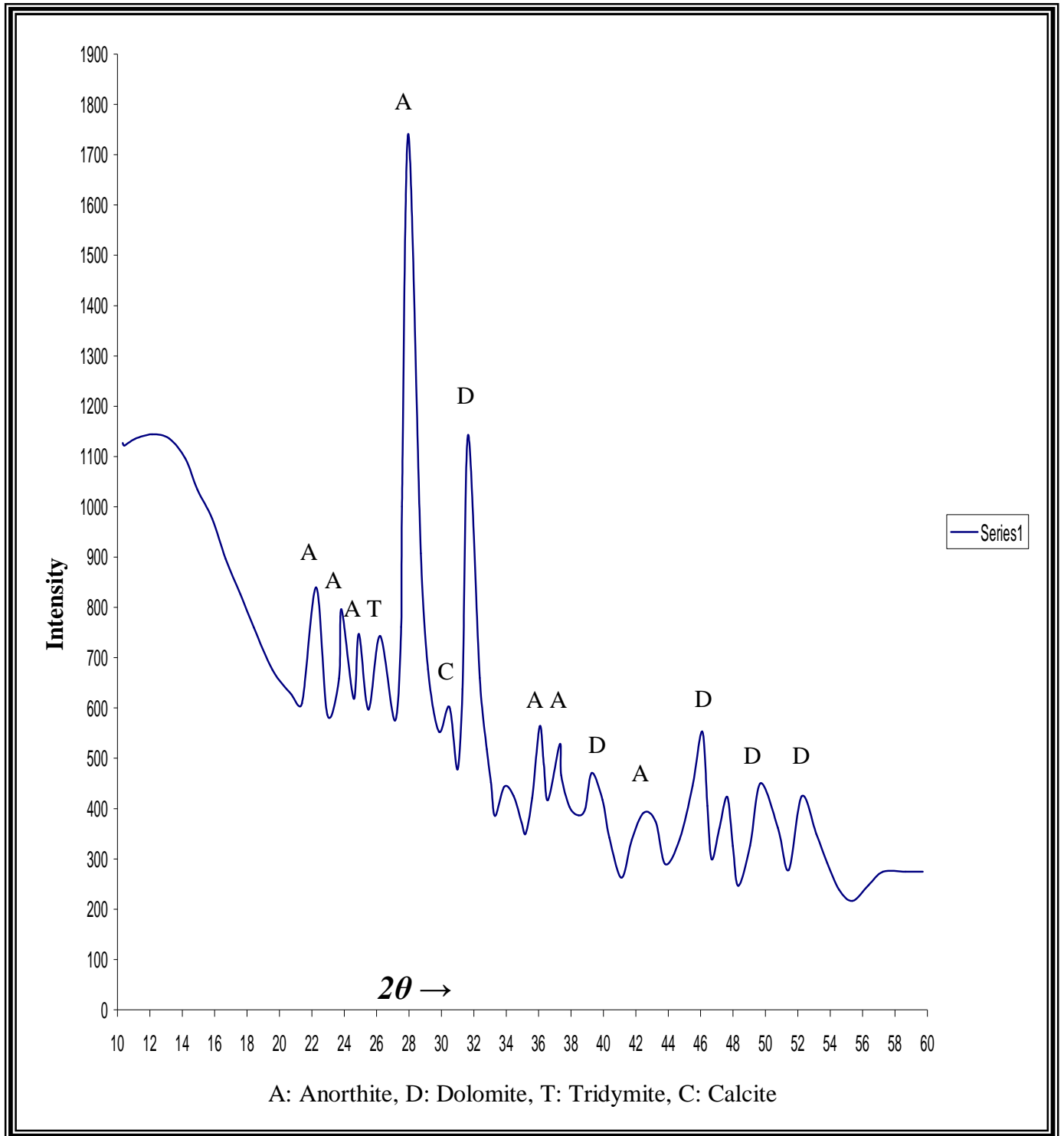


Fig.(3.18)XRD pattern for sample 75% K+25% CaCO₃ fired 1200 °C for three hours [M6]

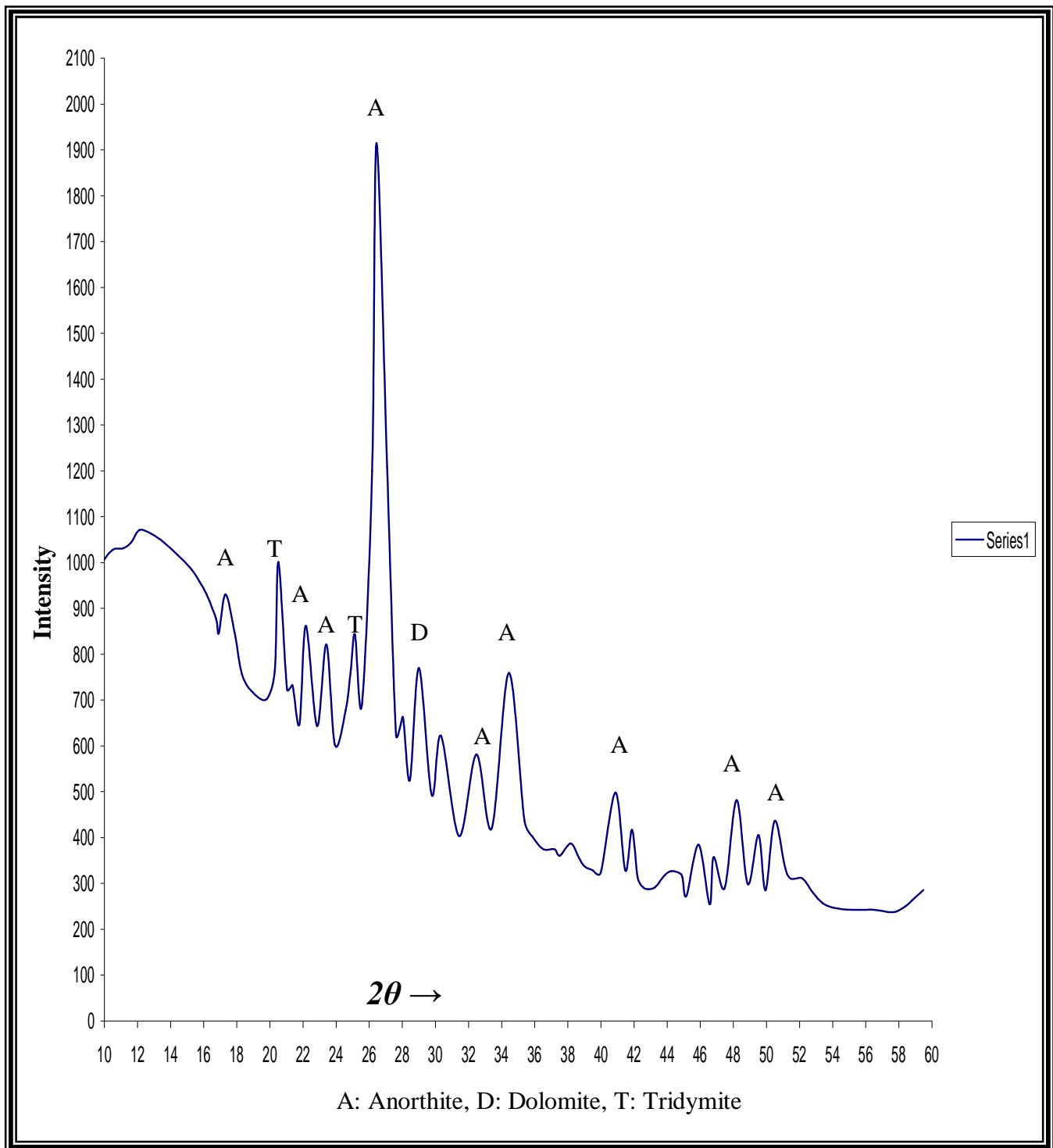


Fig. (3.19)XRD pattern for sample 80% K+20% CaCO₃ fired 1200 °C for one hours [M7]

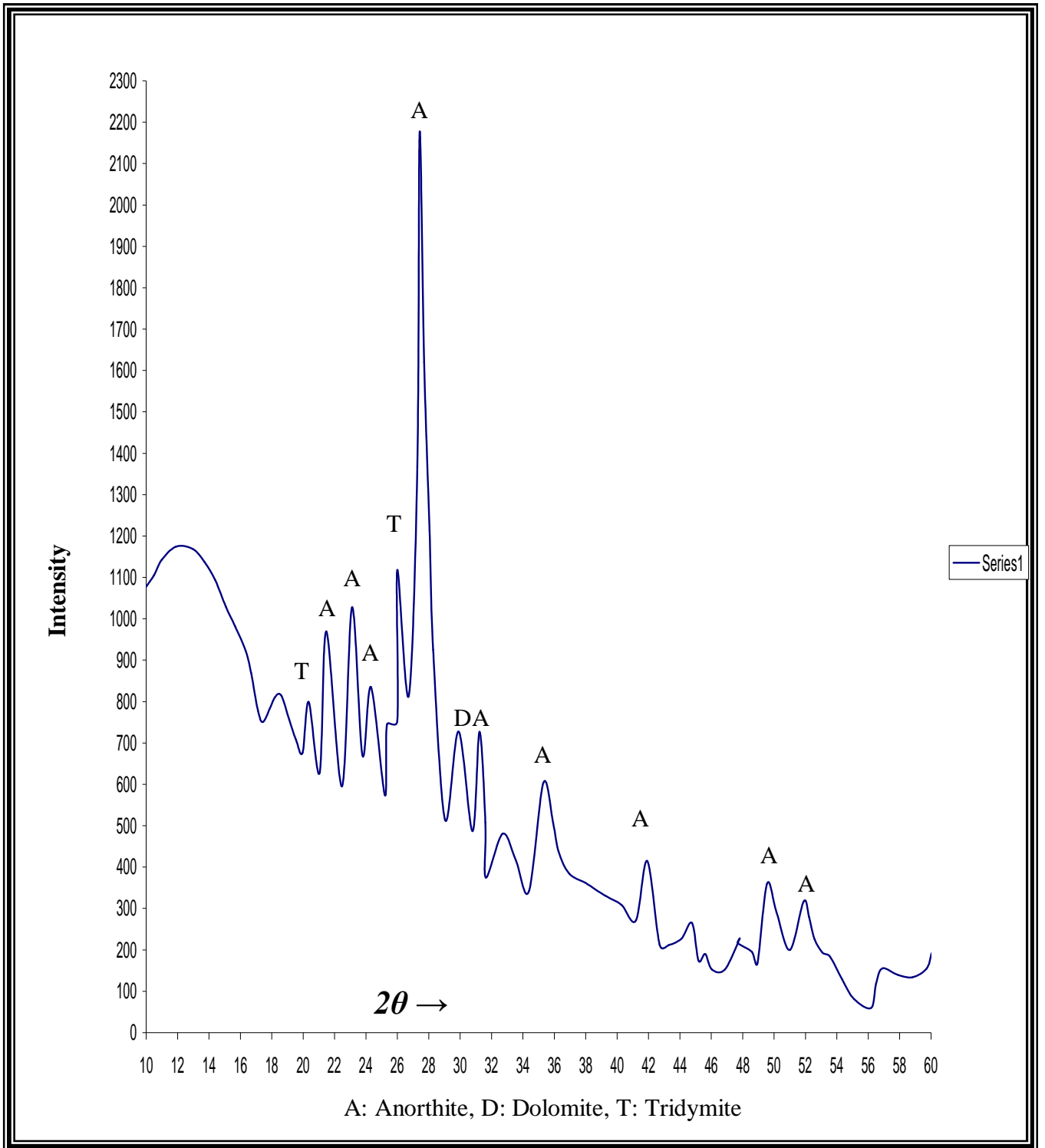


Fig.(3.20)XRD pattern for sample 80% K+20% CaCO₃ fired 1200 °C for two hours [M7]

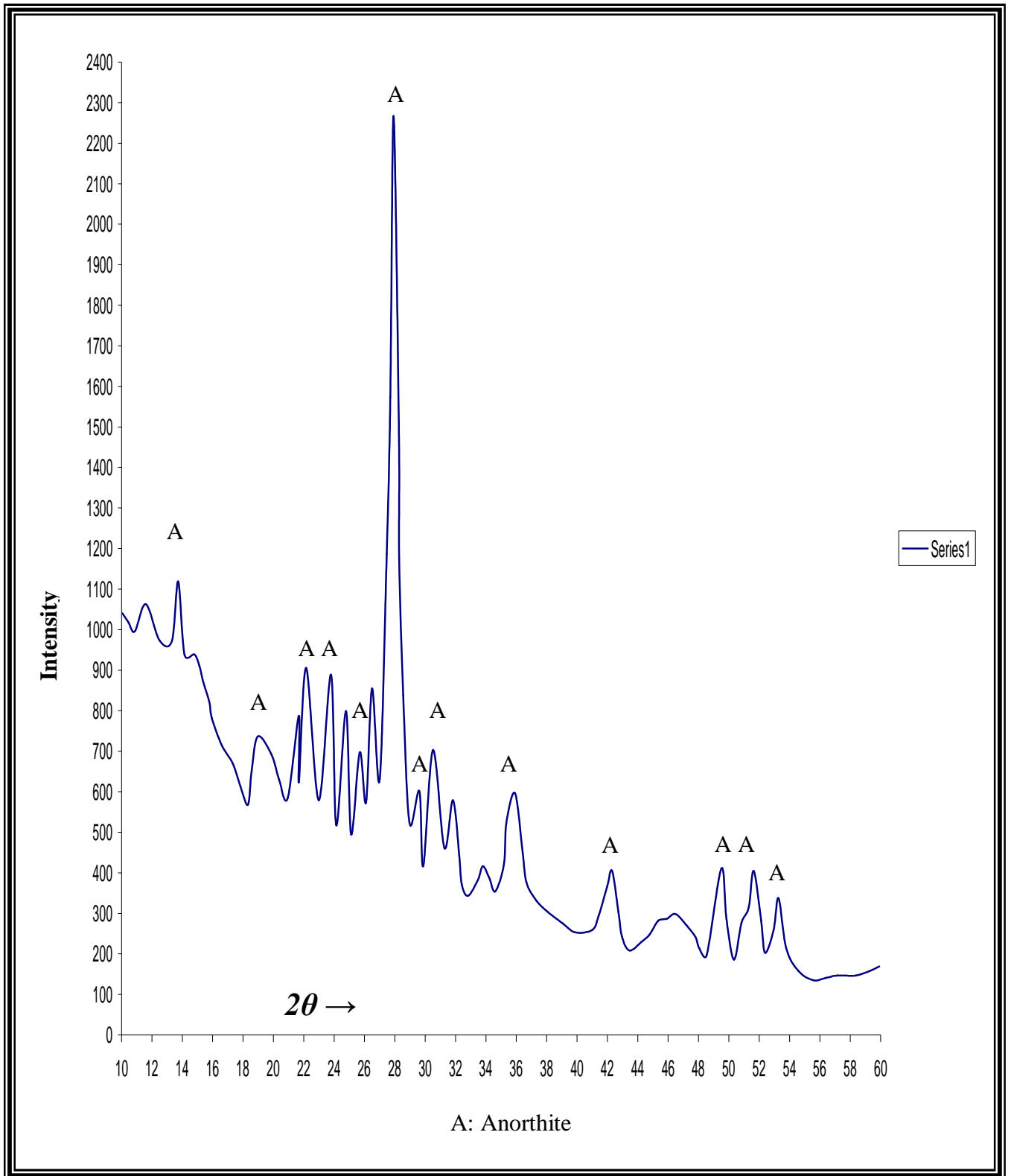


Fig.(3.21)XRD pattern for sample 80% K+20% CaCO₃ fired 1200 °C for three hours [M7]

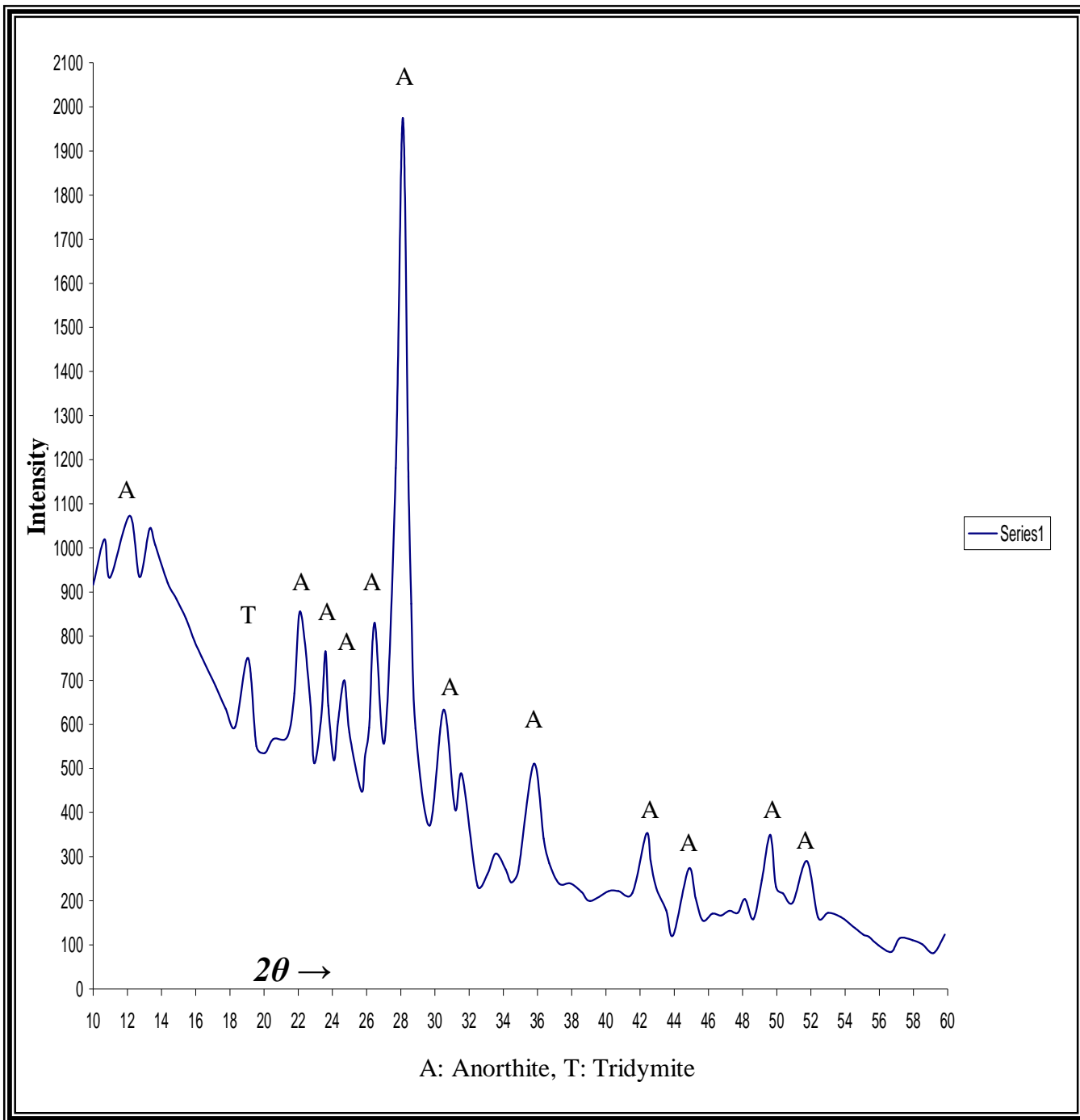


Fig.(3.22)XRD pattern for sample 80% K+20% CaCO₃ fired 1300 °C for one hours [M7]

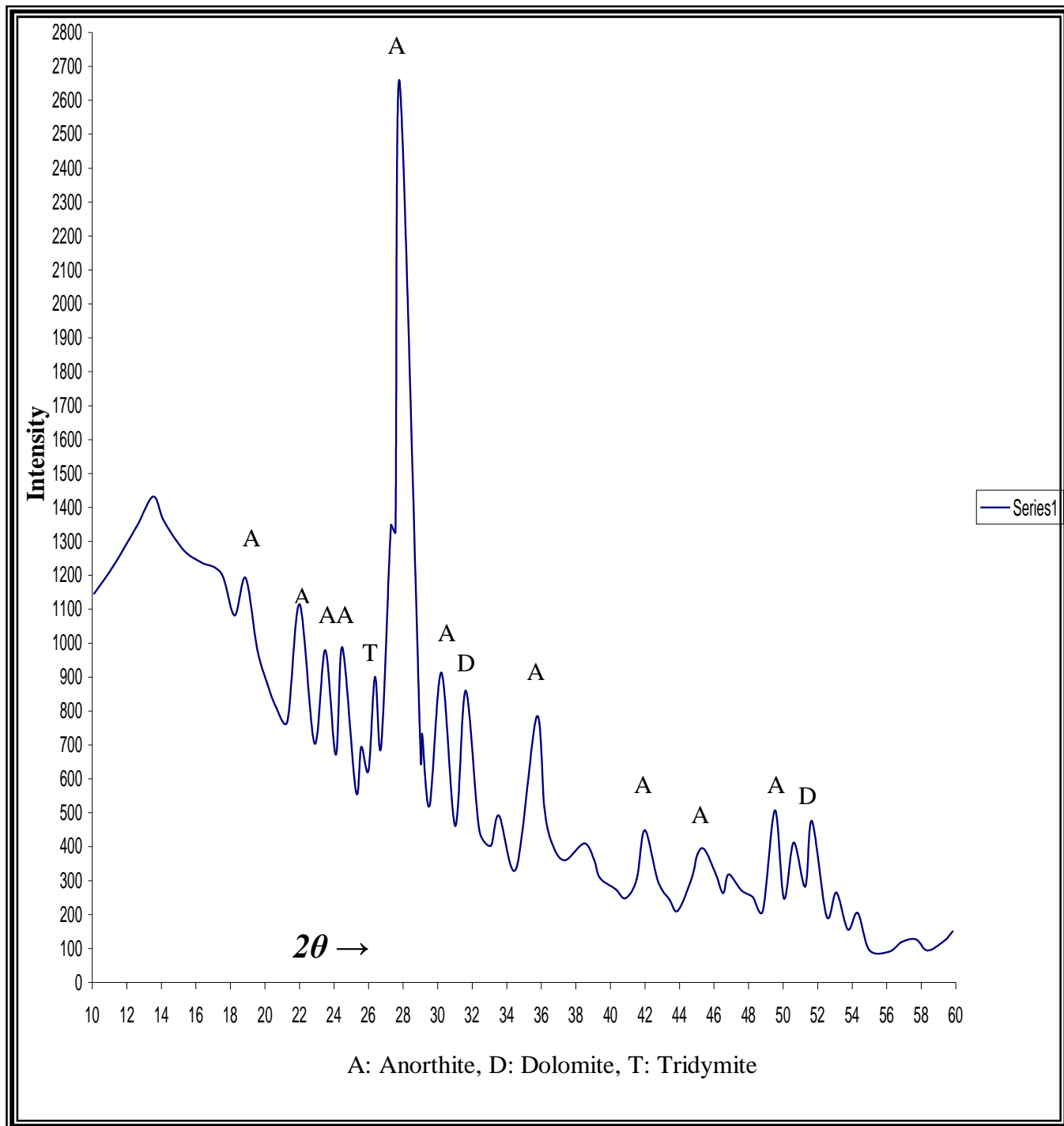


Fig.(3.23)XRD pattern for sample 85% K+15% CaCO₃ fired 1200 °C for one hours [M8]

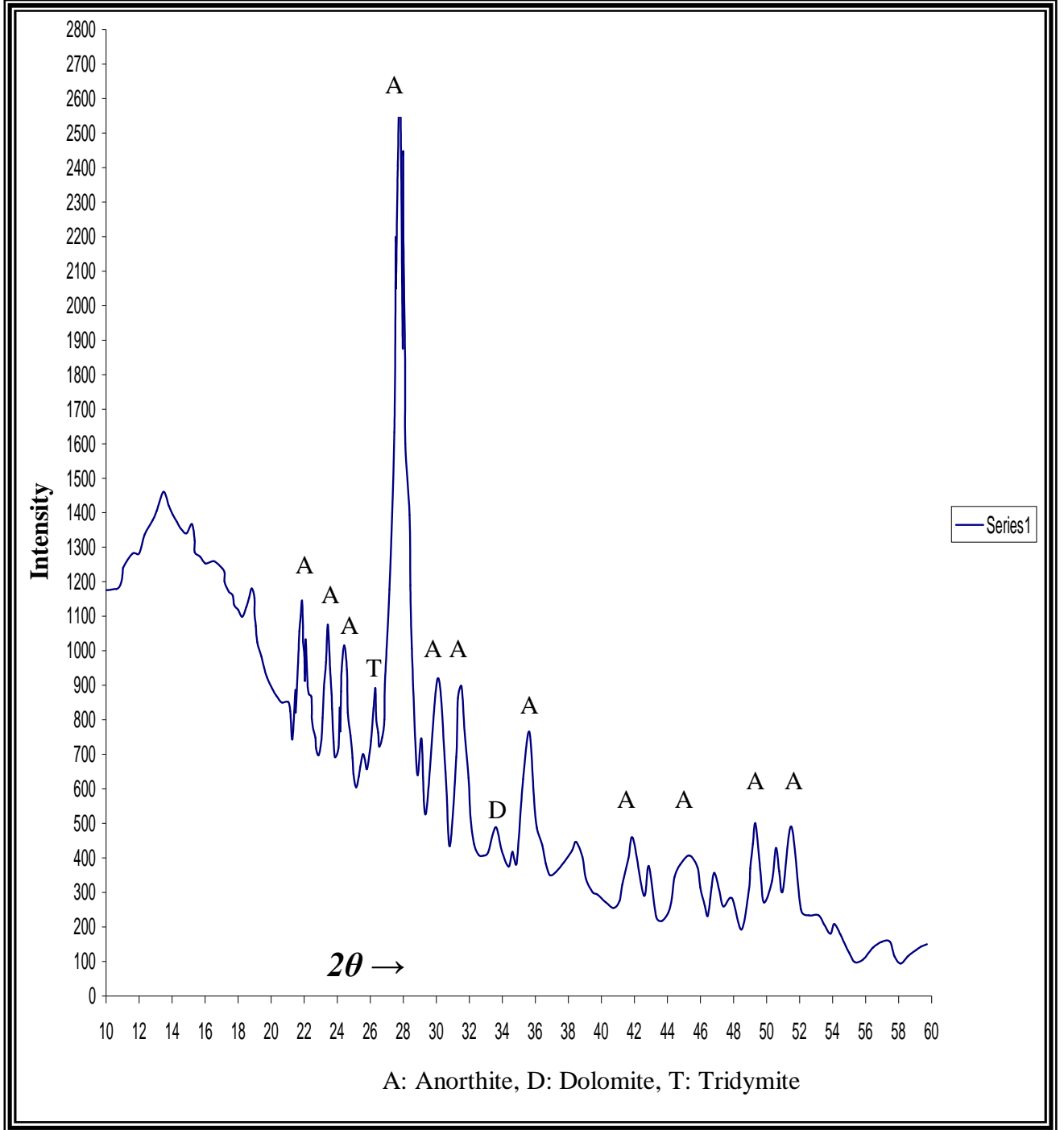


Fig. (3.24)XRD pattern for sample 85% K+15% CaCO₃ fired 1200 °C for 1wo hours [M8]

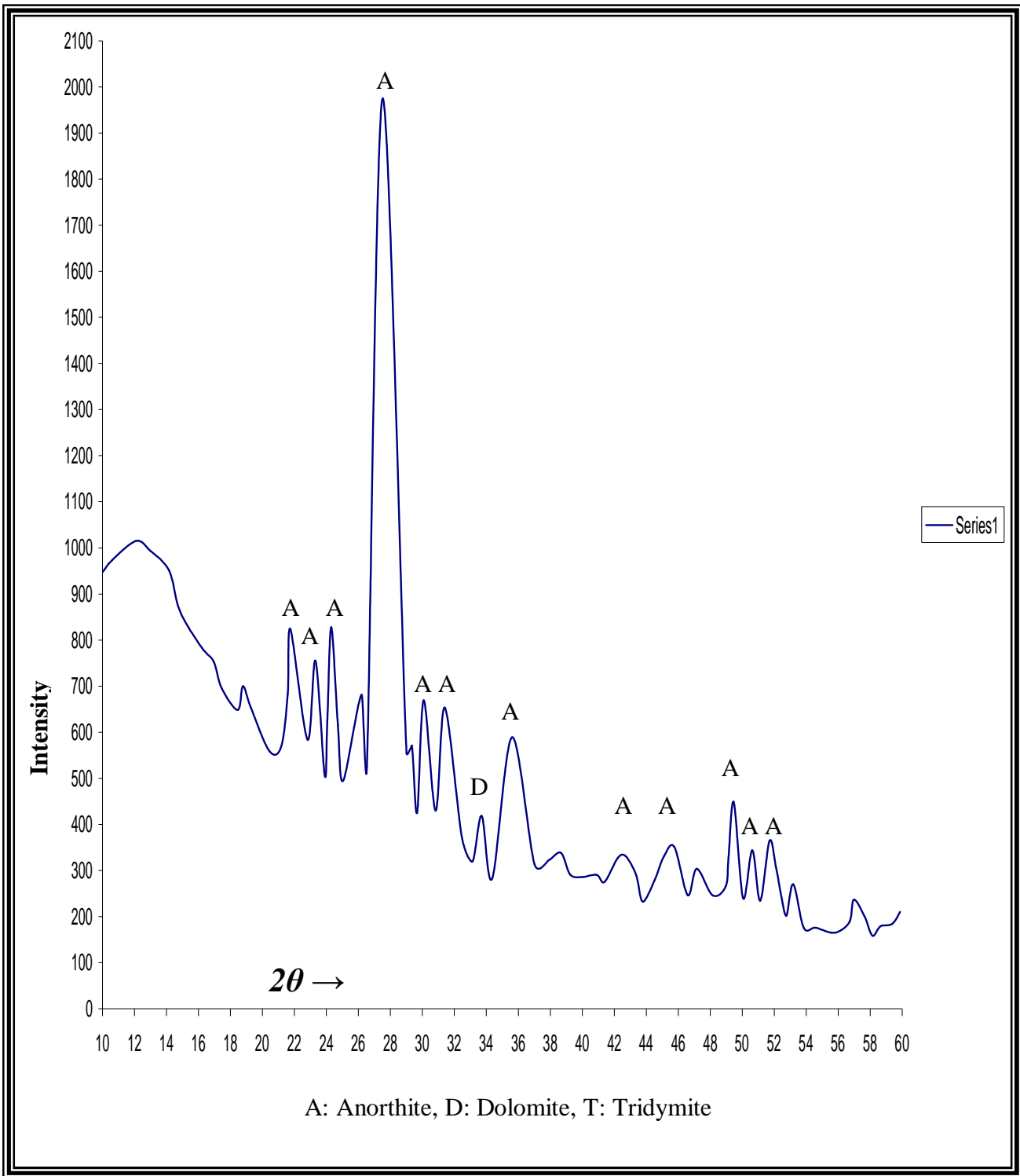


Fig. (3.25) XRD pattern for sample 85% K+15% CaCO₃ fired 1200 °C for three hours [M8]

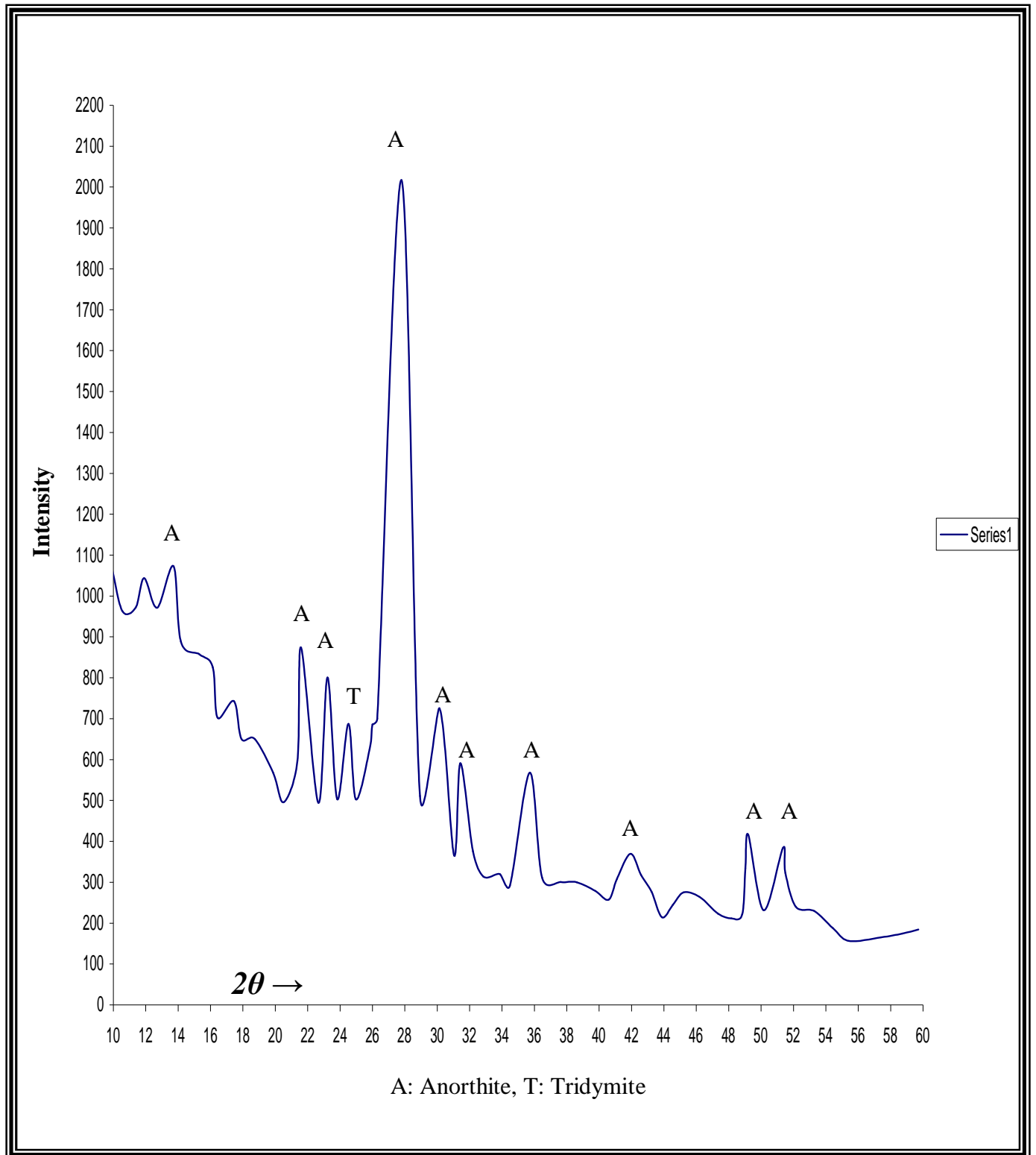


Fig. (3.26)XRD pattern for sample 85% K+15% CaCO₃ fired 1300 °C for one hours [M8]

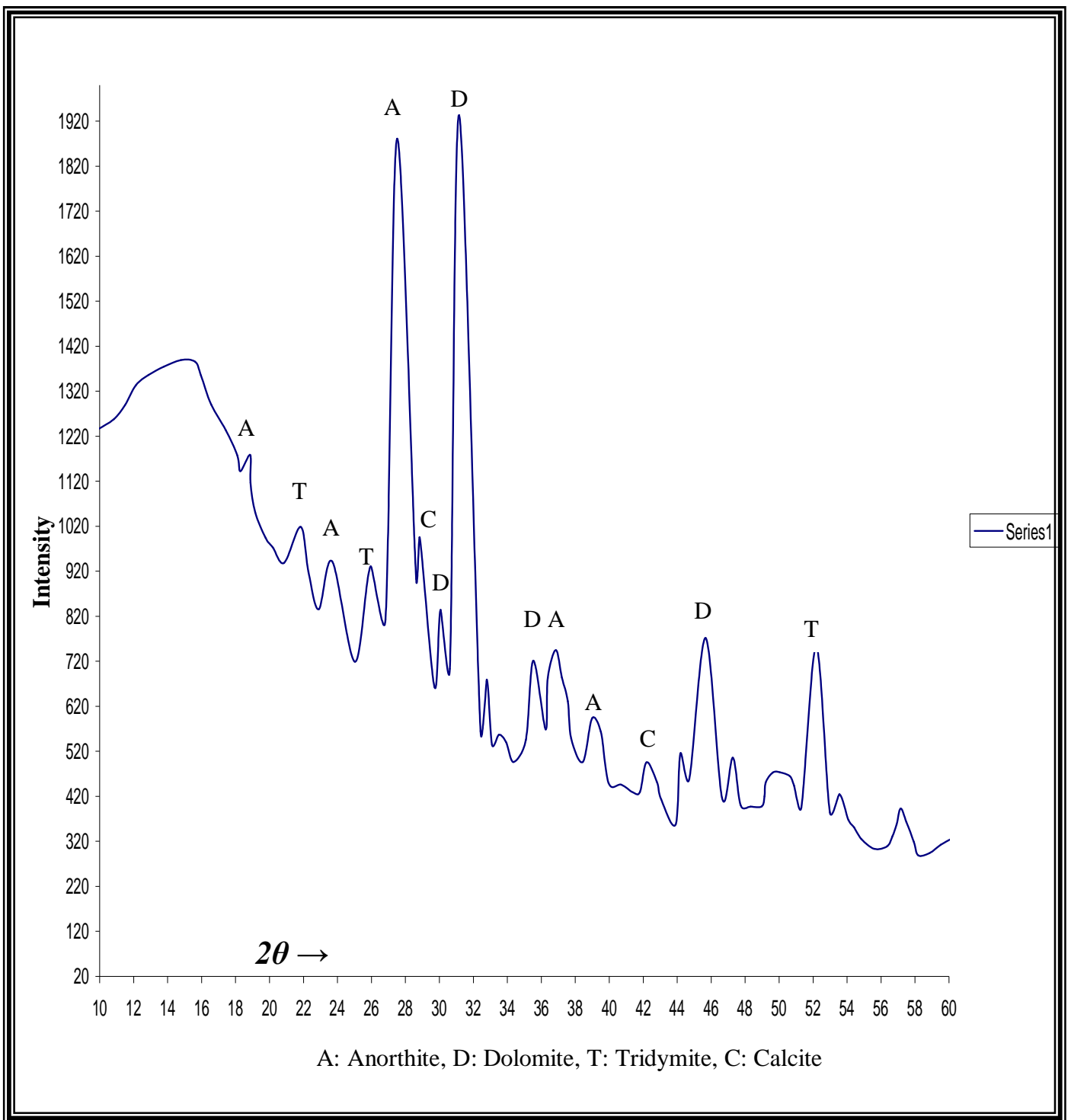


Fig.(3.27)XRD pattern for sample 70%C K+30% CaCO₃ fired 1200 °C for one hours [M1]

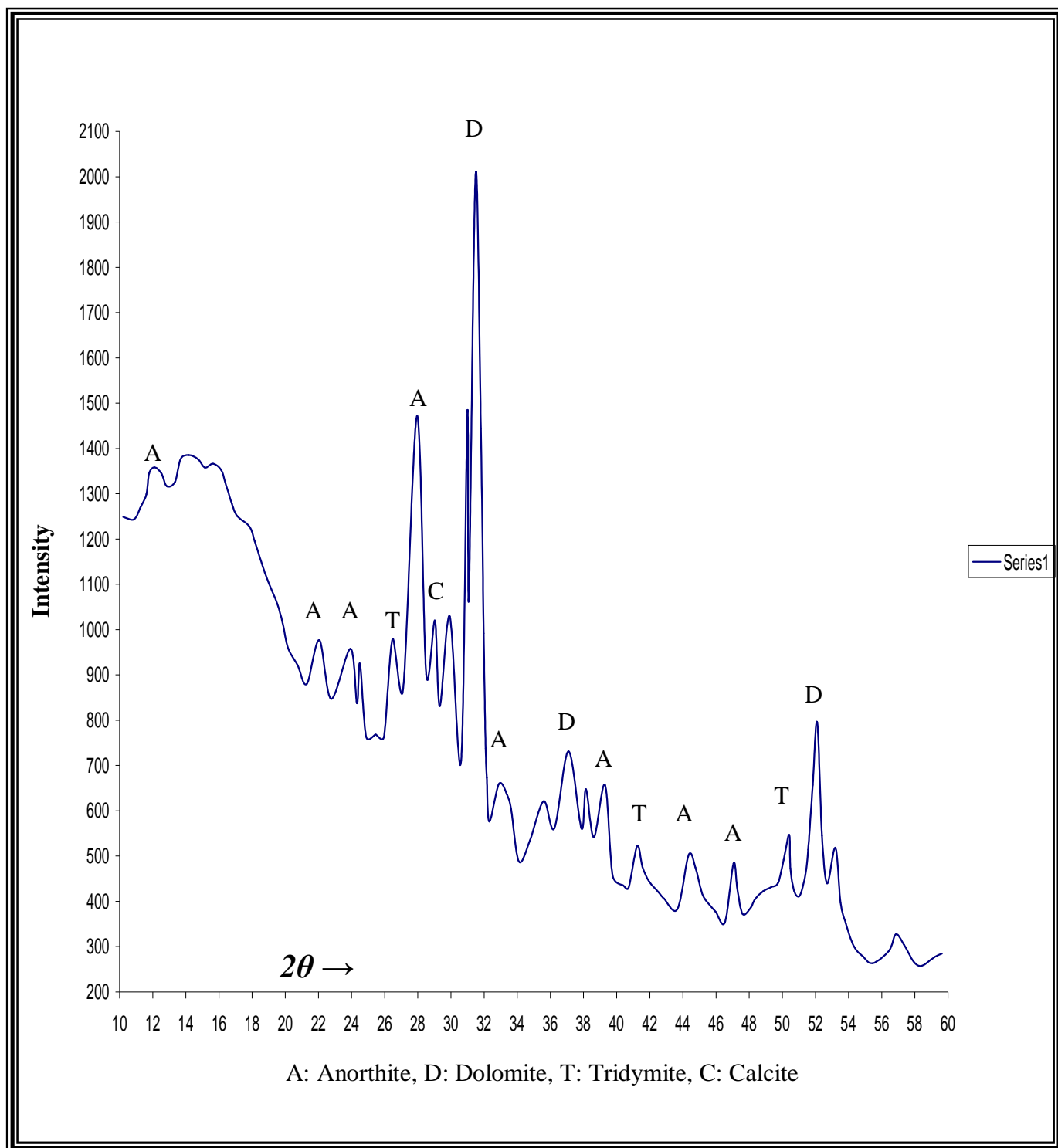


Fig.(3.28)XRD pattern for sample 70%C K+30% CaCO₃ fired 1200 °C for two hours [M1]

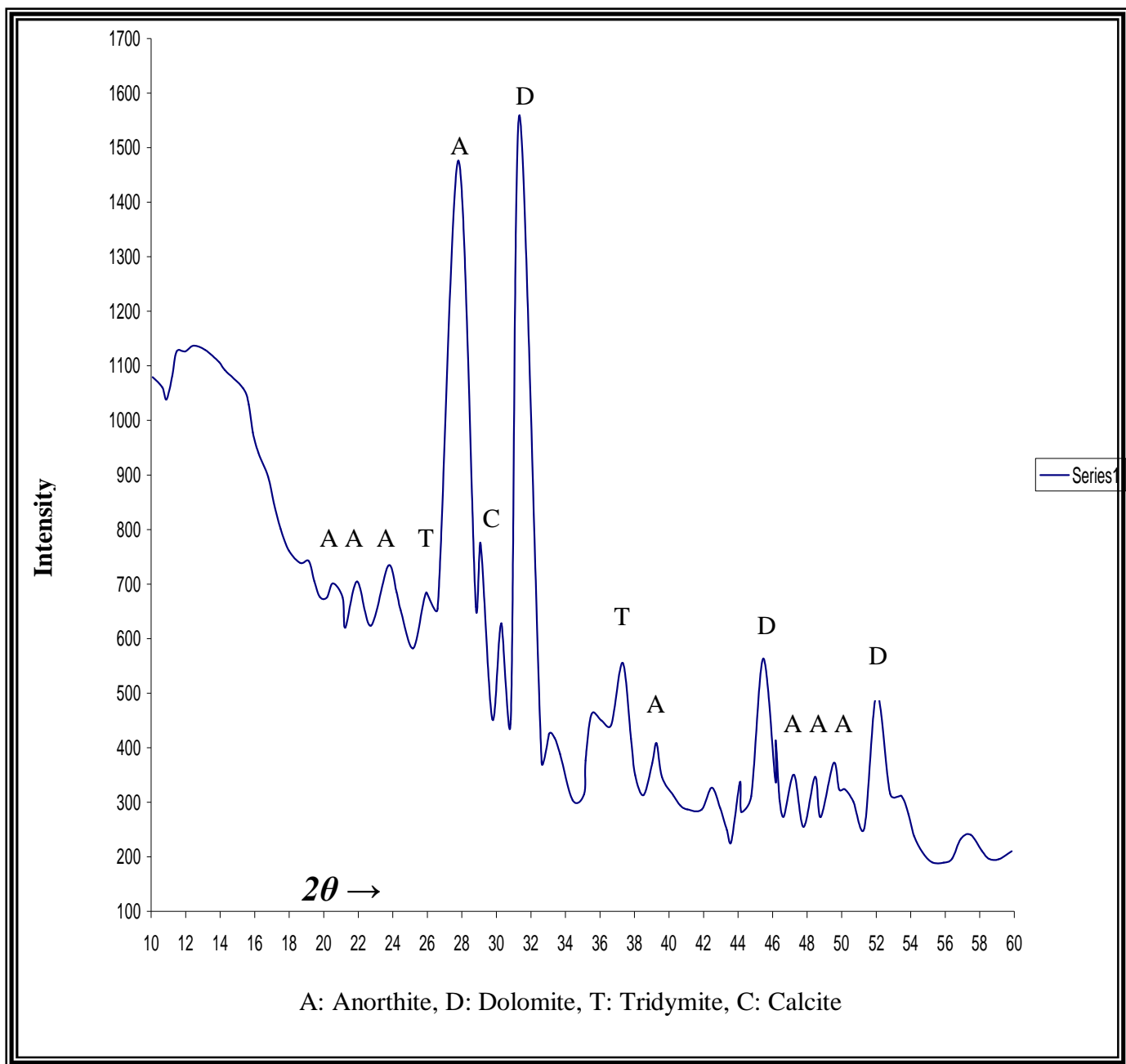


Fig. (3.29)XRD pattern for sample 70%K+30% CaCO₃ fired 1200 °C for three hours. [M1]

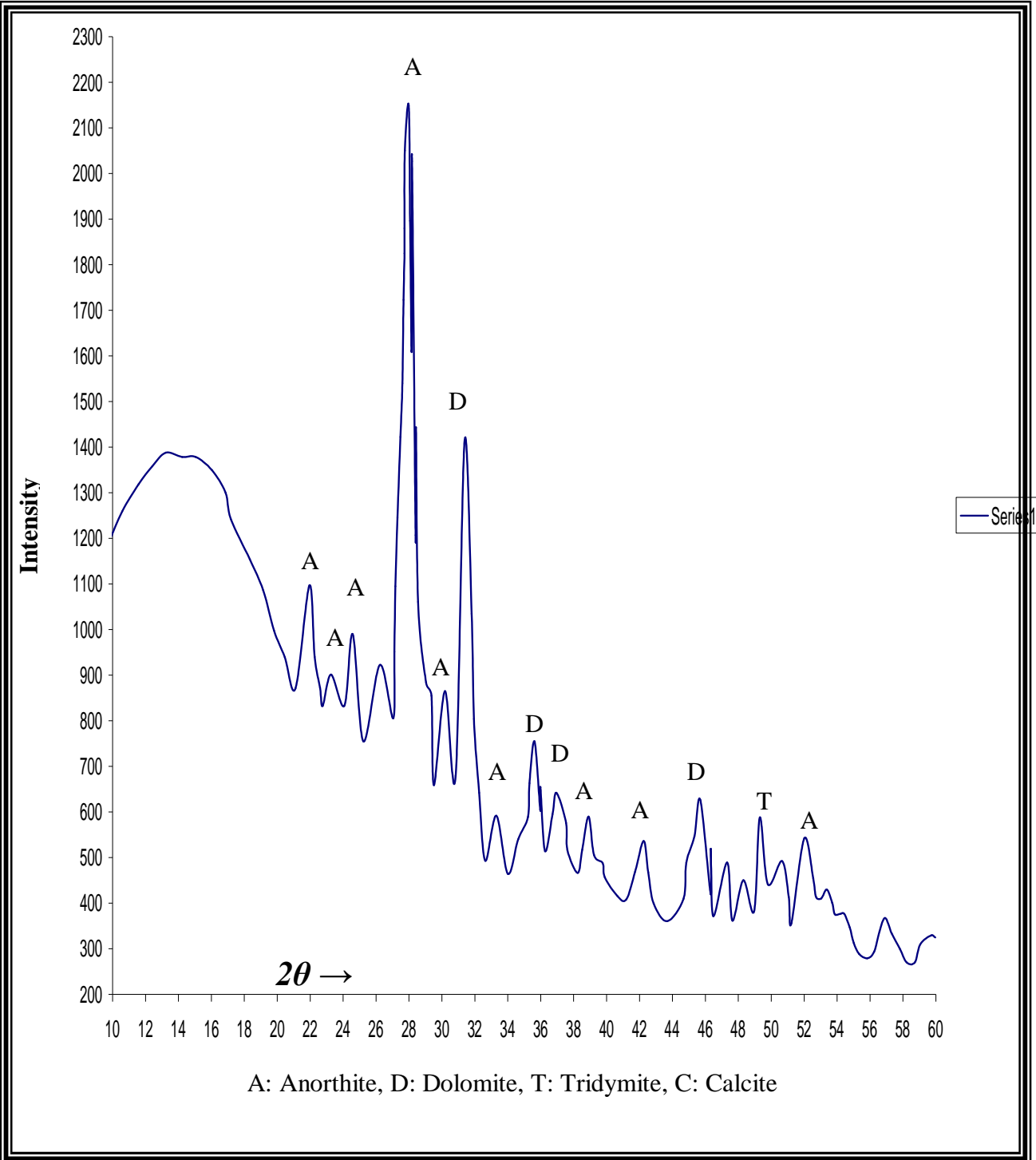


Fig. (3.30)XRD pattern for sample 75%C K+25% CaCO₃ fired 1200 °C for one hours. [M2]

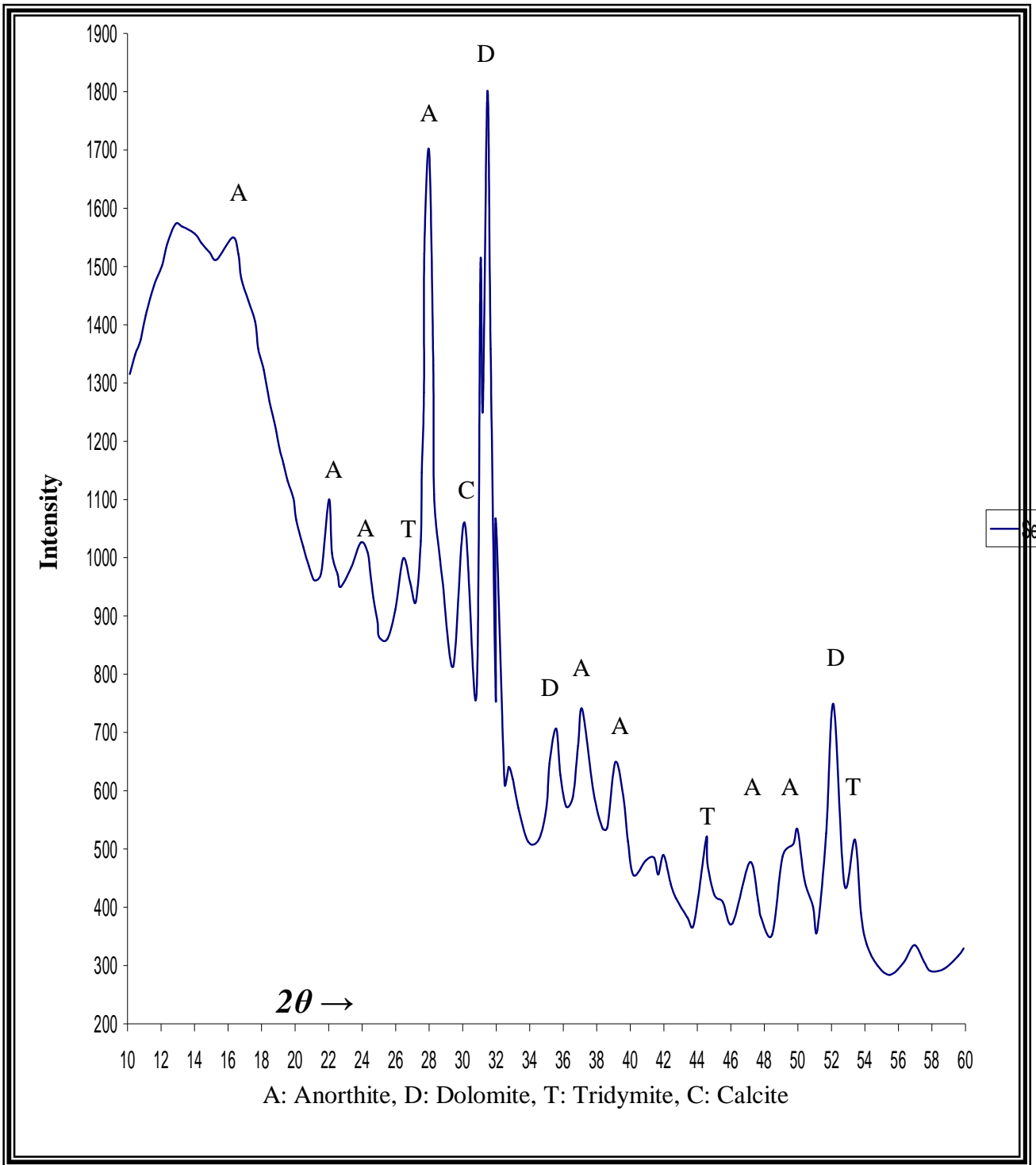


Fig. (3.31)XRD pattern for sample 75%C K+25% CaCO₃ fired 1200 °C for two hours. [M2]

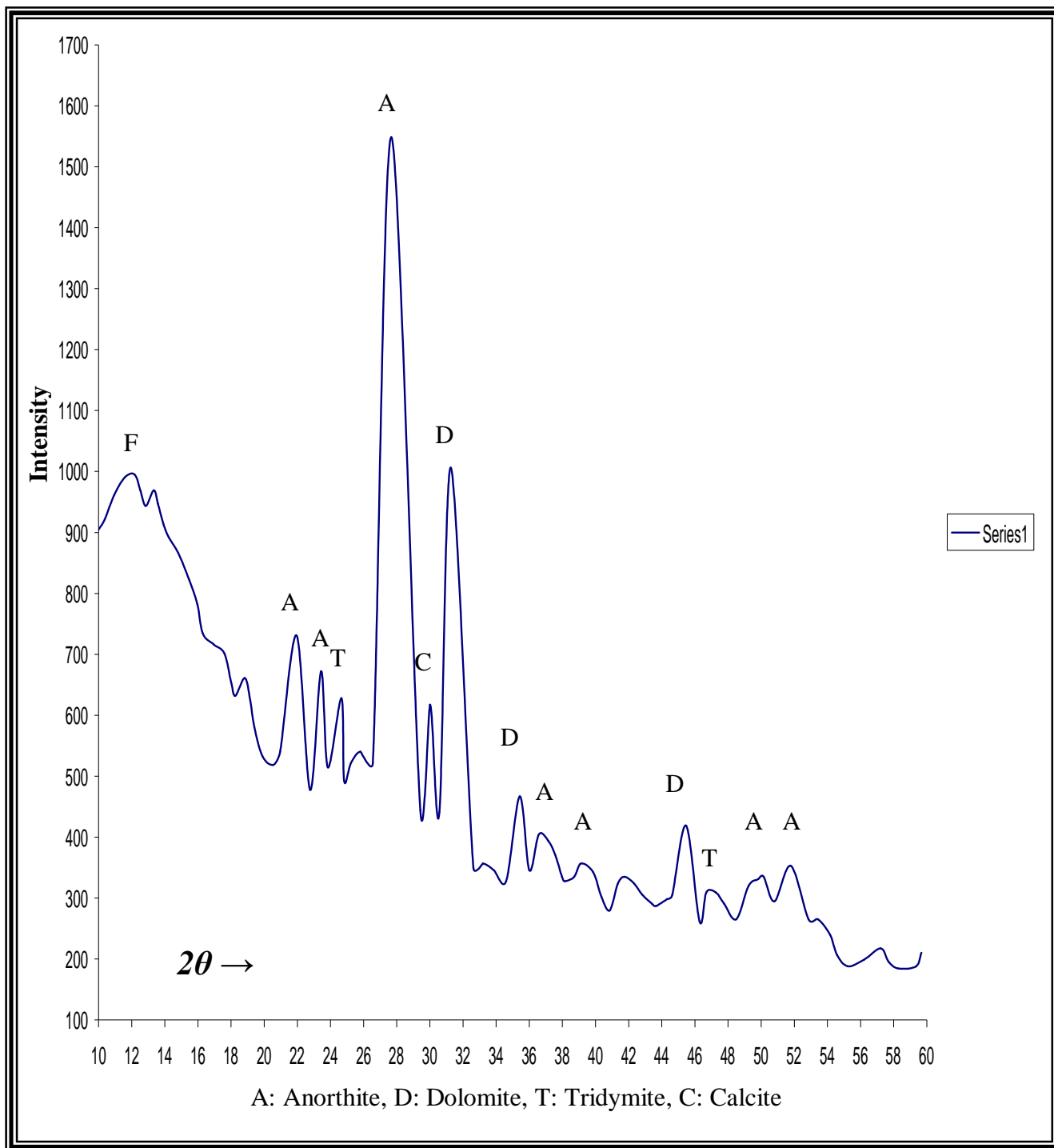


Fig. (3.32)XRD pattern for sample 75%C K+25% CaCO₃ fired 1200 °C for three hours. [M2]

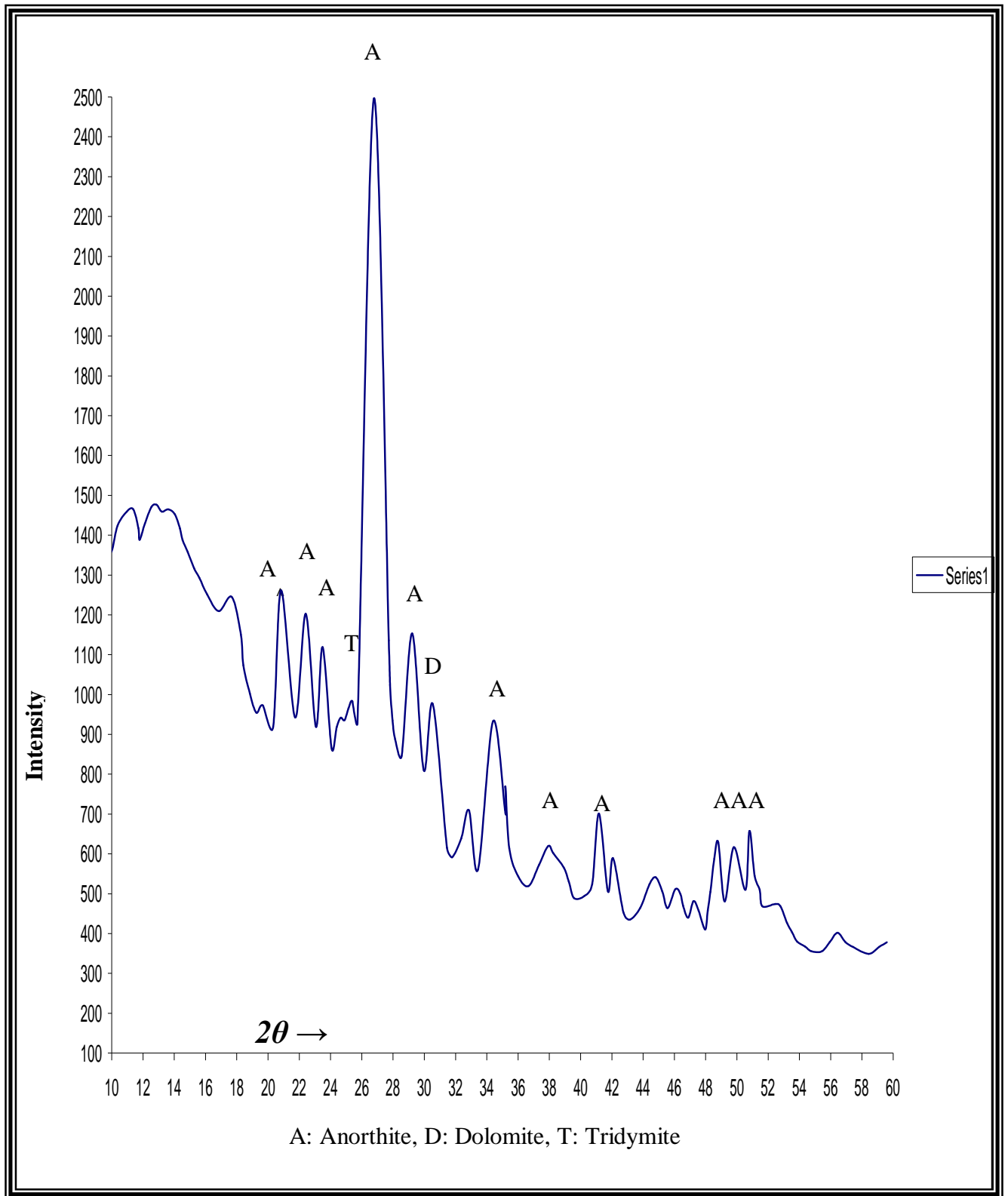


Fig. (3.33)XRD pattern for sample 80%C K+20% CaCO₃ fired 1200 °C for one hours. [M3]

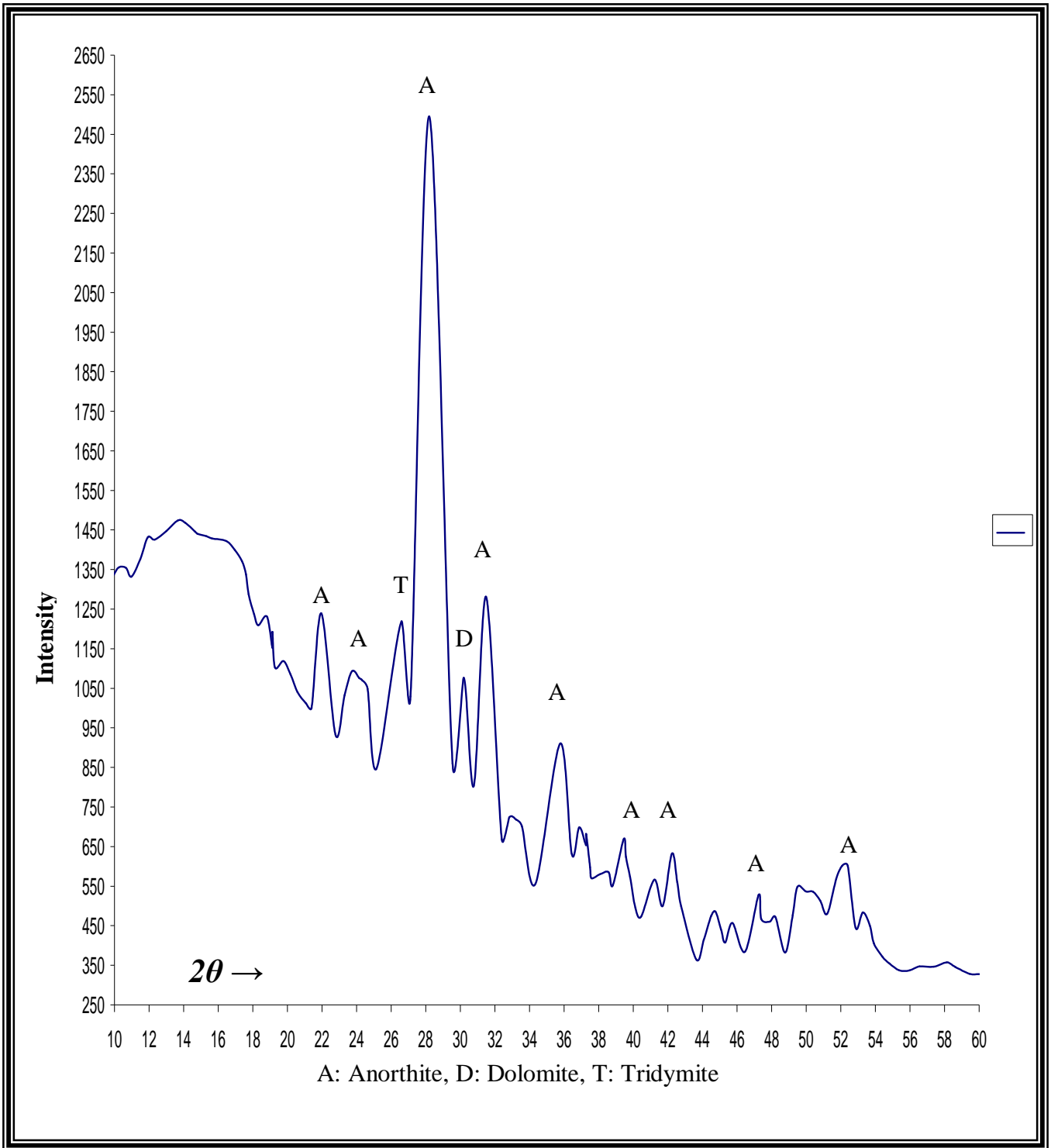


Fig. (3.34)XRD pattern for sample 80%C K+20% CaCO₃ fired 1200 °C for two hours. [M3]

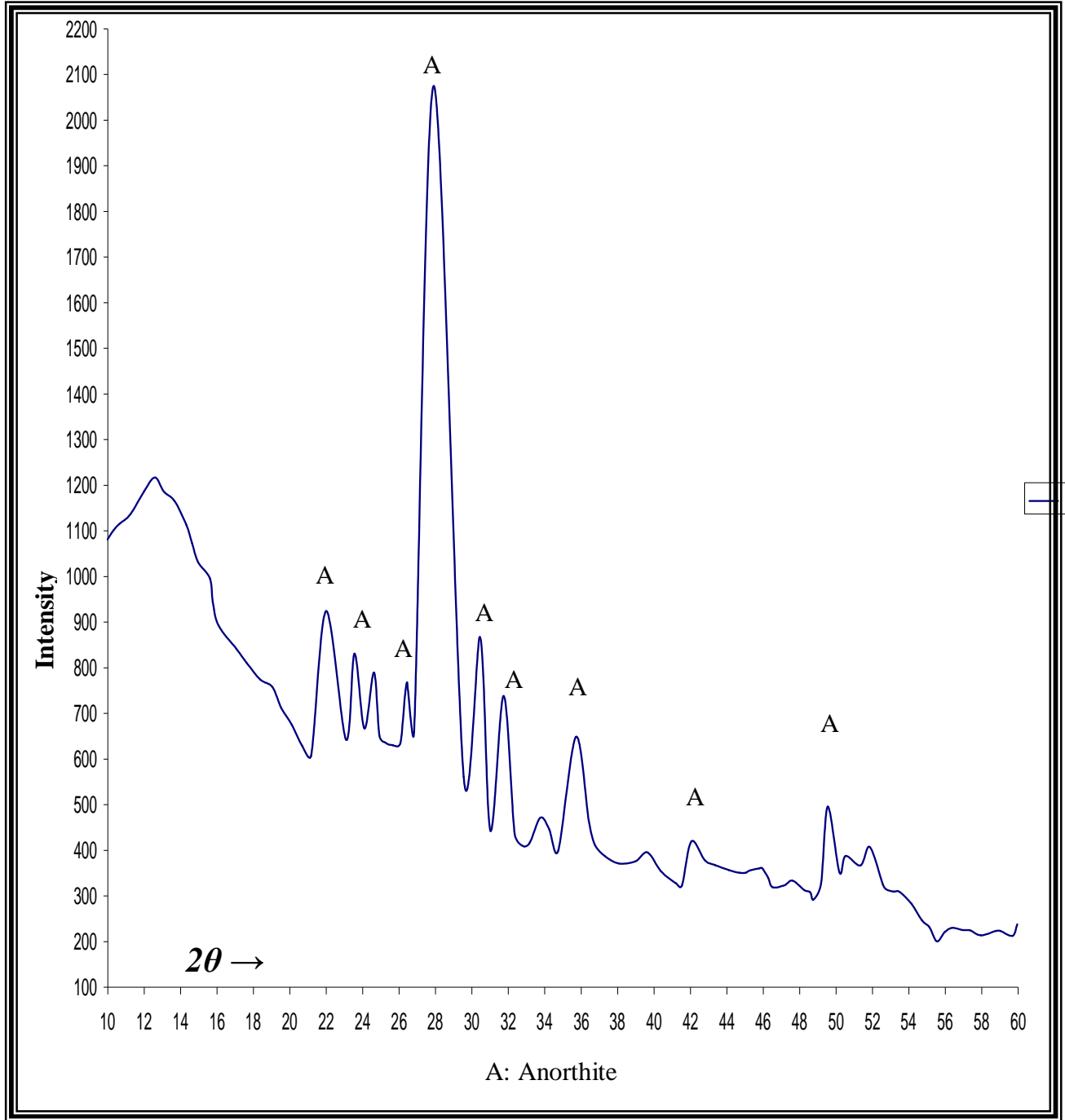


Fig. (3.35)XRD pattern for sample 80%C K+20% CaCO₃ fired 1200 °C for three hours. [M3]

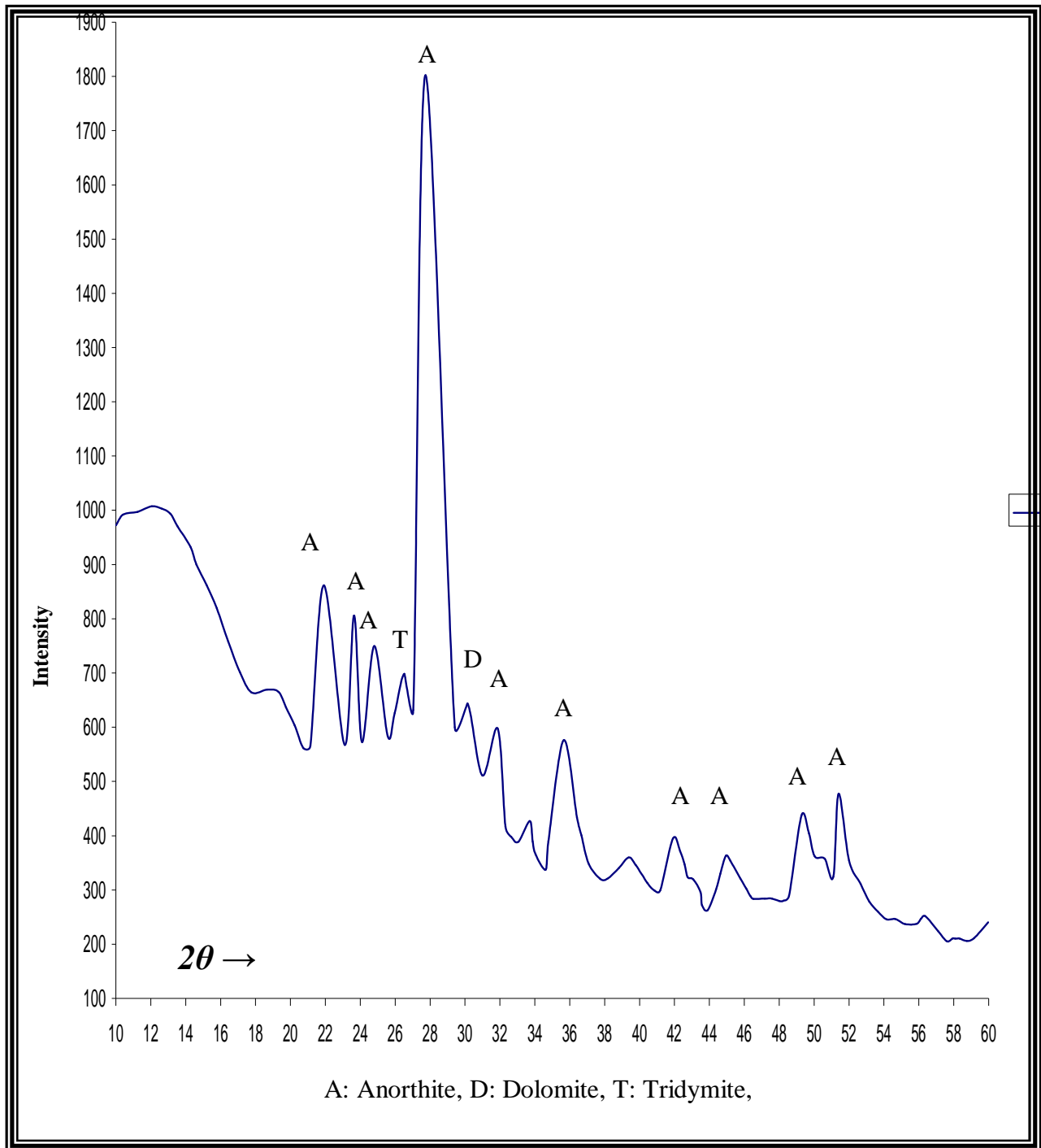


Fig. (3.36)XRD pattern for sample 80%C K+20% CaCO₃ fired 1300°C for one hour. [M3]

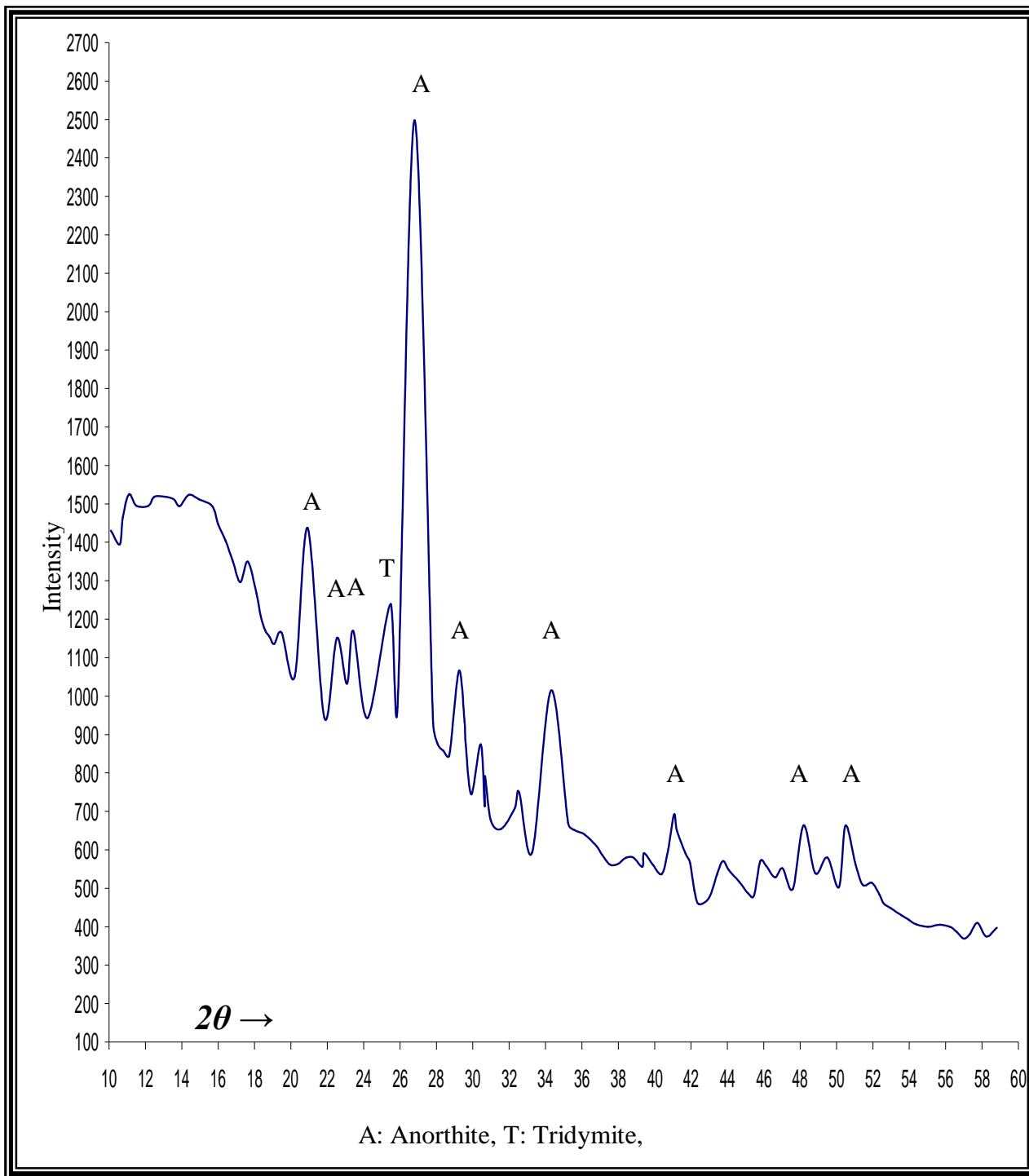


Fig. (3.37)XRD pattern for sample 85%K+15% CaCO₃ fired 1200 °C for one hours. [M4]

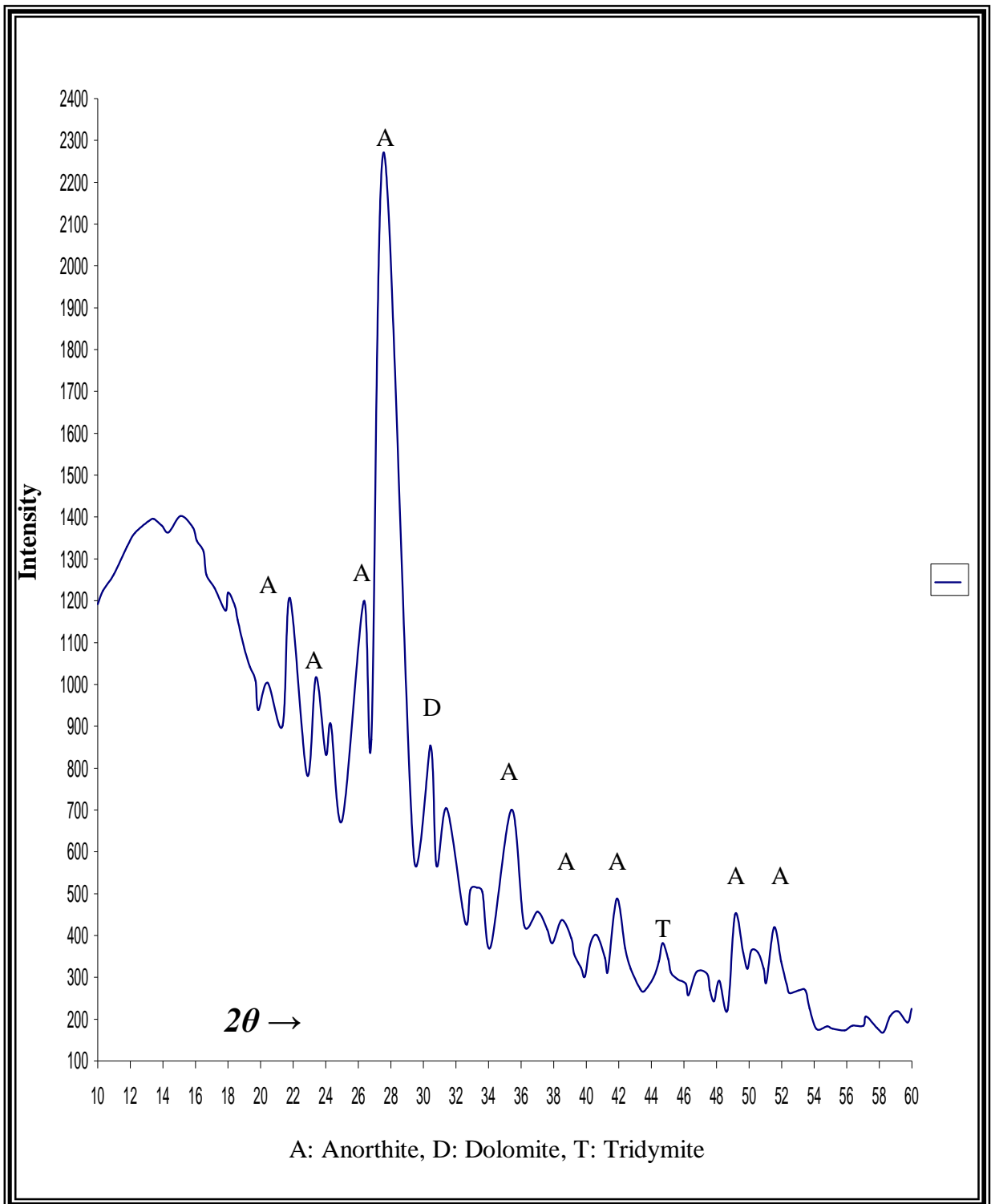


Fig. (3.38)XRD pattern for sample 85%C K+15% CaCO₃ fired 1200 °C for two hours [M4]

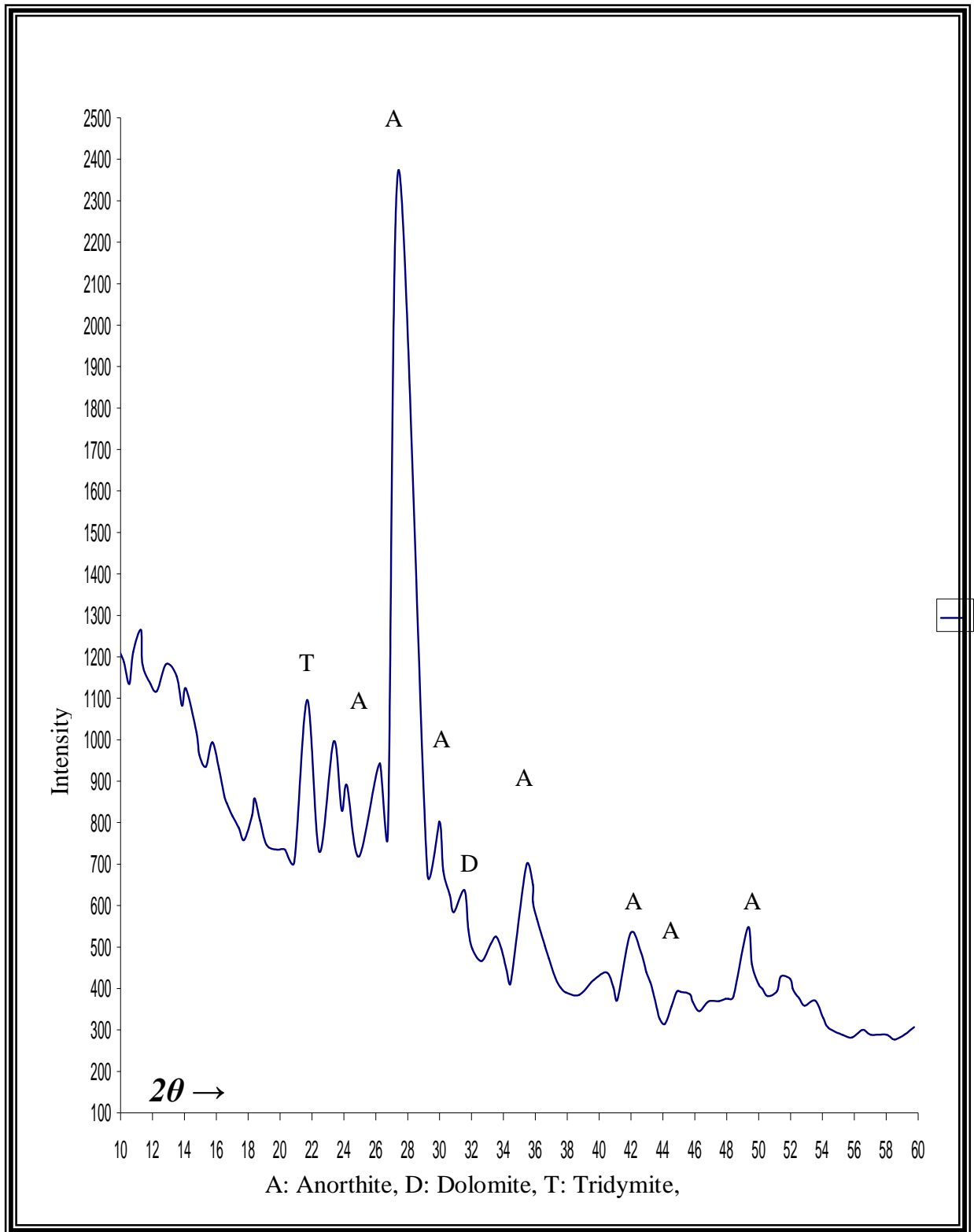


Fig. (3.39)XRD pattern for sample 85%C K+15% CaCO₃ fired 1200 °C for three hours [M4]

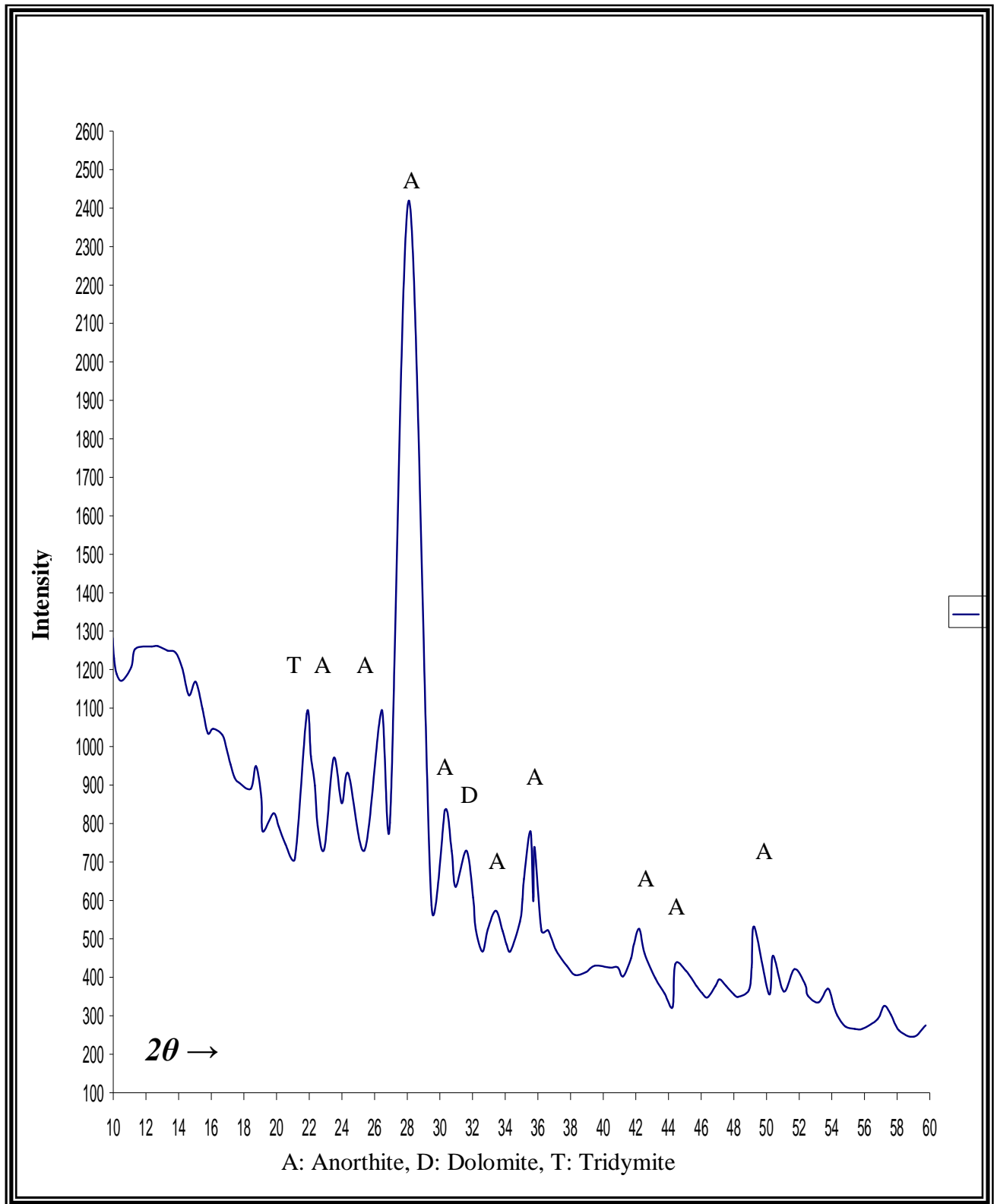


Fig. (3.40)XRD pattern for sample 85%CaK+15%CaCO₃ fired 1300 °C for one hours [M4]

3.2.4 Dielectric Properties Measurements:

The capacitance C_p and $\tan \delta$ of the sample are measured by **LCR** meter (model (Agilent 4294A, Parcition impedance analysis, **40Hz** to **110Hz**)).

Dielectric constant are calculated by using equation (1-4), and dielectric loss index is calculated by using equation (1-13).The results are 3lotted against applied frequency, as a function of sintering temperatures(1200°C /3hrs). The measuring frequency range is from 40Hz to 1 MHz; as table (3-3) which is sufficient to satisfy the requirement for the dielectric measurements in the present work. The behaviors of dielectric constant were taken of each applied frequency as shown in figures from (3-40) to (3-48).

Sintering temperature		1200 for 1 hr	
Group No.	Samples No.	Dielectric constant at 1MHZ	Dielectric dissipation factor
1.calcent Kaolin and calcium carbonate	[M1]70% K+30% C	4.3982	0.059551
	[M2]75% K+25% C	4.3657	0.11162
	[M3]80% K+20% C	5.7788	0.0046658
	[M4]85% K+15% C	4.2873	0.014707
2. Kaolin and calcium carbonate	[M5]70% K+30% C	4.7582	0.073355
	[M6]75% K+25% C	3.6224	0.052853
	[M7]80% K+20% C	5.5014	0.0042969
	[M8]85% K+15% C	4.8255	0.035457
Slandered R. of Anorthite		5.2 - 8	0.006

Table (3.4) dielectric constant and those Dielectric loss indexes at frequency of 1MHZ.

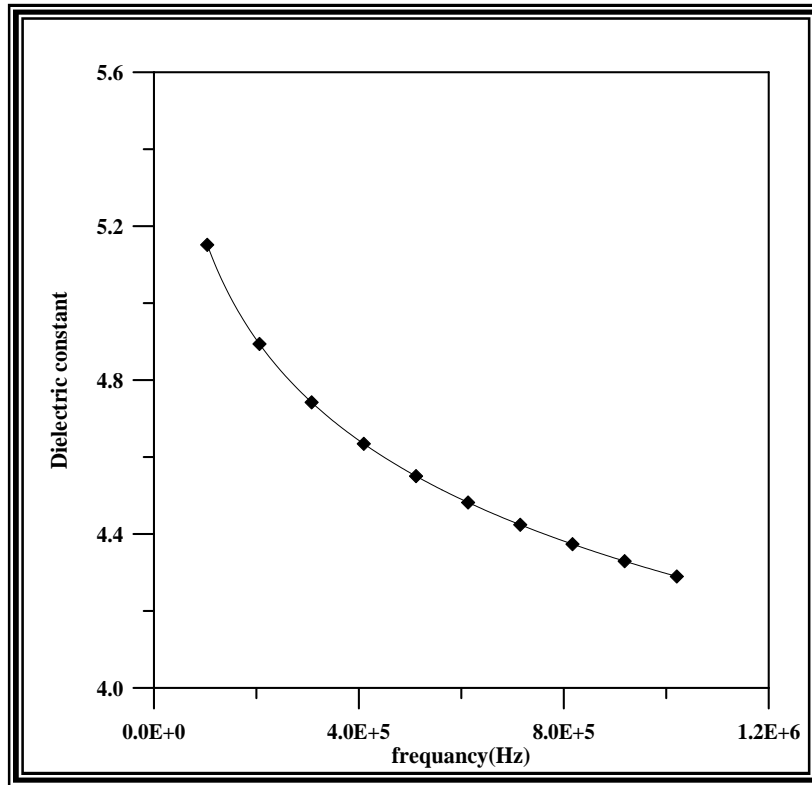


Figure (3.41) Dielectric Constant for sample M₁

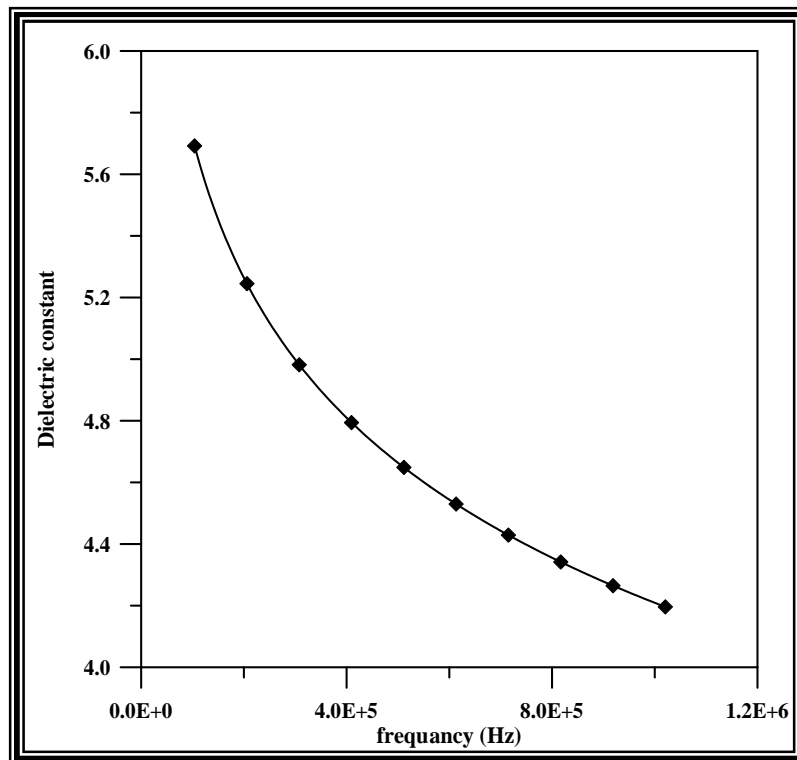


Figure (3.42) Dielectric Constant for sample M₂

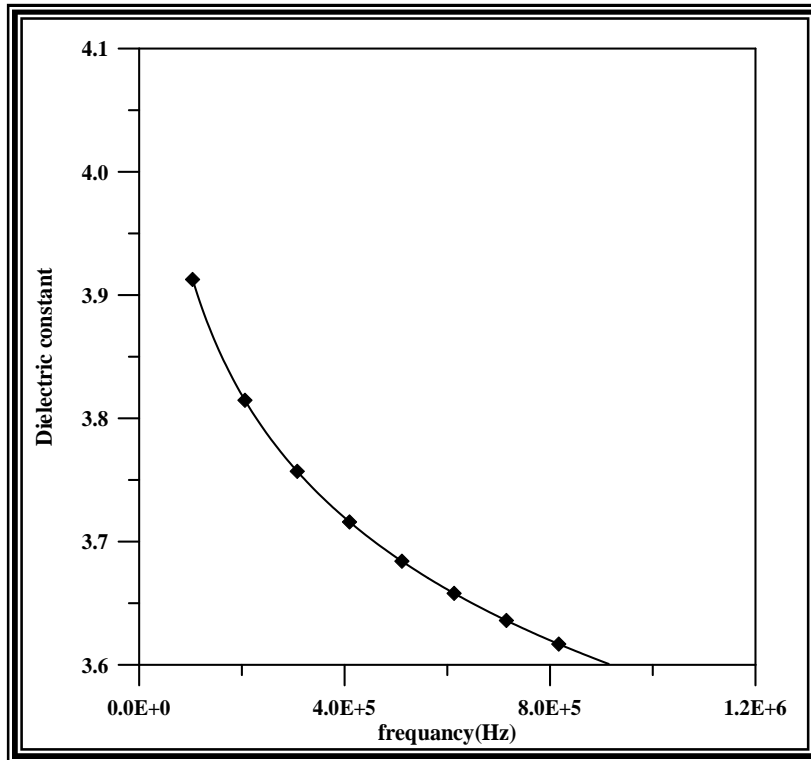


Figure (3.43) Dielectric Constant for sample M₃

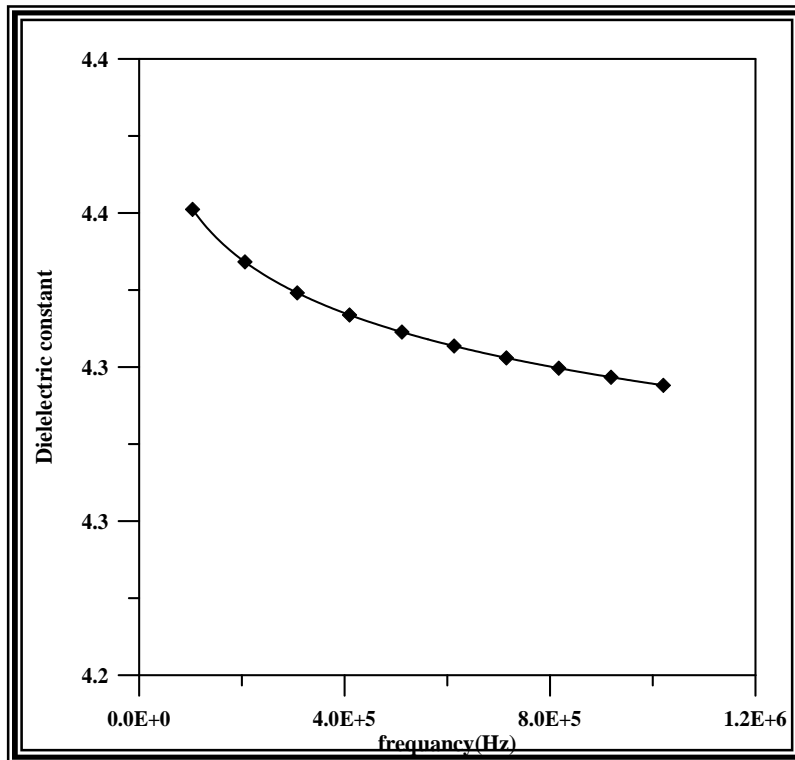


Figure (3.44) Dielectric Constant for sample M₄

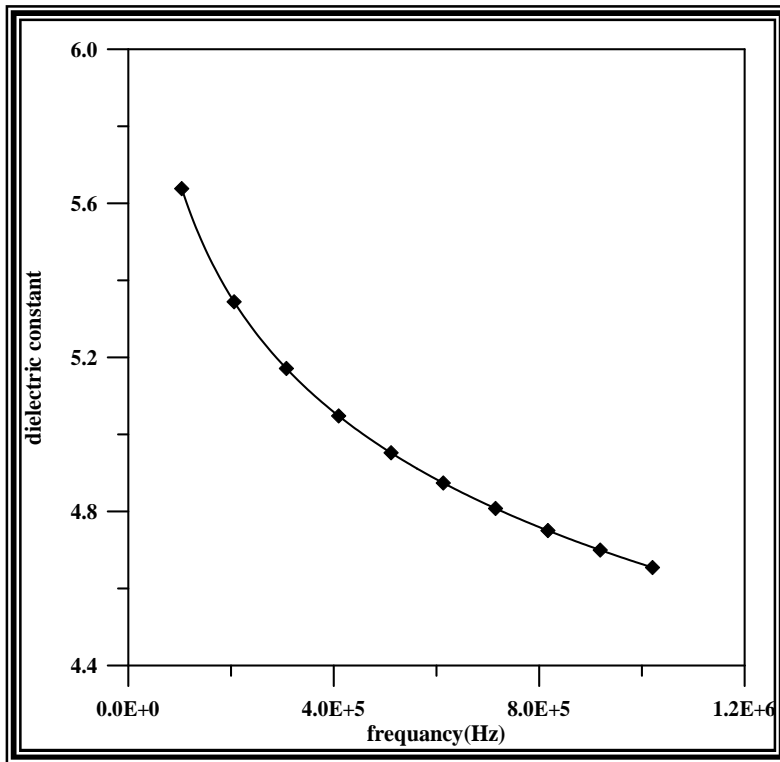


Figure (3.45) Dielectric Constant for sample M₅

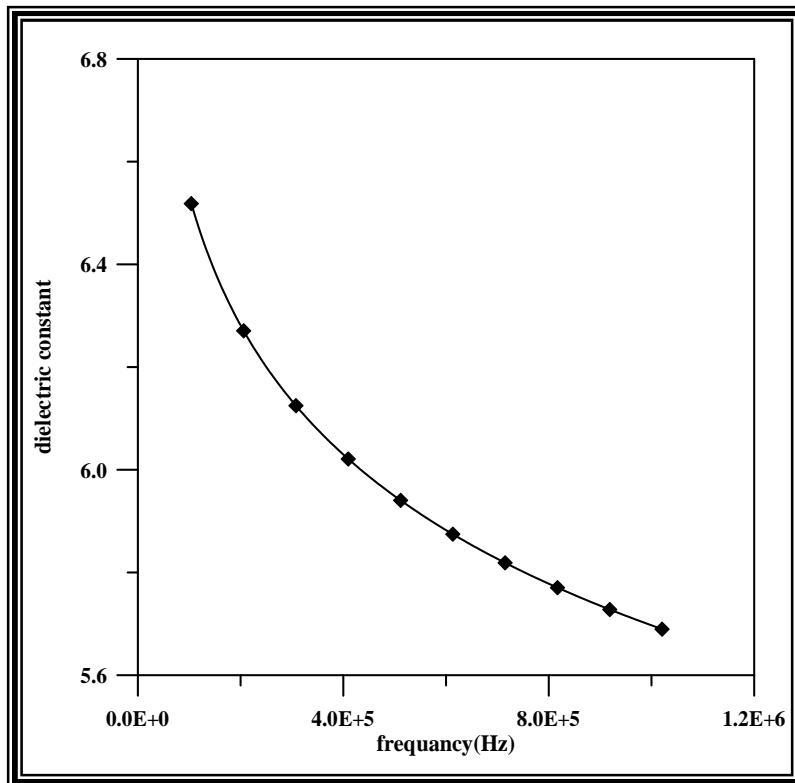


Figure (3.46) Dielectric Constant for sample M₆

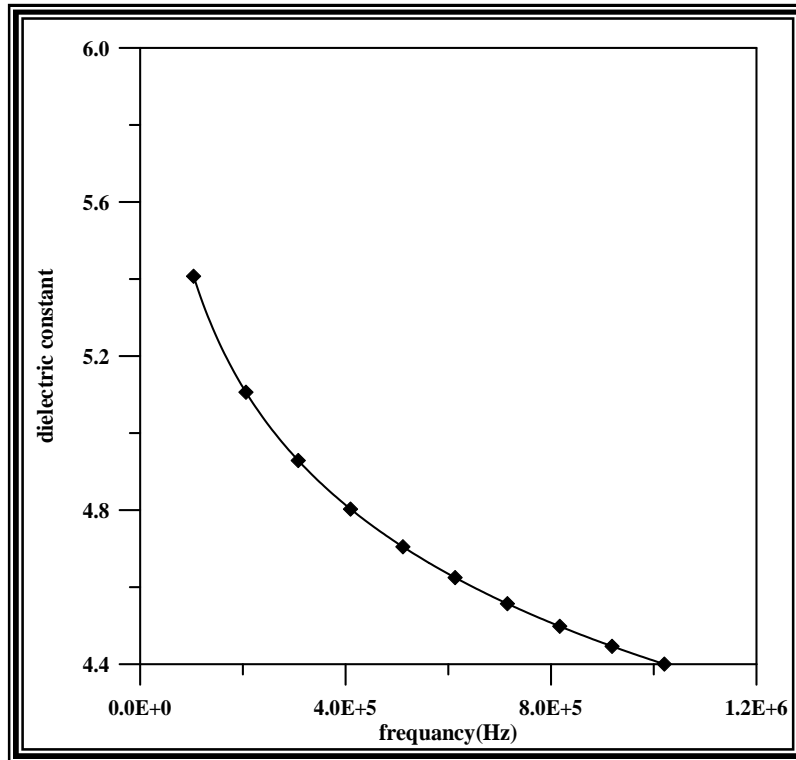


Figure (3.47) Dielectric Constant for sample M₇

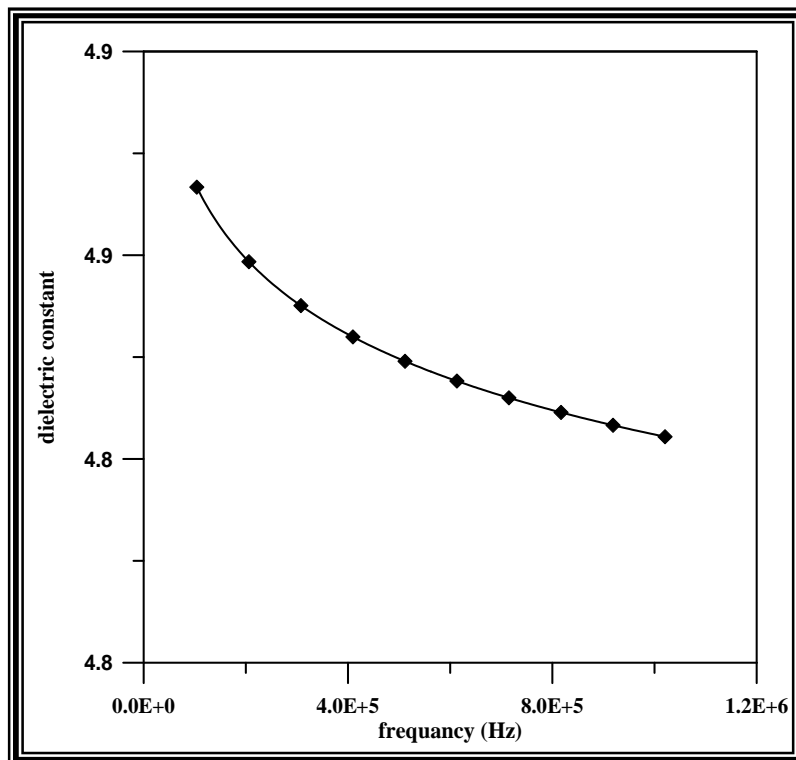


Figure (3.48) Dielectric Constant for sample M₈

Chapter four

Discussion of results, conclusion & future work

4.1 Raw and product Material Characterization:

At the first we must discuss the step of preparing the Kaolin raw material.

1. Processes of washing at the first by distilled water to remove the high ratio of melt in the Kaolin Duekhla.
2. Washing by HCL to remove the free ions of iron in the Kaolin.
3. Another step of washing by distilled water to remove HCL from the solution.
4. Then drying at the temperature rang between (70 -80)°C , milling and sieving to get a fine powder of Kaolin.
5. Sedimentation to get a very fine powder of Kaolin with particle size less than 20 µm.

The second material is calcium carbonate so it applied to some processes, milling with ethanol; to prevent the aggregation in the milling then drying and another step of milling to get a very fine powder of CaCO₃.

Then study the changes of the two materials after these processes by XRD and IR analyses.

4.2 XRD characterization :

The XRD test will be made for all prepared samples gives many of formation about the mixture, so by study these results and comparing with the ASTM of Anorthite material from (The company of Geological survey in Iraq) **table (4, 1)** we saw that the samples will be prepared by mixing 80% of Kaolin Duekhla and 20% of CaCO_3 and heat treatment at 1200°C for 3hrs will given an anorthite material.

So we will discuss the result of XRD test only for these samples (80% Kaolin +20% CaCO_3). If the degree temperature change from 1200°C for 1hr, 2hrs, and 3hrs to 1300°C for 1hr there are many peaks will be pear and disappear, in the figure (3, 19) we saw Tridymite ($\text{Al}_2\text{O}_3 \cdot 2\text{SiO}_2$) material in the intensity peak (1000), (850) and Dolomite ($(\text{CaMg})\text{CO}_3$) material in the intensity peak (800) , Anorthite ($\text{CaAl}_2\text{Si}_2\text{O}_8$) material in the primary intensity peak (1925) and minor intensity peaks for Anorthite in different location.

In the figure (3, 20) saw the intensity peaks for Tridymite and Dolomite will be degrees but the primary intensity peak for the Anorthite will increase and become at (1965).

In the figure (3.21) saw the peaks of Tridymite and Dolomite disappear and the peaks of anorthite will be very clear.

20-20

CALCULATED PATTERN-PEAK HEIGHT
See 20-20A

C

3.19	3.18	3.21	100	91	63	d A	I/I ₀	h k l	d A	I/I ₀	h k l
CaAl ₂ Si ₂ O ₈						5.76	19	112	2.323	8	332
						3.62	33	130,132	2.295	3	133
Calcium Aluminum Silicate						3.51	4	132	2.270	7	332,116
						3.46	14	131,114	2.239	4	352,244
Anorthite (Feldspar)						3.40	7	222	2.158	4	226
						3.36	25	114	2.142	17	242,060
Ref. Borg and Smith, Am. Mineral., 53, 9 & 10, 1709-23 (1968)						3.26	52	220	2.118	4	245
						3.21	63	040	2.095	10	152
Sys. Triclinic						3.19	100	204	2.067	3	045
						3.18	91	004	2.025	3	154
S.G. P1 (2)						3.12	39	220	2.017	5	204,202
						3.04	18	132	2.005	4	312
a ₀ 8.1768						2.952	27	042	1.992	3	136
						2.934	19	024	1.986	4	062
b ₀ 12.8768						2.893	8	224	1.966	4	312
						2.828	20	132	1.958	3	224
c ₀ 14.1690						2.804	9	134	1.932	9	224
						2.655	14	134	1.921	4	224
α 93.17°						2.559	6	222	1.892	4	352,260
						2.526	20	114,242	1.878	7	224
β 115.85°						2.501	28	314,242	1.845	12	333,246
						2.437	6	222,310	1.837	16	064,400
γ 91.22°						2.406	4	152	1.810	5	260
						2.384	4	310	1.801	8	264,170
V 1338.83						2.359	5	152,240	Plus 24 lines to	1.444	
						Scale factor (Integrated Intensities)					
λ 2.5405											
d A	I/I ₀	h k l	d A	I/I ₀	h k l						
6.81	8	111	4.69	14	022						
6.52	8	110	4.24	2	003						
6.42	4	020	4.04	48	202						
5.12	2	111	3.92	11	112						
5.00	1	121	3.78	28	130,131						

Table (4, 1) ASTM for anorthite peaks

4.3 IR characterization:

The results of XRD give the indication about the best samples of Anorthite. The IR analyses were made only for the samples that contain about (80% Kaolin +20% CaCO₃).

These tests are another proves for the Anorthite material by comparing the results we get it by the standard data of Anorthite as shown in the table (4.1). The data of figures (M3, M4) represent the absorption peaks for anorthite, the Anorthite data having shifting from standard data that shifting com from the (1) the different in the particle size (2) the contrition of KBR in the samples (3) resolution of the devise [77].

Standard peaks		Anorthite peaks
1440 w,b		1438.8
1160.35 s		
1085.77 m		
1020.11 b,sh	doublet	1018
987 b,sh	doublet	
950.46 sh	doublet	921.9
773 sh		771.5
758.56 w		
728.27 m,sh		
668.62 m,sh		690.5
624.20 m	triplet	
603 sh	triplet	
575.66 m	triplet	
540.36 m		
470 w,b		466.7
433 sh		

Table (4, 2) standard peaks of anorthite [77]

Where w = weak (< 20% absorption)

b = broad

s = strong (< 80% absorption)

m = medium (< 40% absorption)

Sh = shoulder – just resolved

4.4 dielectric properties:

The dielectric properties of **Anorthite** are measured and the results are presented in figures (3.41) to (3.48) and table (3.4).

Table (3.4) presents a comparison between standard values of dielectric constant and those Dielectric loss indexes at frequency of **1MHZ**. Inspecting table (3.4) and fig. (3.41) to(3.48), it is observed that the samples product under a pressure of (**3 Mpa**) and sintering at 1200 °C for 3hrs that were identified by **XRD** and **IR** analyses as **Anorthite** give the dielectric properties . Thus this considered a standard for the local product presented by the present work that was completed using Kaolin clays of Iraqi Duekhla. From [25] the dielectric constant for the anorthite material abuts (4-6) and the dielectric dissipation factor are (0.006).from the above it will give that M₃ and are the best samples according to the dielectric properties of rang Anorthite material.

4.5 Chemical analyses:

Chemical analyses had done for treated samples at 1200°C /3hrs where the effects of realized firing temperatures, concentrations of added proportions and realized phases has been studied. Those mixes were adopted and analyzed chemically; table (3, 3) illustrates the chemical analysis of these mixes for the prepared samples.

Using the Rational method, oxides ratios were calculated for those composing the Anorthite, as illustrated by table (4.2).The results contained in table (4.2) shows that there is some deviation of the calculated oxide proportions (of the samples) relative to those pure Anorthite. This deviation is attributed, which are.

1. The chemical analyses are an analysis by weight of [2-5] % error percentage.
2. The existence of impurities as shown in table (3.3) which are K₂O, Na₂O, Fe₂O₃.

In order to get Anorthite the excess free SiO_2 must be treated chemically before treating the Kaolin. And the existing Dolomite could be treated by controlling the ratio of added CaCO_3 . This is an optimal situation since the existence of MgO in Kaolin is an impurity that can not be removed. We chose these samples according to the ternary phase diagram as in figure (4, 1).

samples	CaO %	Al_2O_3 %	SiO_2 %
Pure Anorthite	22.4	36	41
M3	19.1	33.45	42.48
M4	23.12	30.08	43.54
M7	19.5	32.57	43.78
M8	21.7	30.47	45.88

Table (4.3) represents the chemical analyses for pure Anorthite and the samples prepared

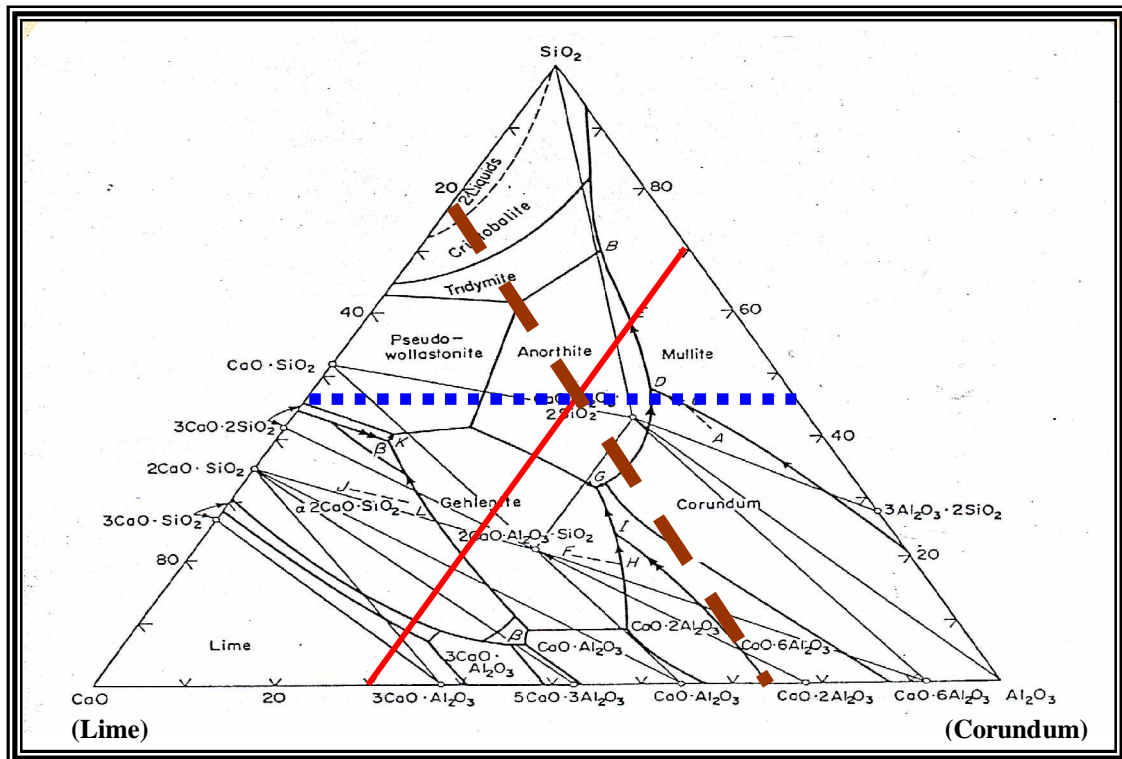


Figure (4, 1) ternary phase diagram

4.6 Conclusion:

1. Kaolin Duekhla mixed with calcium carbonate at limited particle size under the effect of heat treatment (1200°C/3hrs) gives an Anorthite material.
2. XRD and IR analysis explain the required condition to obtain the Anorthite material.
3. Increasing the firing temperature and effected time contribute in increasing % of Anorthite phase.
4. The washing process affects the contrition of the Iron oxides in the Kaolin; this will minimize the Dolomite phase (Ca Mg) CO₃ which comes from oxides existence to raw material.
5. The IR tests were conducted on the samples through XRD measurement at best ratio of 80% and 85% of washed Kaolin that is thermally treated and not thermally treated with 20% and 15% of calcium cabernet respectively because it is the samples that give a phase changing for thermal treatment at 1200°C for 3hrs and 1300°C for 1hr and the results shown in **figures** (3.9) to (3.12)

4.7 Future Work:

1. Studying the effect of granular size of the raw material on the preparing of Anorthite.
2. Studying physical properties (**porosity**), mechanical properties (**compressive strength**) and (**dielectric properties**) for high frequency application.
3. Studying the effect of advanced tech. (Filter press and magnetic separator) to manipulating raw material on the final prepared procedure.

Republic of Iraq
Al -Nahrain University
College of Science



Preparation of Anorthite from Local Raw Iraqi Materials

A Thesis
Submitted to the College of Science
Al-Nahrain University
in Partial Fulfillment of the Requirements for the Degree of
Master of Science in Physics

By
Muamar Abdu Alaziz Kamel

(B.Sc.2000)

Supervised by
Dr. Fadhil A. Rasin

Rabi'a Al-Aw'wal
April

1427A.H.
2006A.D.

Examination Committee Certificat

We certify that we have read the thesis entitled "**Preparation of Anorthite from Local Raw Iraqi Materials**" and as an examination committee, examined the student **Muamar Abdu Alaziz Kamel** on its contents, and that in our opinion it is adequate for the partial fulfillment of the requirements for the degree of **Master of Science in Physics**.

Signature:

Name: Dr. Nadir F. Habubi

Title: Professor

Address: Dep. of Physics College of Education Al-Mustansiriyha University.

Date: / /2006

Signature:

Name: Dr. Jenan H. Al-Mukhtar

Title: Assist Professor

Address: Dep. of Physics College of Science
for Woman Baghdad University.

Date: / /2006

Signature:

Name: : Dr. Fadhil A. Rasin

Title: Assist Professor

Address: Dep. of Physics College of
science Babylon
University.

Signature:

Name: Dr. Azhar J. Dawud

Title: Lecturer

Address : Dep. of Physics College of science
AL- Nahra University.

Date: / /2006

Approved for AL- Nahra University College of Science

Signature:

**Name: Dr. LAITH A. AL-ANI
(Dean of the College of Science)**

Date: / /2006

Supervisor's Certification

I certify that this thesis was prepared under my supervision at the AL- Nahrain University as a partial requirement for the degree of Master of Science in physics.

Signature:

Name: Dr. Fadhil A. Rasin
Title: Assist Professor
Address: Department of physics
College of Science
Babylon University
Date: / / 2006

In the view of the recommendation. I forward this thesis for debated by the examination committee.

Signature:

Name: Dr. Ahmad K. Ahmad
Title: Assist Professor
Address: Head of the Department of physics
College of Science
AL- Nahrain University.
Date: / / 2006

Acknowledgement

I wish to extend my appreciation to my supervisor ***Dr. Fadhil Abed Rasin*** for his kind guidance and encouragement, which make this possible.

I would like to express my thanks to ***Dr. Ahmad K. Ahmad*** the head of physics department and all the staff of physics department, especially ***Mr. Mohammed Tarq*** for their assistance during to preparing of the thesis.

Deep thanks to my father, my mother, my brother my wife and all my friends for their help during the work.

A decorative border consisting of a grid of small, stylized flowers. The flowers are arranged in a rectangular frame around the central text. Each flower has a grey center and white petals with black outlines.

CHAPTER ONE

INTRODUCTION

A decorative border consisting of a grid of small, stylized flowers. The flowers are arranged in a rectangular frame around the central text. Each flower has a grey center and white petals with black outlines.

CHAPTER TWO

*THEORETICAL
PART*



CHAPTER THREE

PRACTICAL and Results
PART



CHAPTER FOUR

*DISCUSSION OF
RESULTS,
CONCLUSION &
FUTURE WORK*

A decorative border consisting of a repeating pattern of small, stylized flowers with five petals and a central dot, arranged in a rectangular frame around the text.

*DEDICATION
TO
MY FAMILY*

A decorative border consisting of a repeating pattern of small, stylized flowers with grey centers and white petals, set against a black background. The border frames the central text.

REFERENCES

1. Schaller, W. T. "**The Genesis of Lithium Pegmatites**" Am. J. Sci., vol. 10: p 207, 1952.
2. Smyth, Ch. Ph. "**Dielectric Behavior and Structure**" Mc Graw-Hill book Company, Inc. New York, (1955).
3. Varley, E. R., sillimante "**chemical of Clays**" vol. 1, 1968
4. Bhaskar V. Velamakauni and Fred F. Lange "**J. Amer. Ceram. Soc**" vol. 74, p 166-172, 1991
5. Rex, W. Grimshaw. "**The Chemistry and Physical of Clays and Allied Ceramic Materials**" 4th edition, 1971.
6. Schairar, J.F. "**The Alkali-Feldspar Join in the System $\text{CaAl}_2\text{Si}_2\text{O}_8\text{-NaAlSi}_3\text{O}_8\text{-SiO}_2$** " J.geol. Vol .58, p 512, 1970.
7. Ilya N.Bindeman and Johan C.Bailey "**Earth and Planetary Science**" vol. 169, p 209-226, 1999.
8. Andrey G.Kalinichev and R.James Kirkpatrick. "**Chem. Mater**" vol. 14, p3539-3549, 2002.
9. D. Traber, U. madder, U. eggenberger "**Mineralogical Magazine**" vol. 62A, P. 1533-1534, 2002.
10. Smith, D. V. "**Feldspar Minerals**" Springer .Volga. New York, 1974.
11. Charles, M. L. "**Engineering Materials Hand book**", 1st edition, by a staff of specialists 1958.
12. R.A.GDULA. "**Anorthite Ceramic Dielectric**" " Journal of geophysical Research, vol.23, p.435,2004.
13. A. I. Andrews. "**Ceramic Tests and Calculation Anorthite**" 2004
14. Ilyan.bindeman, johnc.bailey. "**Earth and planetary science letters**" vol. 169, p.209-226, 1999.
15. R.J.Angel and L. W. Finger "**J. of American Mineralogist**" vol. 75, p. 150-12, 1990.

16. L.klein.and D.R.Uhlmann. **“Crystallization Behavior of anorthite”**Journal of geophysical Research, vol.79, NO.32.1994.
17. Atsushi Yasuda and Kenji Mibe**”J. of Geoph. Research”** vol.107, p. 2072-2085, 2002.
18. Kural G.EtAl.” **Large plates of anorthite”**2003.
19. R.Jaemes Kirkpaticle and James Fred Hays.” **Journal of Geophysical Research”** vol. 81, p.32, 1976.
20. M.cukie Raman and D.R.Uhlmann.” **Viscosity of Liquid Anorthite** “1993.
21. Yuichi Kobayashi and Etsuro Kato. **“J.Am.Ceram.Soc”** vol. 77, p. 833-834, 1994.
22. Takashi Murakami and Toshihiko**”J. of Am. Mineralogist “**vol. 83, p.1209-1219, 1998.
23. Yanting Lin and Laurie A.Leshin .**“Lunar and planetary science”** vol. XXXVI, 2005.
24. Segal, D. **"Chemical Synthesis of Advanced ceramic material"** Cambridge university press, Cambridge, (1989).
25. Yono, T., Sato, M. and Terashita, k. **"Resent Work in Japan on the Mixing of Solids"** powder Technology, Vol.20, and pp.9 – 14,(1978).
26. Brownell, W. E. **"Structure Clay Products"** Spring–Verlag, New York, (1976).
27. Norton, F. H. **“Element of Ceramics”** 2nd edition, Addison Wesley publishing company, London, (1974).
28. Grim, R. **“Applied Clay Mineralogy”** McGraw–Hill book company, Inc. New York and London (1962).
29. Fard, R. W. **“Ceramic Drying”** pergamon press; Oxford, New York, (1986).

30. Ask eland, D. R. **“The Science and Engineering of Materials”**,
Van no– strand Reinhold international Co. Ltd, Hong Kong (1988).
31. Petrzzelli, G. Guldi, G and Sequi, P. **“Electro–Optical
Measurement of Clay Shrinkage”**. Clay minerals, Vol.11, pp. 81 –
84 (1976).
32. Callister, W. D. **“Material Science and Engineering an
Introduction”**, 5th edition, by John WIELLY & Sons (2000).
33. Send, T. and Richard C. Bradt, **“J. Am. Ceram. Soc.”** 73[1] 106–
114 , (1990)
34. Kohen, M. & Norton F.H. **“Physical Ceramics for Engineers”** by
Addison – Wesley publishing Company, (1964).
35. Cullity, B. D. **“Elements of X – ray Diffraction”**(1978).
36. Klug, H. P. and Alexander, L. E. **“X – ray Diffraction Procedures
for Polycrystalline and Amorphous Materials”** 2nd edition (1974).
37. Omar, M. A. **“Elementary Solid State Physics ;Principles and
Applications”**(1975).
38. Alpert, N. L. & Keiser, W. E. **“IR Theory &Practice of Infrared
Spectroscopy”** 2nd by plenum press, New York, (1970).
39. Buswell, A. M. and Dudenbostel, B. F. **“J. Am. Chem.
Soc.”**Vol.63, pp 2554 – 2558. (1941).
40. Sarasota, J. M. **“Dehydration Rehydration Studies of Clay
Minerals by Infrared Absorption Spectra”** by pergmon press,
New York, (1962).
41. Miller, J. G. **“J. Phys. Chem.”** Vol. 65, No.5, pp. 800– 804, (1961).
42. Grim, R. E. **“Clay Mineralogy”** 2nd edition, MC Geaw Hill book
Company, New York, (1968).
43. Farmer, V. C. **“Infrared Spectroscopy”**. Vol.3, No.11, pp.29 – 35
(1979).

44. Reson, F.A. **"The Use of Iraqi Siliceous Rocks as Electrical Insulators Industry"**, Ph.D Thesis College of science, Nahrain University, (1998).
45. Omar, M. A. **"Elementary Solid State Physics"**, principle and application, Addition–Wesley publishing company, Inc.London, (1975).
46. Kingery, W. D. **"Introduction to Ceramics"**, John wiely, New York, (1976).
47. Jansen, L. **"Phy. Rev."**Vol.112, No.2, pp 434 – 444, (1958).
48. ASTM Designation D150 – 68. **"Standard Methods for Test A.C Loss Characteristics and Dielectric Constant (Permittivity) of Solid Electrical Insulating Material"**.
49. Kawakuho, T. and Yamamota, N. **"Thermal Properties"**Advanced technical ceramics (Sh. Somiya ed) Academic press Inc. scan Diego, California, New York, (1989).
50. Askeland, D. R. **"The Science and Engineering of Materials"**, 2nd edition, KENT publishing company, Boston, (1989).
51. Van der Marel, H. W. and Spacher **"Atlas of Infrared Spectroscopy of Clay Mineral and their Admixed "**. Elsever Scientific publishing company, New York, (1976).
52. John, O.F. **"Physical Phenomena in Clays"** vol. 27, p.270 – 277 (1999).
53. Berry, R. S. & Flynn, G. P. **"Physical Chemistry "**by john wiely &Sons, Inc. New York (1980).
54. Rex, W. Grimshaw. **"The Chemistry and Physical of Clays and Allied Ceramic Materials"**4th edition, p. 593-597, 1971.
55. Rex, W. Grimshaw. **"The Chemistry and Physical of Clays and Allied Ceramic Materials"**4th edition, p. 599-603, 1971.

56. Rex, W. Grimshaw. "**The Chemistry and Physical of Clays and Allied Ceramic Materials**"4th edition, p.345-375, 1971.
57. Geologists and Soil Scientists, H.Van Olphen." **Clay colloid chemistry for clay technologists**" 2nd Edition, 1977.
58. Rex, W. Grimshaw. "**The Chemistry and Physical of Clays and Allied Ceramic Materials**"4th edition, p. 605-606, 1971.
59. Newton, R. C." **J. Amer. Ceram. Soc.**" Vol.151, p.1223, 1966.
60. Haskell, R. W. and DeVries, R. C." **J. Amer. Ceram. Soc.**" Vol.47, p.203 and 236, 1964.
61. Rex, W. Grimshaw. "**The Chemistry and Physical of Clays and Allied Ceramic Materials**"4th edition, p. 608-609, 1971.
62. Rex, W. Grimshaw. "**The Chemistry and Physical of Clays and Allied Ceramic Materials**"4th edition, p. 606-608, 1971.
63. Rex, W. Grimshaw. "**The Chemistry and Physical of Clays and Allied Ceramic Materials**"4th edition, p. 712-715, 1971.
64. Williamson, J. and Glasser, F. P." **Science**" Vol.148, p.1589, 1965.
65. Rex, W. Grimshaw. "**The Chemistry and Physical of Clays and Allied Ceramic Materials**"4th edition, p. 623-625, 1971.
66. H.Zahang and A. I. Cooper"**Chem. Mate.** " vol. 14, p.4017-4020, 2002.
67. Rankfn, G. A. and Menvin, H. E." **J. Amer. Chem. Soc.**" Vol.38, p.571-578, 1978.
68. H. F. W. Taylor and A . Cooper " **Clay Mineral Bull**" vol. 3, No. 16, 1959.
69. Dcman, R. C., Barr, J. B., McNally, R. N. and Alper A. M." **J. Amer. Ceram. Soc.**" Vol. 46, p.313. 1963.
70. Johnson, R. E. and Muan, A." **J. Amer. Ceram. Soc.**" Vol. 48, p. 360, 1965.

71. Gentile, A. L. and Foster, W. R.” **J. Amer. Ceram. Soc.t.”** Vol.46, p.76, 1963.
72. Jianzhong and Huagao “**Journal of Chemical Physics**”vol.120, No.15, (2004).
73. Farmer, C. N.” **Clay Mineral Bull**” vol. 5, No. 27, 1962.
74. Phillips, B. and Muan, A.”**J. Amer. Ceram. Soc.”** Vol.45, p.590, 1962.
75. Berry, R. S. & Flynn, G. P. “**Physical Chemistry** “by john wiely &Sons, Inc. New York (1980).
76. Alberty, R. A. and Silbey, R. “**Physical Chemistry** “2nd edition, by john wiely &Sons, Inc. New York, (1997).
77. J. A. Gadsden “**infrared spectra of minerals and related inorganic compounds** “(1975).